Imperial College London

Evaluation of Tomographic 3D Ultrasound for the Assessment of Vascular Pathology

Adel Ahmad Al Zahrani
CID: 00955602

A thesis submitted in partial fulfilment of the requirements for the degree of

Doctor of Philosophy

In the Faculty of Medicine

Department of Surgery and Cancer

Imperial College London

&

Imperial College NHS Healthcare Trust, Hammersmith Hospital

London, United Kingdom

April 2023

Abstract:

Tomographic 3D ultrasound (t3DUS) is a promising imaging technique for quantifying vascular diseases by measuring the degree of stenosis and plaque volume. However, its accuracy and reliability for the assessment of vascular diseases need to be investigated. Therefore, this thesis aims to assess the accuracy and reproducibility of t3DUS for quantifying vascular diseases, including grading stenosis and measuring plaque volume *in-vitro and in-vivo.*

A literature review was performed to evaluate the use of three-dimensional ultrasound (3DUS) for assessing carotid stenosis in patients with carotid diseases showing that 3DUS is more accurate in quantifying carotid diseases and has a low level of inter and intra-observer variability when compared to 2DUS. However, it requires prolonged time for images to be reconstructed into 3DUS, which may currently limit its use in clinical practice.

The analysis from the *in-vitro* study on the vascular phantom, including channels with different grades of stenosis, demonstrated that t3DUS has an excellent inter-operator agreement with low variability and is more accurate than 2DUS for grading stenosis when compared to the reference values with an Intra-Class Correlation (ICC) value of 0.96 (95% confidence interval (CI) 0.90 – 0.98, $p < 0.001$. Based on these findings, two clinical studies were conducted investigating the reproducibility and accuracy of t3DUS for measuring carotid plaque volume (CPV) within the internal carotid artery (ICA) in patients undergoing carotid endarterectomy (CEA) (n=25), and the potential benefits of t3DUS in providing more precise measurement of stenosis in the superficial femoral artery (SFA) in patients with the peripheral arterial disease (PAD) (n=50). The results showed an excellent agreement level between

t3DUS and reference test (i.e., *Ex-vivo* carotid plaque volume from carotid endarterectomy specimen) and intra-observer agreement in measuring carotid plaque volume. This result demonstrates that t3DUS can measure the disease severity of SFA in patients with lower limb arterial disease with a correlation value *(r)* = 0.99, $p<0.001$.

The findings of this thesis indicated that t3DUS is a reliable and reproducible method for quantifying vascular diseases, including grading stenosis and measurements of CPV. Further research investigating the potential of the added value of t3DUS in assessing the different ranges of vascular diseases, including aneurysms, arteriovenous fistula (AVF) for haemodialysis access, and venous mapping, should be considered.

Table of Contents:

Statement of Originality:

This is an original thesis, and no component of the work in the thesis has been submitted in support of an application for another degree or qualification at this or any other University.

Copyright Declaration:

List of Publications:

Parts of this thesis have been published in a scientific journal and presented at scientific conferences:

Published Article:

- Alzahrani A, Alotaibi SA, Aslam M, Sultan SR. Reliability and Accuracy of Tomographic 3-Ultrasound for Grading Vessel Stenosis: A Phantom Study. Ultrasound in Medicine & Biology. 2022 Sep 1;48(9):1899–906. Alternatively, please refer to *Appendix C 1.*
- Alzahrani A, Sultan SR, Aslam M. Tomographic 3D Ultrasound for Grading Stenosis of Superficial Femoral Artery.

Articles Under Review for Publication:

- Alzahrani A, Sultan SR, Aslam M. Reliability of Tomographic 3D Ultrasound in Measuring Internal Carotid Artery Plaque Volume.

List of Published Abstracts and Conference Presentations:

- Alzahrani A, Aslam M, Sultan SR. Reliability and Accuracy of Tomographic 3D Ultrasound for Grading Vessel Stenosis: A phantom study. Charing Cross symposium 2022, UK. https://www.cx2022online.com/on-demand-single/3320/0
- Alzahrani A, Sultan SR, Aslam M. Reliability of Tomographic 3D Ultrasound in

Measuring Carotid Plaque Volume - Adel Alzahrani. European Society of Radiology 2022, Vienna. https://connect.myesr.org/?esrc_course=vascular-imaging-miscellaneous. Alternatively, please refer to *Appendix C 2*

- Alzahrani A, Sultan SR, Aslam M. Comparison between 2DUS and t3DUS for the assessment of the lower limb artery. Accepted for poster presentation in the vascular society annual meeting, 2022, Brighton, UK.
- Alzahrani A, Sultan SR, Aslam M. Comparison between 2DUS and t3DUS for the assessment of the lower limb artery. Charing Cross symposium 2023, UK. https://www.cxsymposium.com/cx-events-2023/?set=3.0300
-

Acknowledgement:

First and foremost, praises and thanks to God, the Almighty, for His showers of blessings throughout my research work to complete this research successfully.

I am extremely grateful to my parents for their love, prayers, care, and sacrifices in educating and preparing me for my future. I am very thankful to my wife and my sons for their love, understanding, prayers and continuous support in completing this research. Without their constant support, none of my work would have been achieved.

I would like to express my deep and sincere gratitude to my research supervisor, Dr Mohammed Aslam, lecturer and research supervisor at the Imperial College London, for allowing me to do this research under his supervision and for providing valuable guidance throughout this research. His dynamism, vision, sincerity, and motivation have deeply inspired me. Many thanks to Mr Usman Jaffer, Consultant of Vascular Surgery, for his support and help. I also would like to thank Dr Salahudeen and Dr Mohammed Al-Sadi for their support during my educational journey.

Dedication:

I dedicate my work to my brother Mohammad who passed away 25 years ago. I have always wished to celebrate the achievement of this research with him as we used to do for our school graduations in the past. Sadly, he could not see me graduate, and we could no longer celebrate in our lives.

List of Tables:

List of Figures:

Abbreviations:

2DUS	Two dimensional US
3DUS	3-Dimensional Ultrasound
AAA	Abdominal Aortic Aneurysm
AGES	advanced glycation end-products
ALARA	As Low As Reasonably Achievable
AR	Area Reduction
ATA	Anterior Tibial Artery
AVF	Arteriovenous fistula
B Mode	Brightness mode
CAD	Coronary Artery Disease
CCA	Common Carotid artery
CEA	Carotid Endarterectomy
CFA	Common femoral artery
CFV	Common femoral vein
CI	Confidence Intervals
CIMT	Carotid IMT
CPV	Carotid Plaque Volume
CT	Computed Tomography
CTA	Computed Tomography Angiography
CV	Coefficient Variation
CVA	Cerebral Vascular Accident
CVD	Cardiovascular Disease
DM	Diabetes Mellitus
DPA	Dorsalis pedis artery
DR	Diameter Reduction
DSA	Digital Subtraction Angiography
DUS	Duplex Ultrasound
ECA	Eternal Carotid Artery
ECST	European Carotid Surgery Trial
EDV	End Diastolic Velocity
GSM	Grey Scale Median
HZ	Hertz
ICA	Internal Carotid Artery

ICC	Intra-Class Correlation
ICH	Intracerebral haemorrhage
ICH - GCP	International Conference of Harmonisation of Good Clinical Practice
IICS	Intraclass correlation coefficients
IMB	Intima-Media boundary
IMT	Intima-Media Thickness
IMU	Internal Measurement Unit
KHZ	Kilohertz
LOA	Limit Of Agreement
LSV	Long saphenous vein
MD	Mean Difference
MRA	Magnetic Resonance Angiography
MRI	Magnetic Resonance Imaging
NASCET	North American Symptomatic Carotid Endarterectomy Trial
NHS	National Health Service
NICE	National Institute of Clinical Excellence
OTO	Outer wall to Outer wall
PAD	Peripheral Arterial Disease
PFA	Profunda Artery
PL	Peroneal Artery
PSV	Peak Systolic Velocity
PTA	Posterior Tibial Artery
PZT	Piezoelectric crystals
RIND	Reversible Ischemic Neurological Deficit
SD	Standard Deviation
SFA	Superficial Femoral Artery
t3DUS	Tomographic Three-dimensional Ultrasound
TIA	Transient Ischemic Attack
TVA	True volume analysis
TWV	Total Wall Volume
US	Ultrasound
VA	Vertebral artery
VR	Velocity ratio
VWV	Vessels Wall Volume

CHAPTER 1

BACKGROUND

1.1 Cardiovascular disease:

Cardiovascular disease (CVD) is a serious condition that can seriously impact people's lives worldwide. CVDs take nearly 18.65 million lives per year globally (1). It is estimated to be the leading cause of death and disability globally. The death rate of various diseases in males and females is shown in Figure 1.1. CVD is regarded as the primary cause of death compared to other diseases (2). As in almost all CVDs, the fundamental pathophysiology and development are primarily atherosclerotic sources, causing coronary artery disease (CAD), Stroke and Peripheral Arterial Disease (PAD).

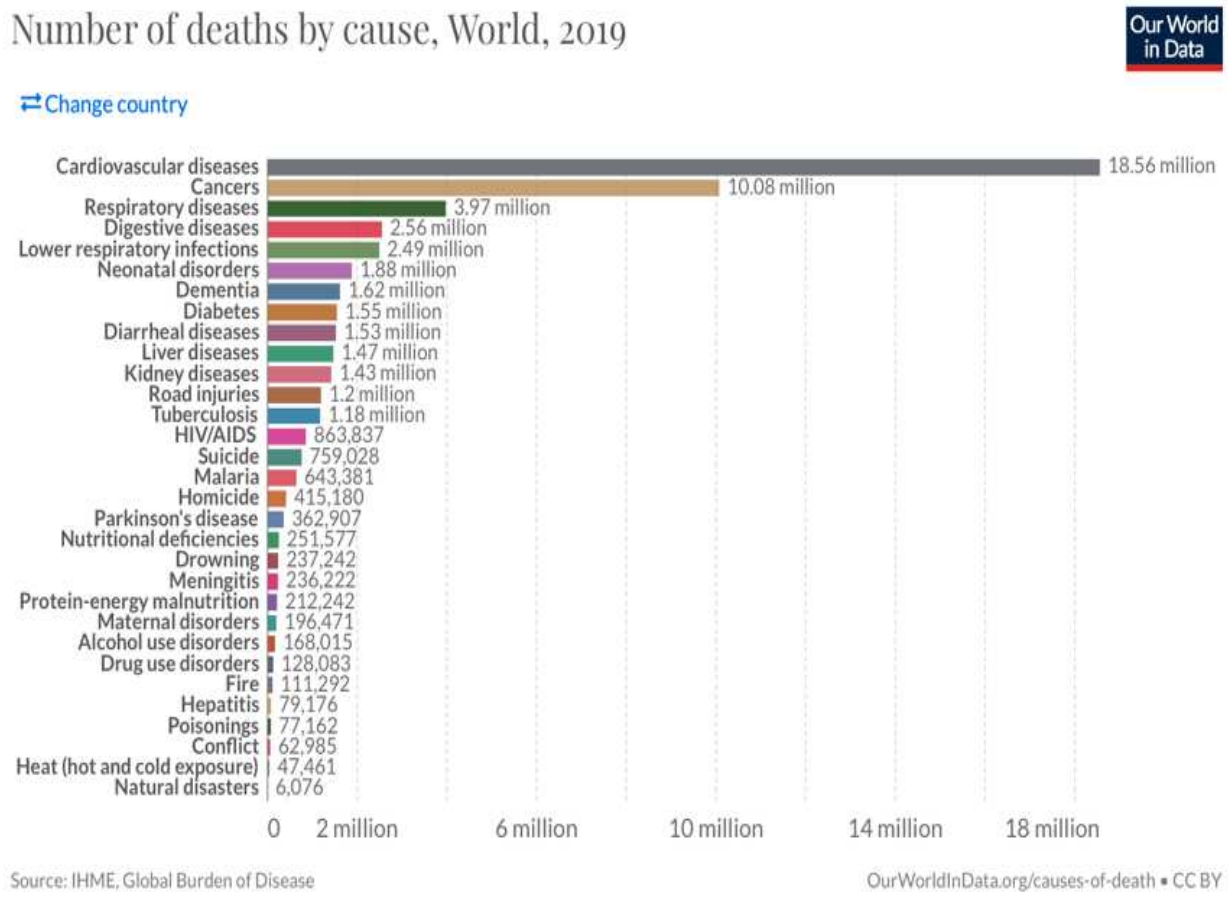

Figure 1.1 causes of death in the world (1)

1.1.1 Coronary Arterial Disease (CAD)

CAD is the leading cause of death worldwide, and it is caused by the build-up of plaques within the arterial wall, which can cause an occlusion to the blood flow in the heart and cause a medical condition called a myocardial infarction. Because of the high mortality rate associated with CAD, cardiovascular researchers prioritise developing medical interventions that repair and replace diseased arteries (3). Advances in arterial regenerative medicine could benefit from a better understanding of how coronary arteries develop during embryogenesis and how these pathways can be reactivated during disease. Recent research has advanced our understanding of how coronary vasculature is formed and revealed unexpected aspects of neural stem cell implementation that may have consequences for organ development in general (3). Recent research using cutting-edge technology has discovered novel origins of, in addition to, new molecular and cellular mechanisms that govern the development of coronary vessels in the postnatal heart, such as collateral artery structure, endocardial-to-endothelial differentiation, and bone marrow stromal cell transition. These novel coronary vessel formation regeneration mechanisms provide new possibilities for promoting cardiac repair and regeneration by targeting microcirculation (4).

1.1.2 Stroke

A stroke is a neurological disorder characterised by blood vessel occlusion. There are two main types of strokes, Ischaemic and intracerebral haemorrhage (ICH). In ischaemic stroke, clots form in the brain, interrupting or reducing the blood flow and causing tissue death in the affected area. ICH stroke occurs when one of the brain arteries becomes

aneurysmal, causing blood vessels to rupture, resulting in bleeding, and causing sudden death of brain cells due to a lack of oxygen (5). Stroke can also cause depression and dementia. It is the world's second leading cause of death and a significant cause of disability. Stroke is most common in developing countries, with ischemic stroke being the most popular type (5). Stroke is the "incoming epidemic of the twenty-first century," according to the World Health Organization. Recent data shows that 85% of all strokes may be preventable (6).

Two main ICAs anteriorly and another two vertebral arteries (VA) posteriorly supply and control blood flow to the brain; this is known as (the circle of Willis). as previously stated, Ischemic stroke is caused by an insufficient amount of blood and oxygen in a specified area within the brain. In contrast, ICH stroke is a consequence of bleeding caused by a ruptured blood artery (5). Another type, Ischemic occlusions, cause about 85% of stroke mortalities which are caused by a thrombotic incident in the brain (7).

Plaque accumulation will ultimately narrow the arterial lumen, resulting in ischaemic stroke. An embolism is caused by decreased blood flow to the brain area in an embolic stroke; the blood flow to the brain decreases, leading to severe stress and early cell death, a condition known as (necrosis). Necrosis is accompanied by plasma membrane damage, inner membrane swelling and leaking of cellular contents into extracellular space, leading to neuronal function loss (8). Other medical conditions such as Inflammation, energy failure, loss of homeostasis, acidosis, increased intracellular calcium levels, excitotoxicity, free radical-mediated toxicity, cytokine-mediated cytotoxicity, complement activation, impairment of the blood-brain barrier, activation of glial cells, oxidative stress, and leukocyte infiltration are all considered to make a significant contribution in stroke pathology (9). A high

mortality rate is associated with ICH stroke, which accounts for 10–15% of all strokes. Stress in the cerebral tissue and internal damage cause blood vessels to rupture. It has toxic effects on the vascular system, causing infarction (10) It is divided into two types: intracerebral and subarachnoid haemorrhage. ICH, resulting in an abnormal accumulation of blood within the brain. The most common causes of ICH are hypertension, vasculature disruption, excessive anticoagulants and thrombolytic agents (11).

1.1.3 Peripheral Arterial Diseases (PAD)

PAD is an atherosclerotic vascular disease affecting more than 200 million people worldwide. It has higher cardiovascular event rates than the rate of coronary artery disease (12). Ischemic leg pain is a defining feature of PAD, which is also associated with an increased blood pressure response to exercise, impaired vascular function, and an increased risk of myocardial infarction and cardiovascular mortality. PAD is distinguished by intermittent claudication, defined as tiredness, discomfort, muscle cramps, or pain of vascular origin in the lower extremity calf muscles that are consistently induced by mainly walking or exercise and consistently relieved within a time range of 10 minutes by rest (13).

Diabetic Mellitus (DM) is a significant risk factor for PAD. The increased risk of PAD in diabetic sufferers is multifactorial and complex. Lower extremity function and ability are worse in diabetic patients with PAD than in patients with PAD alone. Furthermore, diabetic patients with PAD are more likely to experience sudden ischemia of arterial thrombosis and ischemic ulceration of the lower extremities (11). As a result, a better understanding of the pathophysiology of PAD in DM is required to shed light on its diagnosis, prevention, and

treatment (14). However, in diabetic patients, overproduction of advanced glycation end-products (AGEs), increased oxidative stress, increased inflammatory factors, and dyslipidaemia may directly or indirectly worsen PAD (15) In other words, these DM abnormalities complicate the pathophysiological mechanisms of diabetic PAD.

1.1.4 Atherosclerosis

Atherosclerosis is a process in which lipid-leaden macrophage deposits and other material, such as cholesterol, calcium, thrombus, and protein, accumulate within an artery, most commonly at the site of microtrauma, and cause an inflammatory response (16,17) (Figure 1.2) Microtrauma is more likely to occur at curvature points, branching, or dilatation. Microtrauma can result in increased flow disruption, resulting in increased stress between blood flow streams and the arterial wall (18,19). This turbulence results in cholesterol infiltration into the endothelial cell wall, accumulating over time, hardening to form a plaque, and narrowing the arterial lumen. Increased shear stress caused by atherosclerosis creates a virtuous circle, predisposing the artery to plaque build-up (20). Patients may develop symptoms when atherosclerosis progresses to critical flow-limiting stenosis or diffuse disease load.

Several medical conditions lead to atherosclerotic diseases, such as obesity, diabetes, dyslipidaemia, hypertension, and smoking. These conditions are the primary risk factors for cardiovascular disease (21–26). Being physically inactive is a significant risk factor for all these problems. Atherosclerosis-related symptoms and conditions include myocardial infarction,

angina, stroke, cerebral vascular accident (CVA), reversible ischaemia without neural deficit (RIND), and transient ischemic attack (TIA), resulting in vascular mortality.

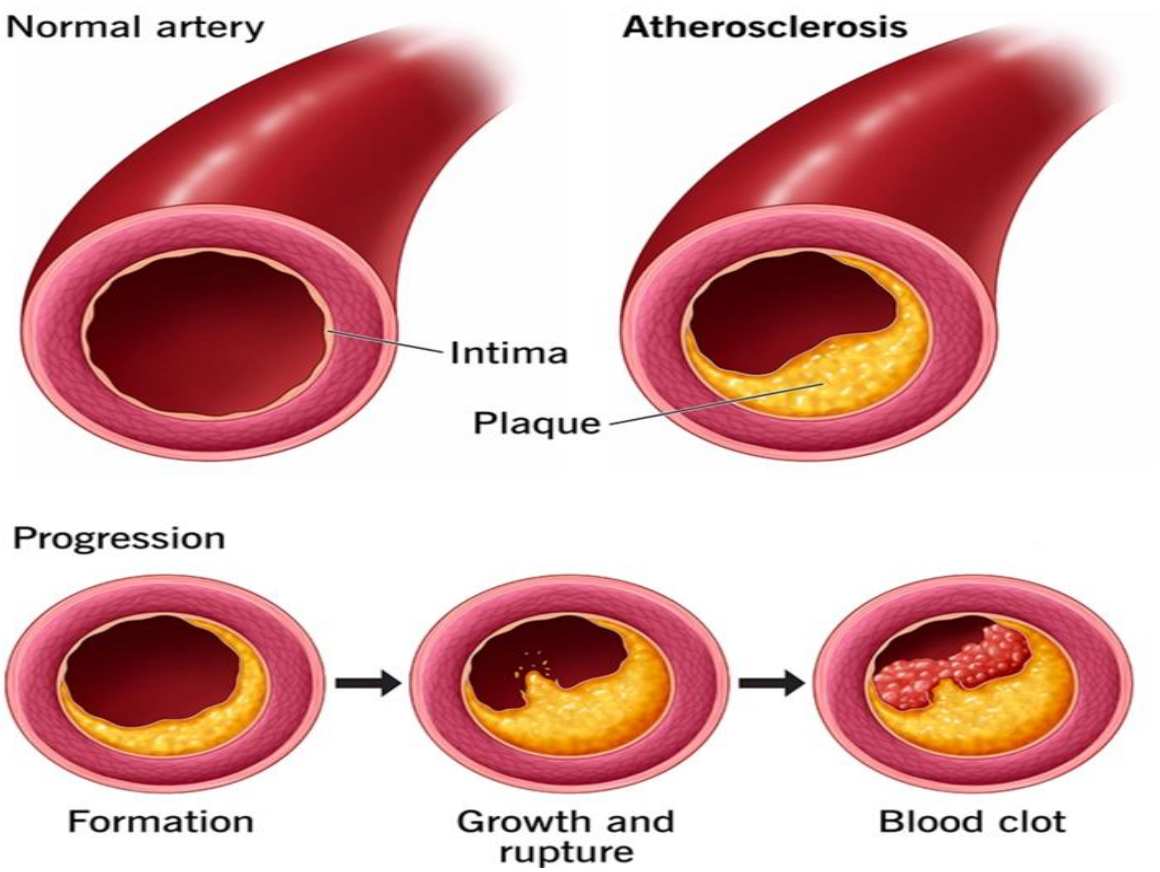

Figure 1. 2 stages of atherosclerosis. (17)

Surgically treating atherosclerosis at the symptomatic stage is prohibitively expensive for the national health service (NHS) and frequently results in a lengthy terminal treatment plan. Antiplatelet medications, such as Clopidogrel, are beneficial in reducing risk when used early and long-term (27). Additionally, there is compelling evidence that statin-based lipid-lowering therapy reduces cardiovascular and all-cause mortality, emphasising obtaining an LDLc level of less than 1.8 mmol/L (28). While optimising medical care at the outset of symptoms can help lower cardiovascular risk, it is too late to prevent the risk from forming in the first place.

Cardiovascular screening and vigorous early medical treatment can considerably reduce cardiovascular mortality and morbidity (29). From here, accurately diagnosing vascular disease has a significant impact on patients and service providers.

1.2 Diagnostic Methods of Cardiovascular Disease:

Cardiovascular imaging can be either prospective or preventive. Imaging is critical in cardiovascular screening since it has increased patient adherence to medical care and decreased cardiovascular events (30). Despite its significance, most vascular imaging is now used for diagnostic purposes and surgical planning.

1.2.1 Magnetic Resonance Imaging (MRI)

Compared to computerised tomographic angiography (CTA), Magnetic resonance angiography (MRA) is pricier because it does not use ionising radiation and frequently employs a gadolinium-based contrast medium. Gadolinium contrast increases the risk of nephrogenic systemic fibrosis in patients who suffer from renal failure (31), and patients whose glomerular filtration rates are close to boundaries for gadolinium use require pre-admission for intravenous hydration. This procedure is essential to protect the kidneys and increases the cost. The benefit which MRA can provide is the evaluation of the crural calcified arteries (Figure. 1.3).

Kreitner et al. (32) demonstrated that MRA is as accurate as DSA in evaluating the crural arteries and the foot arteries, suggesting that diagnostic digital subtraction angiography (DSA) for PAD should not be performed where MRA is available. Because of semi-automation, image

processing in MRA is much faster than in CTA, but acquisition times are longer and more operator-dependent. When imaging for PAD, MRA scans can easily be mistimed, resulting in an undiagnostic image due to venous contamination (33), although this depends on the imaging technique. Conventional high-dose chase imaging methods have a much higher incidence (34). Because of the risk of overheating, MRA cannot be used with metallic implants, such as older vascular stents or pacemakers. Vascular stents are also problematic because they frequently fill voids (as with iliac stents), leading to occlusion misdiagnosis. 2DUS can reduce this with waveform profiling. Availability of the MR scanner and its availability within the hospitals and diagnostic centres can also be a problem; vascular clinics and studies centres within health care facilities with Cardiac or Neurosurgical specialities may struggle to gain access to MR scanners, forcing them to rely on other scanning modalities such as CTA which has its own set of risks and potential side effects.

It is also possible for MRA to overestimate the severity of stenoses due to the way data is computer generated to generate what can be visually spectacular images. This is mainly due to the sampling frequency (35) when a higher intensity projection is used, implying that source data must be assessed continuously to avoid misdiagnosis. The misclassification rate of carotid stenosis has been around 15% (36).

Because Vascular Surgeons rely on these alternative imaging techniques, Interventional Radiologists spend more time performing diagnostic catheter angiograms and reporting CTA and MRA scans. As a result, intervention waiting lists are growing, leading to longer waiting lists.

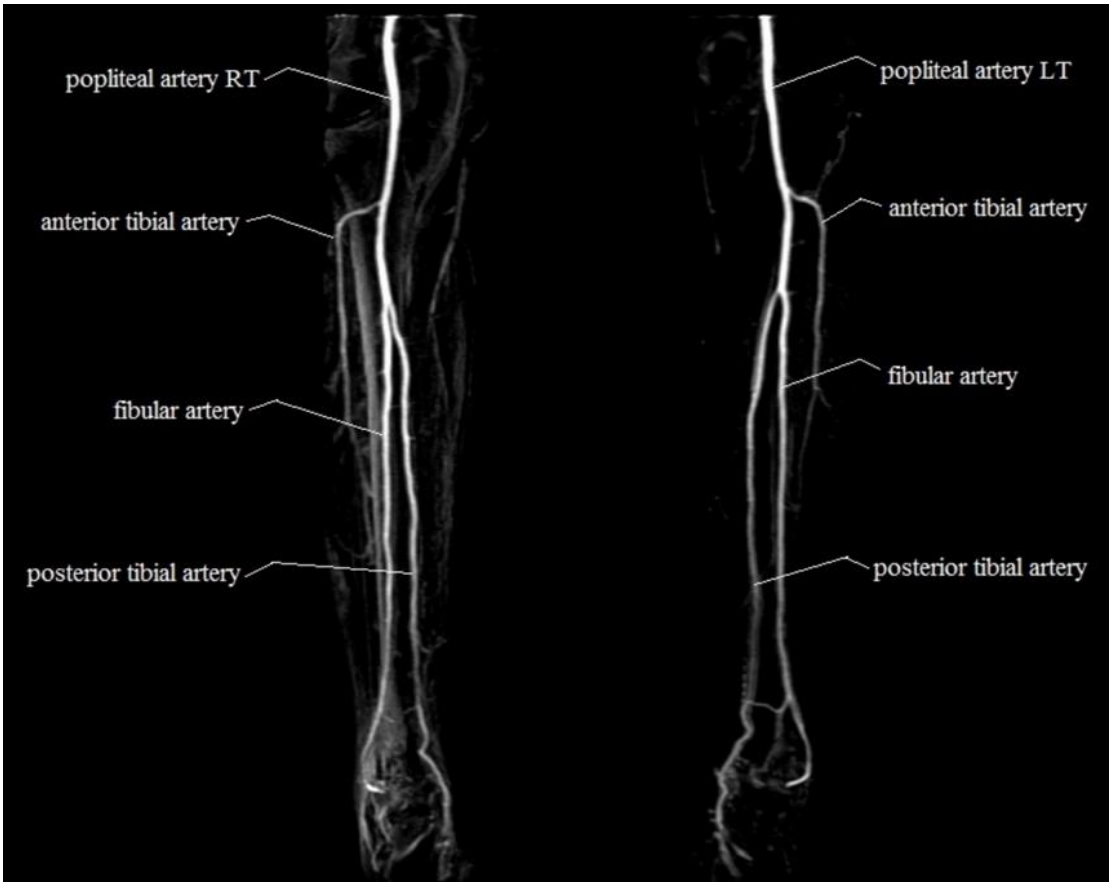

Figure 1. 3 Bilateral MRA of crural arteries (37)

1.2.2 Computerised tomography (CT) scan

CT scan is the fastest compared to MRI and DUS due to its computerised generation. CTA uses ionising radiation and nephrotoxic contrast medium (generally iodinated), which causes accumulated potential nephropathy and therefore is not appropriate for some groups of patients with impaired renal function (38). CTA avoids the limitations of 2DUS and has higher sensitivity and specificity, for example, for PAD, which has been noted to be between 92 and 99.2% (39). This is due to several factors, and the most important one is that it is less operator-dependent. Regardless of its greater sensitivity and specificity and overall improved image efficiency over 2DUS for lower limb vessels and iliac arteries, CTA may still be performed technically incorrectly; these technical errors significantly limit its diagnostic accuracy. The

specificity and sensitivity for arterial pathology have been reported to be 91% and 85%, respectively, and 92% and 94% for iliac arterial disease(39). Overestimation of the grade of calcified stenosis by CTA is thought to be a significant limitation, mainly due to two main factors. Firstly, modern CT scanners use maximum intensity projections, which may lead to false lesions when scanned vessels are close to bones; Secondly, the calcified walls are highly attenuative. As a result, CTA requires skilled interpretation and experience to ensure that these are not misreported and to increase diagnostic accuracy.

Although MRA and CTA can provide better image quality and details when compared to traditional Ultrasound, using radiation in CT scan and contrast agents in both may be obstacles to some patients with poor renal function (40). The waiting list for the MRI scanning is also another issue. In addition, some patients are claustrophobic and cannot stay stationary whilst scanning using those two modalities (41). Ultrasound can provide real-time images and assessment of the blood velocities along with the spectral waveforms, indicating the severity of the stenosis where detected (42).

1.2.3 Angiography

Angiography is considered the gold standard imaging technique for assessing PVD. It can provide anatomical details of the disease and play a significant role in the treatment. Compared to CT angiography, there is evidence of a 95.2 per cent agreement between 3DUS results of stenosis. Using CTA as a gold standard, this figure corresponds to the sensitivity of previously published research, which is around 95%. This was evaluated in 40 individuals, and the data compared stenosis assessments using diameter reduction rather than measuring

plaque volume. Of 20 patients undergoing carotid endarterectomy, 11 had >95 per cent stenosis, 8 had >75 per cent stenosis, and 1 had less than 75 per cent stenosis, which was consistent and demonstrated good agreement across all modalities (3DUS, 3DCTA, and 3D angiography). There were two examples in this investigation where the differences in the degree of stenosis determined by each approach were significant. However, the researchers explain why these discrepancies exist. In one case, the common carotid artery (CCA) bifurcation was severe, preventing the 3D probe from detecting distal ICA (43). As a result, subtotal stenosis seemed to be an occlusion on 3DUS.' In the second example, the disparity was caused by a calcified plaque, which prohibited 3DUS from assessing the degree of stenosis, but angiographic procedures could overcome this. This shows that CTA should be used in conjunction with 3DUS in more complex situations and that it should be utilised in all patients diagnosed with the external carotid artery (CEA), as an error could result in an erroneous treatment plan. Nonetheless, 3DUS is a good screening technique with a significant association with gold-standard CTA findings (43).

DSA is frequently utilised as a gold standard, and 3DUS has been compared to it. A study has shown that only 32 of 36 stenosis defined as high-grade in 3DUS - the remaining four were diagnosed as insignificant. This miscalculation was magnified when looking at the 17 critical level stenosis, of which 3DUS recognised only ten as high grade. Despite these underestimations, the overall agreement with DSA was better than 2DUS velocity ratio (44). However, DSA has limitations, including contrast media, low spatial resolution, artefacts, and a small field of vision (45).

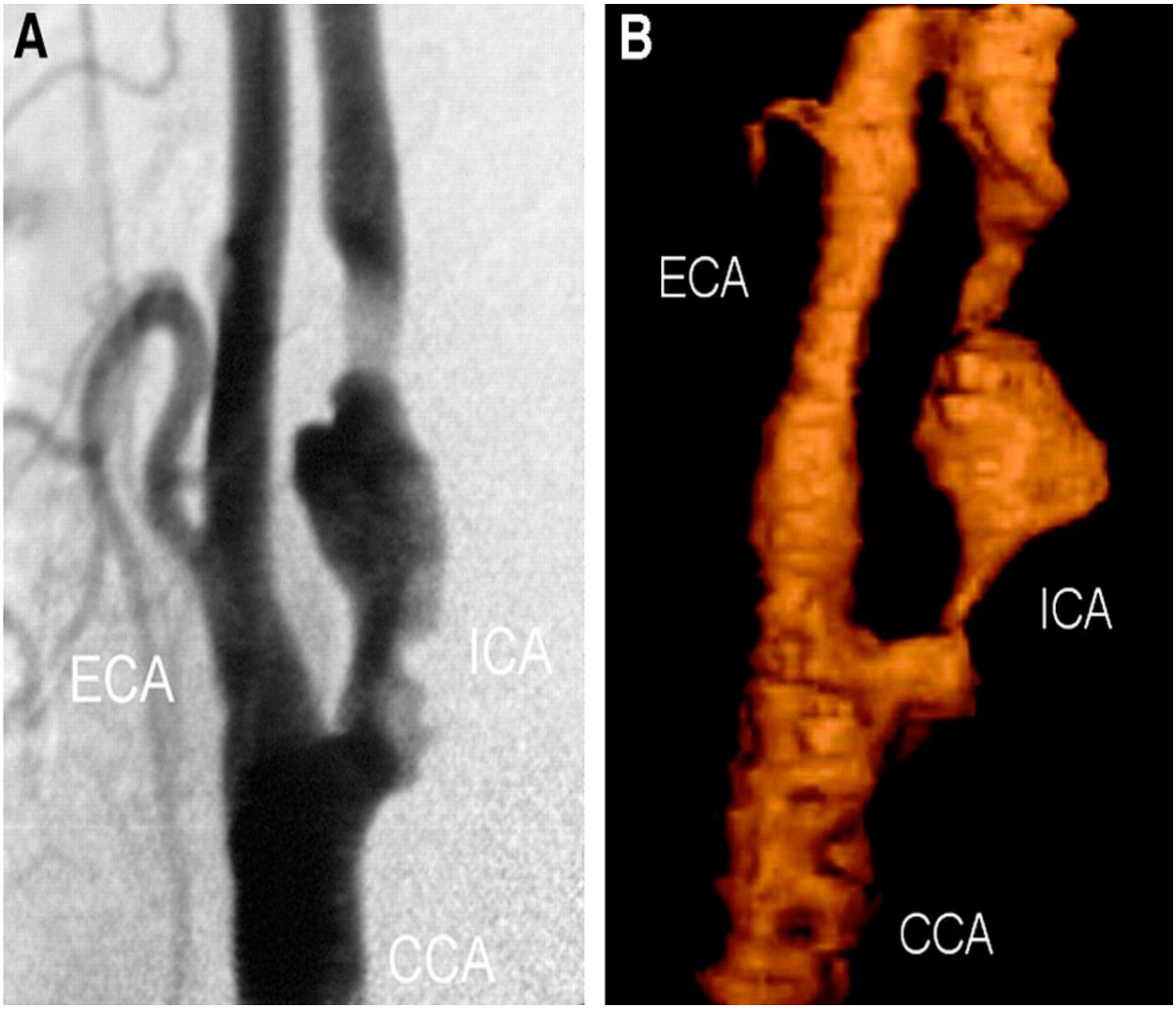

Figure 1. 4 Comparison of carotid stenosis between DSA (A) and 3DUS (B). Proximal stenosis measured by DSA is 73% and measured by 3DUS is 74% (44).

1.2.4 Ultrasound

Ultrasound (US) traces its origins to Sonar, first developed to detect German U-boat forces during World War II. The first successful application of diagnostic ultrasonic transmission was not reported until 1942 (46). Ian Donald, who described the use of pulsed sound in the imaging of abdominal masses, stated the first successful application of Ultrasound in the medical field in the UK in 1958 (47). Due to the high cost and limited diagnostic capability, the US was first adopted by just a few hospitals. However, it did contribute to the early

development of modern diagnostic radiology; with the commercialisation of brightness mode imaging (B-Mode) in 1963, Homes and Howry made the subsequent extensive development in the United States (48). Since then, the Doppler effect had been incorporated into greyscale (B-Mode) imaging to detect blood flow, and in 1974, Barber et al. (49) announced the first commercial Duplex scanner.

The US has already been established for routine vascular investigation in hospitals throughout the industrialised world, and it is critical to vascular centres. The simultaneous use of B-mode, colour Doppler, spectral waveforms Doppler analysis, triplex imaging, and Duplex ultrasonography (DUS) are essential vascular ultrasound prerequisites. Recent advancements in DUS devices, such as contrast and B-Flow imaging, have transformed vascular US monitoring. Moreover, a recent development in US technology, the introduction of t3DUS reconstructions, could usher in a new era of vascular surgery. However, little research has been conducted on t3DUS accuracy, variability, reproducibility, and utility.

The fundamental physics of Ultrasound are essential physical principles of US and US instruments. Sound is classified as infrasound, audible sound, and Ultrasound, and it travels in cycles of oscillating high and low pressure, referred to as a longitudinal wave. To visualise this in terms of an object, consider the backward and forward movement of a Slinky. Traditionally measured in decibels, the sound is frequently assessed in terms of frequency in the unit of Hertz when applied to imaging (Hz). Infra-sound is any sound with a frequency less than 20 Hz, with an audible range of 20 Hz to 20 kilohertz (kHz). These basic principles are thoroughly detailed in *Appendix B* in order to optimise clinical understanding of US imaging.

1.3 Role of Ultrasound in Vascular Disease:

The clinical assessment followed by a 2DUS scan is the first line of investigation; DUS mode in the ultrasound scans is commonly used along with 2DUS mode and the colour mode to assess blood flow circulation and estimate the blood velocities in both significant (large) and minor (small) vessels of the body. The spectral Doppler technique can display normal and abnormal sign waveforms to indicate the disease's severity in the scanned vessel (50). However, there is a wide subjectivity in assessing the grade of stenosis among vascular scientists due to the operational dependency on Ultrasound.

DUS is a helpful tool for vascular patients due to the introduction of multi-element compound transducers with electronic beam steering and focuses on high frame rates (51). Their comparatively compact size and inexpensive cost compared to other diagnostic modalities such as CT and MR scanners. DUS is also non-invasive and safe for long-term patient monitoring because it does not use ionising radiation or nephrotoxic contrast. DUS can detect velocity variations across diseased segments to assess the disease severity, which is essential for surgeons to decide the best treatment plan for the patient. This means the disease can be quantified in functional severity, providing extra flow data and diameter reduction estimates like angiography.

As current DUS transducers are small, various scanning angles are feasible, allowing insonation around artefacts. Unlike other radiology-based assessments, vascular DUS imaging reporting is typically conducted by the individuals who acquire the images, usually after the

scan. The primary benefit of DUS is its portability. It can be utilised in the community, outpatients, at the bedside, in surgery, or even in intensive care.

1.4 Limitations of US in Vascular Disease Assessment:

DUS for surgical treatment is highly operator-dependent and is conducted in the UK by highly skilled vascular scientists or Sonographers and less typically by Vascular surgeons or Radiologists (52). Professional operators use typical DUS images to create a 3D mental image of the vascular disease and accompanying anatomy along the length of the relevant vessel (53). Practitioners who are not well trained may not be confident in making the correct assessment and diagnosis because of the lack of clinical skills and scanning experience when scanning or reading images. Consequently, unnecessary and expensive other imaging modalities such as CTA, MRA, and catheter angiography may be needed for more vascular evaluation (53).

Although safer for patients, DUS monitoring is prone to inaccuracy since it represents a narrow slice of 3D anatomy. Hence, anterior, medial, and posterior transducer positions/scanning planes mean that the same site cannot be ensured during follow-up. The most significant constraint is the presence of artefacts that cause acoustic shadowing, such as intestinal gas and arterial calcification (Figure. 1.5), which obscure the pathology image and can be limited further by vascular depth. Severely calcified plaque or arterial wall is a particular obstacle for carotid assessment, as alternate scan planes can avoid total obscurity and shorten depth while avoiding absolute anonymity. Other artefacts, such as reverberation and mirror images, might misrepresent DUS images, making it difficult for the operator to

determine what is real. When employing DUS pictures, measurements are also tricky. Volumetric evaluation using DUS, such as for Carotid tumour size, estimated from circumferential and length measures, is typically imprecise. It is not achievable for complicated structures like a carotid plaque with conventional technology. A severely tortuous, kinked, or coiled vessel can also cause the flow to centrifuge and become turbulent, elevating Doppler velocities and rendering blood velocity grading criteria obsolete. Medical conditions such as heart failure, sepsis, or changes in vascular haemodynamic, can significantly alter the pressure gradient induced by vasodilation, which can mislead Doppler velocities and make stenosis severity testing difficult. These difficulties lead to CT and MR) imaging's continuous significance in surgical education.

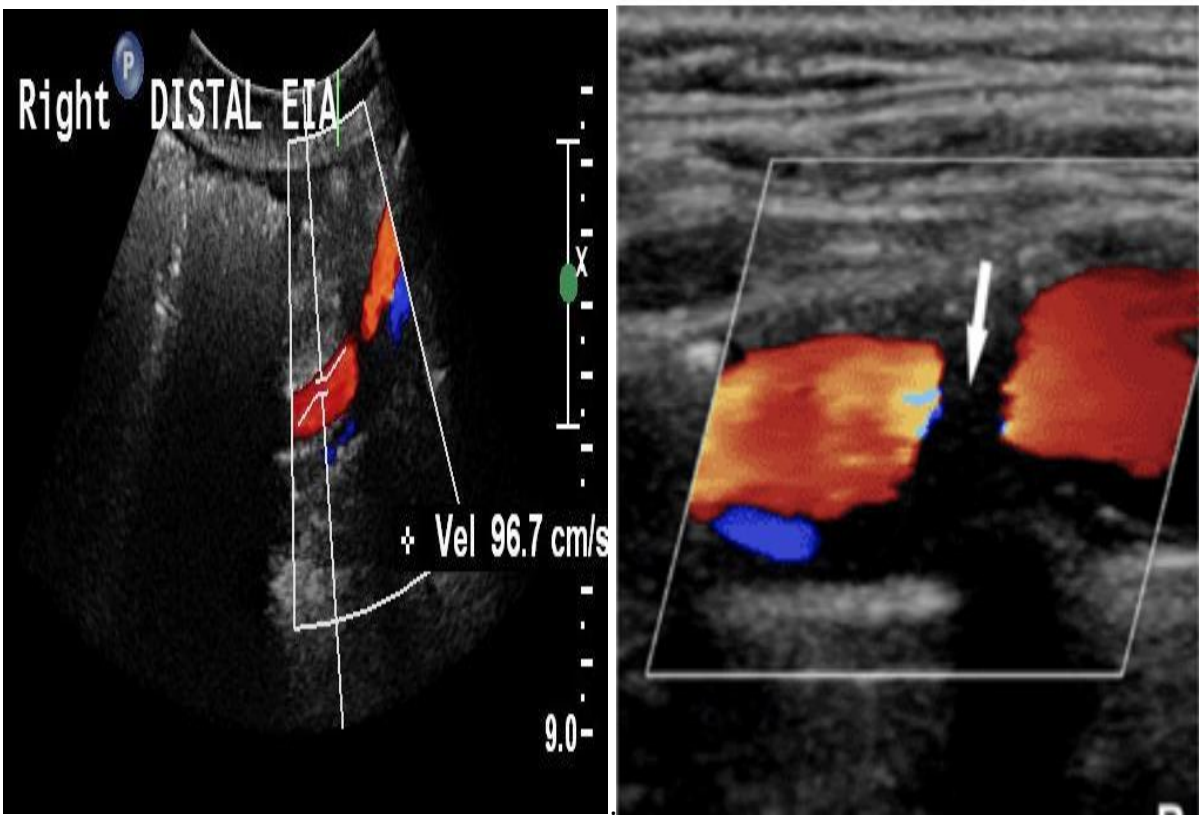

Figure 1. 5 Left shows bowel gas prevents visualisation of the iliac arteries. Right, acoustic shadowing covers carotid plaque (54).

The most challenging example of the current use of 2DUS in vascular disease assessment includes operator dependency, Interobserver variation, artefacts, difficulty in assessing pelvic and abdominal vessels and calcification presence. These are serious difficulties confronting most professionals when using ultrasound to evaluate vascular disease. These will reduce the US image quality and the overall image of vascular circulation. Additional techniques and advanced imaging are required to improve and overcome these limitations. t3DUS could be an excellent alternative scanning method for better image quality and more medical details in assessing vascular pathology.

1.5 3 Ultrasound Imaging:

t3DUS optimises disease visualisation from all angles, eliminating the need to form a mental impression (53,55,56). Accurate monitoring becomes reproducible as the same anatomy is visualised each time, and parts of anatomy previously inaccessible to DUS imaging, such as near the jaw for high carotid bifurcations, may become visible (53,55,57). With t3DUS imaging, many additional metrics, such as volume, become available. Through improved surveillance and assessment approaches, t3DUS may benefit patients by detecting those at risk of severe morbidity and mortality sooner (55,57).

1.6 Types of 3DUS Ultrasound scanners:

There are four general types of 3DUS ultrasound equipment:

1.6.1 Mechanical 3DUS Ultrasound

A mechanical arm linked to a DUS transducer or a motor-driven crystal within the t3DUS transducer housing can perform 3D mechanical imaging (55,57). Motors move the arm or piezoelectric crystal (PZT) a predetermined amount between each 2D image frame. A succession of 2D image frames spaced by a predetermined distance are captured, and each image is sequentially put into a 3D reconstruction of the anatomy. The 3D volume reconstruction is highly accurate since the orientation of the 2D frames is already known, resulting in rapid and high-quality 3D image acquisition and reconstruction. Still, the machine can be heavy and burdensome (55).

Mechanical arms are frequently acquired individually, resulting in significant expenses. Motor-driven crystals also result in a more extensive transducer housing than typical DUS probes, which can be challenging to move to provide perpendicular views of the anatomy and necessitate significant volumes of ultrasonic gel to assist heel-toeing.

To enable colour Doppler imaging, the transducer can be stationary in the mechanical arm or kept on the belly at a non-perpendicular angle (55). The transducer or crystal can be rotated, tilted, or fanned to visualise slightly larger volumes while the transducer footprint stays stable in the patient's abdominal area. However, using probe manoeuvres such as rotating or tilting

whilst the transducer stays on the abdomen results in non-specular reflection and more ultrasound waves are transmitted. This leads to more attenuation resulting in further ultrasound energy loss. As a consequence, reduced 3D volume resolution and poor image quality (58). Mechanical components indicate that the systems are likely to fail more than electrical or software 3DUS approaches.

Because of the mechanical limitations, crystals can only be driven over limited space, allowing only small anatomical structures to be scanned and viewed (Figure 1.6). As a result, multiple scans needed to be performed and assembled together in order to obtain a full visualisation of the anatomical structure, which impairs the image quality. Mechanical 3D scanning has the advantages of quick and near real-time volume reconstruction. By adopting a mechanical arm, conventional DUS transducers may be employed, allowing customers to take advantage of US technology/imaging advancements on a budget (59).

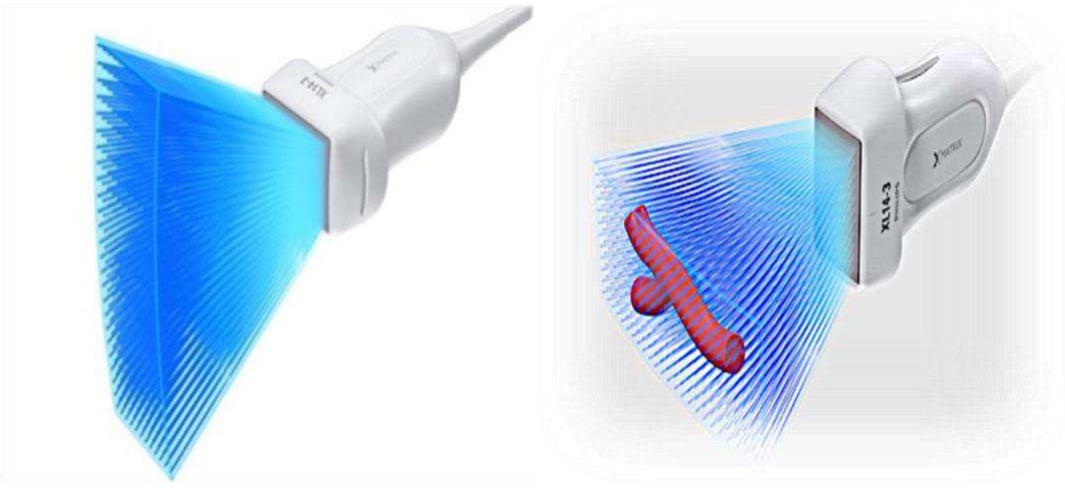

Figure 1. 6 An example of mechanical 3D probe (60).

1.6.2 3D and 4D Matrix Scanning

Electronically imaging solutions were created to avoid the need to move 2DUS transducers coupled to heavy mechanical arms around the anatomy. Matrix array transducers are a grid of a large number of PZT crystals aligned in both the lateral and elevational planes to produce non-real-time 3D volumes. Because of the large number of crystals in matrix probes multiplexing, signal processing and phasing of element excitation must be used to reduce the number of wires required to excite each crystal while keeping the transducer functioning (59,61). These methods can also allow matrix systems to analyse and show real-time 3D picture volumes, a technique known as 4D matrix imaging (61). 4D matrix scanning has been found to improve abdominal aortic aneurysm (AAA) diameter and volume evaluation over CT (61,62), as well as endoleak detection and visceral vessel revascularisation in fenestrated endovascular aortic repair (EVAR) (63). 3D and 4D volumes are typically shaped like a truncated pyramid. The transducer is electrically swept across all the PZT elements in 3D and 4D matrix scanning. The probe is held steady and generates a small 3D reconstruction with isotropic resolution. A fixed number of grid elements means a maximum fixed reconstruction size that can be less than the required anatomy. Choosing a suitably sized Matrix (e.g., 50 × 50 or 128 x 128 elements) is therefore critical, although, as with mechanical scanning,' stitching' numerous scans together is feasible to visualise the entire anatomy. Because matrix transducers are delicate and costly, high-volume reconstructions were not commercially possible until recently (64). Philips company has had commercial success with matrix transducers (61,62), but other companies are starting to catch up.

1.6.3 Freehand with Position Sensors

3DUS imaging using the freehand within vascular surgery has the most promise. Tracking sensors are fitted to a typical DUS transducer and allow the Sonographer to move the probe freely, hence the moniker "freehand." The DUS instrument must have a 3D software package installed or be linked to an external 3D system such as Curefab CS or Piur tUS. Freehand tracking methods are also as precise and dependable as mechanical systems (65). Sensors (Figure. 1.7) detect transducer position and orientation as they sweep over the body, annotating 2D image frames from a 2DUS scanner with space and time information. Based on this information, structures are recreated, allowing the volume to stay precise while giving the operator more discretion. Transducers can easily move over a vast area and past obstacles like bowel gas and acoustic shadowing, but the resolution is not isotopic. Various tracking technologies, including potentiometers, acoustic, magnetic (preferable due to greater freedom), and optical-based systems (most accurate), have been used (57).

Figure 1. 7 3DUS freehand sensor tracked system (66).

1.6.4 Freehand without Position Sensors

This approach has the same advantages as tracked systems, except that no location or orientation information is tagged to the DUS frames. It assumes a pre-defined scan distance, requiring a high level of operator expertise when scanning (57). Due to a lack of positional data, 3D volumetric reconstruction quality is inadequate; consequently, measurements cannot be made, but immediate reconstructions are produced (57). This results in qualitative images better suited for real-time imaging but with minimal diagnostic utility. Although this procedure does not require specialised hardware and can be performed with regular DUS transducers, it is rarely used in the literature. Because accuracy is critical in Vascular Surgery, this procedure is unlikely to acquire traction.

Thesis Aims:

The current ultrasound imaging technique using 2DUS, colour and spectral Doppler cannot provide satisfactory medical details in arterial geometry, even though details of anatomical and Doppler waveform analyses are provided. There is a lack of optimum, non-invasive imaging technology to assess arterial plaque volume at different angles, which requires further improvement in this model by using novel technology such as t3DUS for better imaging and treatment plans. Therefore, this study aims to assess the t3DUS accuracy and reliability for the assessment of vascular disease as well as correlating 2DUS with t3DUS for grading lower extremity arterial stenosis.

Thesis Hypothesis:

1) t3DUS is a better diagnostic tool than the 2DUS imaging modality for assessing vascular disease.
2) t3DUS is an accurate method for measuring carotid artery plaque volume.

Thesis Objectives:

- Conducting a literature review to better understand what has been published in 3DUS carotid plaque volume measurement.
- Performing a phantom study to evaluate the accuracy of t3DUS for grading stenosis, using the manufacturer's measurements as a gold standard.
- Comparison of conventional carotid arteries stenosis criteria with t3DUS plaque volume assessment.
- Comparison between 2DUS and t3DUS in the assessment of peripheral arteries for grading stenosis.

CHAPTER 2

GENERAL METHODOLOGY

2.1 Tomographic 3D Ultrasound:

t3DUS employs a freehand electromagnetic sensor tracking system that uses a frame-grab technique (Figure 2.1). Once the DUS scanner has been optimised for the anatomical area of interest, the transducer is swept over the vessel. The image is collected by the t3DUS computer but not in real-time. All equipment used is shown in (Figure 2.3). This technology can be applied to most commercially available ultrasound systems and employs software explicitly designed for vascular surgery. PIUR tUS medical set adds tomographic images based on the 2DUS available images. The 3D analysis of ultrasound data is comparable to CT or MRI medical imaging. Examining operators can use both 2D and 3D ultrasound data to generate the image, diagnose, and improve diagnostic image quality. t3DUS keeps the ability to visualise amid obscurity. The software has a mechanism for precisely computing volume, resulting in a high-accuracy geometric mesh. Certain elements, such as vessel detection and image presentation, are semi-automated and have manual error correction, reducing waiting times (replacing alternative imaging) and speeding up patient throughput. This is the only system currently available with this capability, designed explicitly for Vascular Surgery.

An Internal Measurement Unit (IMU) sensor attached to the transducer and tracks the ultrasonic probe during a free-hand scan generates the high-resolution t3D digital information. Bluetooth technology is used to transmit the data received from the sensor during the scan to a small box that works as a control unit. The ultrasound images are continuously transmitted to the PIUR tUS Infinity box through the ultrasound scanning machine's video output and wirelessly transmitted to the control unit via a Wi-Fi connection before the scan. The system determines the 3D volume based on these two data. All essential

points required for data creation, including frame rate, depth, and the ultrasound transducer, are automatically recognised, analysed, and transferred to the computer through Wi-Fi from the video signal.

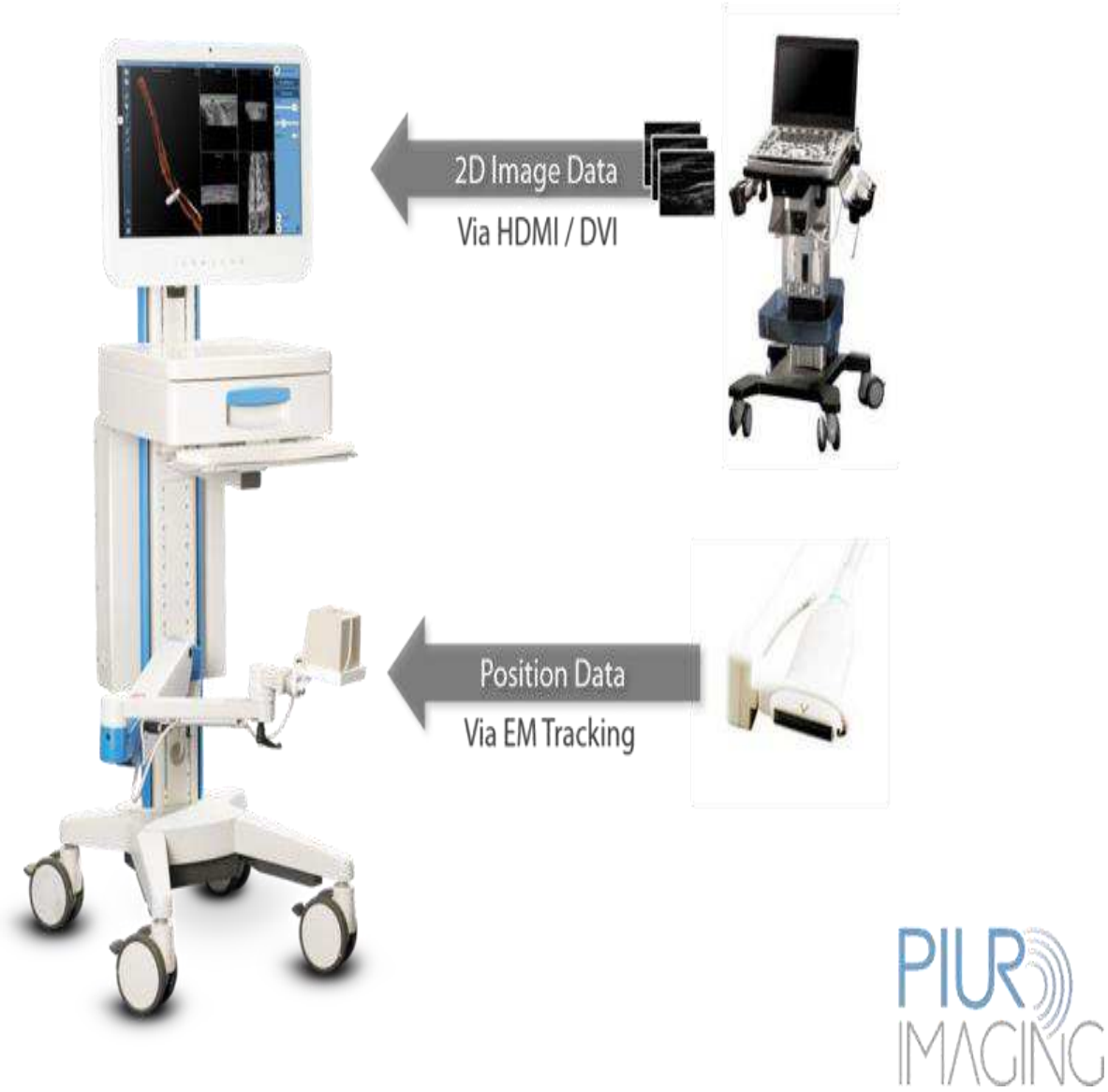

Figure 2. 1 Piur imaging tomographic 3DUS electromagnetically tracked device. Reproduced with permission of PIUR imaging GmbH) (66).

Figure 2. 2 PIUR t3DUS Infinity system setup (66).

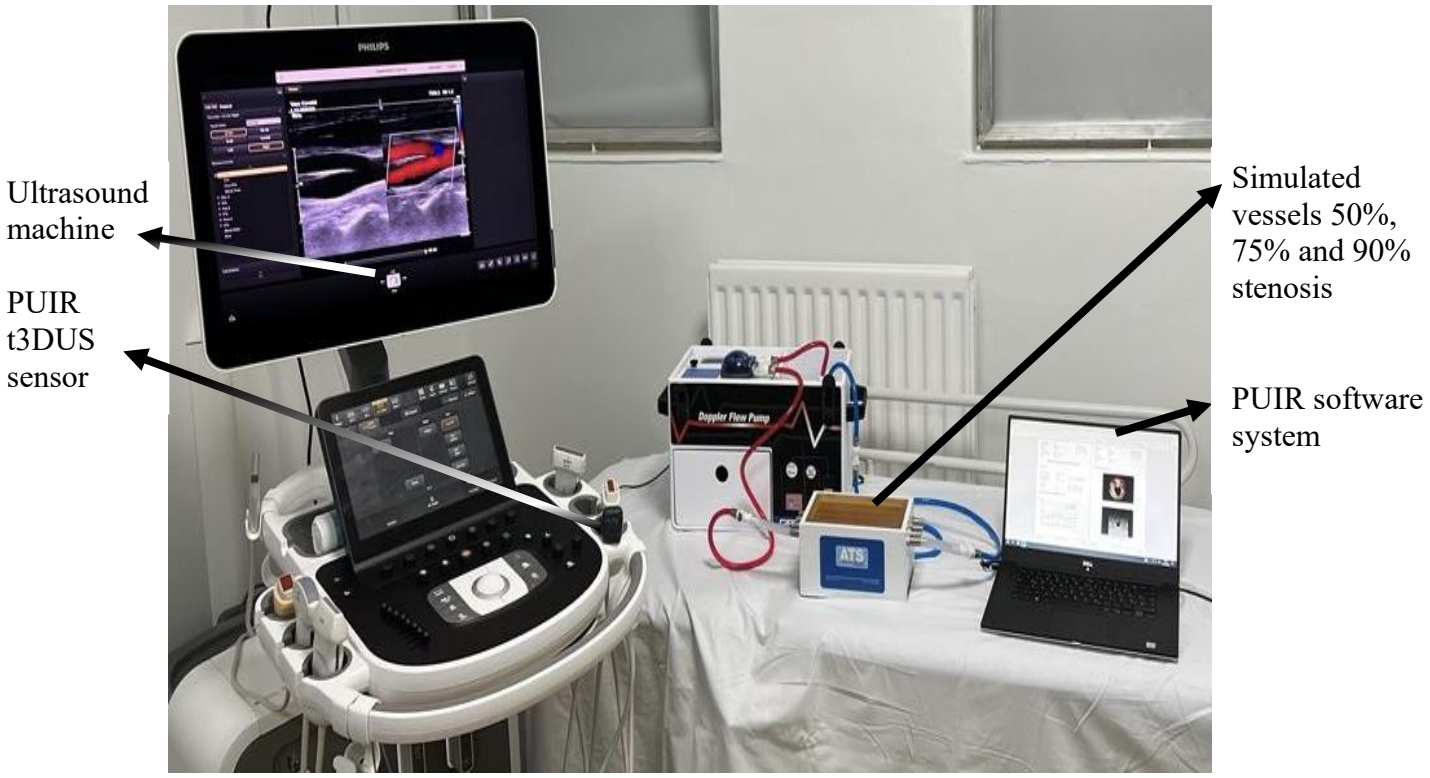

Figure 2. 3 illustrates the equipment used in the present studies.

2.2 Phantom:

The phantom used in the study was created with specific requirements and designs that suit the research aims. It was made to provide valid data for assessing a new medical device's accuracy, reliability, and repeatability. The phantom was made of a rubber-based substance resembling blood vessels and the surrounding tissue. This substance increases the operational life of the phantom by avoiding usage complications associated with (water-based) gel, which is usually applied to the phantoms. These complications include melting, freezing, and surface damage. The phantom's longevity, quality, and dependability last for approximately three years by overcoming these issues.

Temperature fluctuations affect the acoustic characteristics of all non-biological and biological materials. In most diagnostic imaging systems and vessels, tissue-simulating phantoms are calibrated at 23°C; it is the room temperature where the phantom is kept. To achieve accurate measurements, ATS attaches a thermometer strip to the exterior surface of the phantom and clearly shows the room temperature changes.

The simulated vessels used were initially designed by the researcher to simulate blood flow. The manufactory company collaborated with the researcher to make a suitable tissue-mimicking phantom with appropriate and accurate simulated vessels with different stenosis grades. The first simulated vessel was clear with no stenosis, which is to set the pumper within the normal velocity range. The second simulated vessel was made with 50% stenosis, which is considered the luminal significance borderline. The third simulated vessel was made of 75% stenosis, which is considered a significant stenosis. The last simulate vessel was made of 90%,

which reflects near occlusion stenosis. The simulated vessels were made based on engineering precision and the flow pump supports routine Doppler quality assurance measurements of velocity accuracy, directional accuracy, sample volume accuracy and sensitivity (Appendix A).

2.2.1 In Vitro phantom study

Simulated vessels in a 525-model phantom, produced by Computerised Imaging Reference Systems, Inc. (CIRS, Norfolk, Virginia, USA), were used for establishing a baseline and evaluating intra-inter-observer variation. The four simulated vessels were initially drawn and sent to the company to exemplify this study's aim (Figure 2.4). The phantom was then made with different grades of stenosis, as requested. There was no difference between simulated vessel size, length, and stenosis length for more accuracy. The first one was made clear with no stenosis, whilst the second was made with 50% stenosis. The third simulated vessel was made with 70% stenosis, and the fourth was made with 90% stenosis (Figure 2.5).

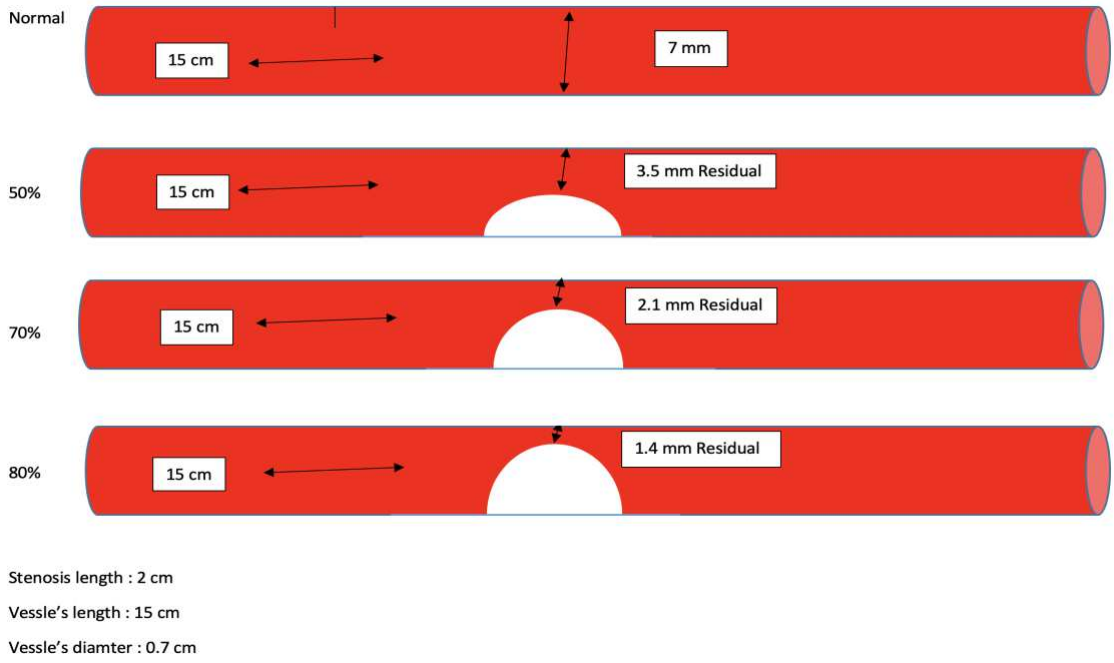

Figure 2. 4 Initial drawing for the simulated vessels requested.

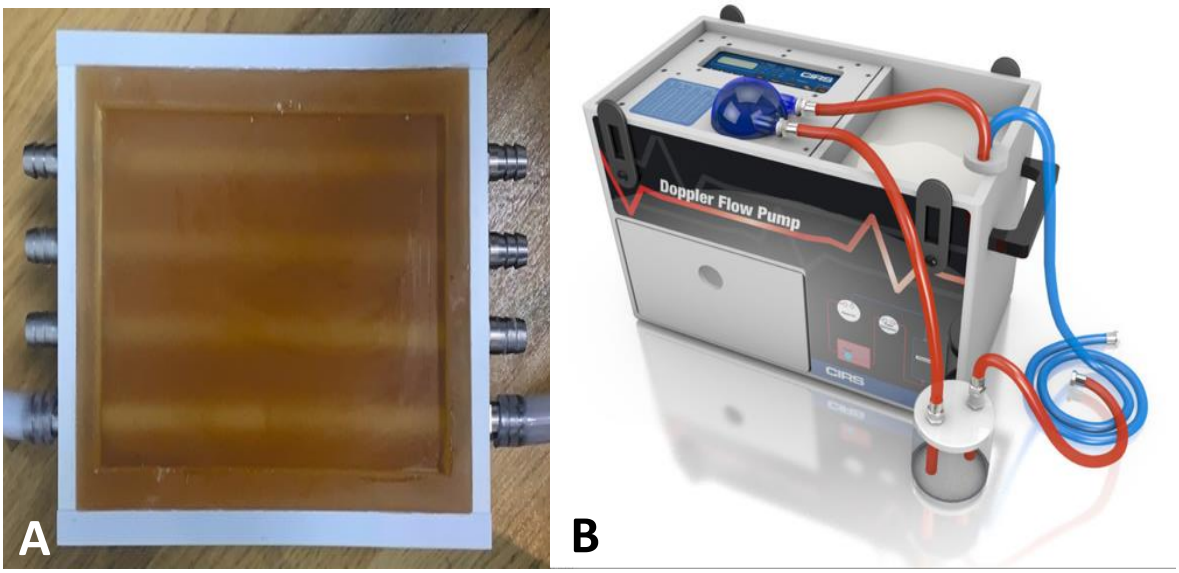

Figure 2. 5 simulated vessels requested with a Doppler flow pump. (A): Simulated vessels with different grades of stenosis (B): Doppler flow pump (67).

For intra-observer agreement, the researcher assessed each simulated vessel above several times "99" using three ultrasound modes on a high-resolution premium Philips Elite ultrasound imaging system (Philips Healthcare, Bothell, WA, USA). The modes used are

brightness mode, also known as B mode, colour Doppler mode and pulse wave mode. All three simulated vessels were measured using the area reduction method in transverse. In longitudinal, all simulated vessels were measured using a diameter reduction. Following the 2DUS scans, a t3DUS scan was performed using t3DUS (PIUR imaging GmbH, Vienna, Austria) imaging techniques. The package of the t3DUS is a small sensor, smart Wi-Fi box and Dell laptop for analysis of the picture taken. For both 2DUS and t3DUS, the same ultrasound machine setting was used. The images were taken in transverse for 2DUS and t3DUS scans. For inter-observer agreement, two senior vascular scientists from Hammersmith vascular laboratory were involved and assessed the vessels “33” times for more accuracy.

2.3 Clinical Studies:

This research aimed to assess four different vascular areas: Carotid artery, arteriovenous Fistula (AVF), Superficial veins and lower limb arteries. Based on the statistical power calculation, a total number of 38 participants is required for each group. As this research was conducted during Covid-19 crisis, the initial plan has been changed due to lack of data as less participants were able to attend their appointments. Hence, a new plan was created based on participants ability to attend and two of the initial four groups were recruited which re 31 Carotid arteries and 50 participants for the lower limb arterial studies. Six participants of Carotid plaques endarterectomy were excluded as plaques were not fully extracted.

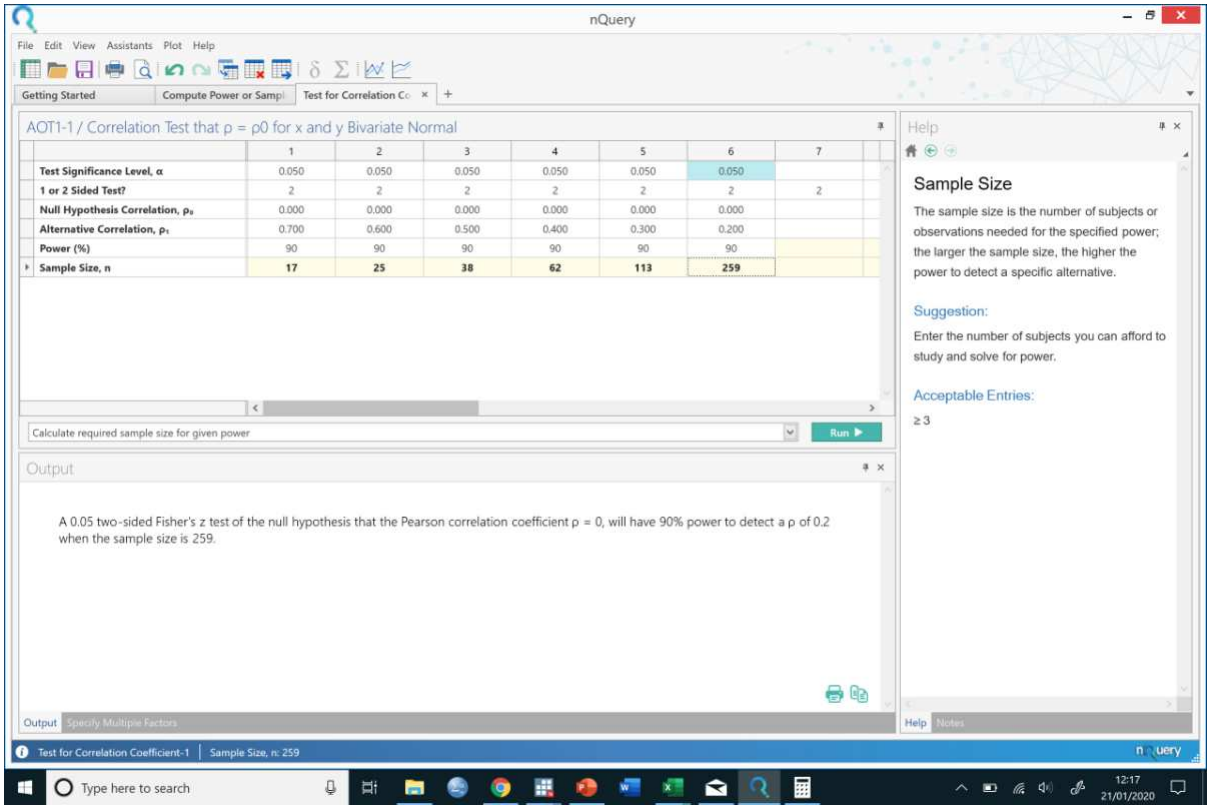

In this research, the equipment used was Philips EPIQ 7 ultrasound machine (high-resolution premium Philips Elite ultrasound imaging system (Philips Healthcare, Bothell, WA, USA). Philips L12-4 for ClearVue Broadband linear array transducer with a Frequency range of 12-4 MHz was used for scanning. And PUIR t3DUS system (PIUR imaging GmbH, Vienna, Austria).

This study has been approved and gained ethical approval from the Health Research Authority (HRA) and Health and Care Research Wales (HCRW) under number 20/LO/0814. The study was registered (NCT04318171) with the US National Library of Medicine clinical trial.

2.3.1 Carotid Plaque Volume

A total of 25 patients were recruited. Patients were fully aware of the research aims, and written consent was obtained. The participants attended their pre-operation routine scan. The nationally approved protocol was followed as the following:

The patients were made aware of the scan's steps, and the assessment was explained. The examiner used his right hand to scan both the right and left carotid arteries.

After confirming the patients' identification, they were asked to expose the neck area and lie on their backs on the couch. The patients were also asked to turn their heads away from the side being assessed to ensure maximum access to the vessels to be examined with good access. Dignity and privacy were always maintained.

Bilateral CCA, carotid bifurcation, ECA and ICA were assessed using a B-mode in transverse view. The scan started from the proximal segment of the CCA to the very distal level of the ICA bilaterally. Followed by scanning the same vessels in longitudinal view in a colour mode from the proximal level of the CCA to the distal ICA level bilaterally. The pulse wave mode was then applied, and a peak systolic velocity was recorded from the CCA proximally, mid-level and distally. The ICA Peak systolic velocity (PSV) was also taken from the proximal level within the stenotic area and distally. ECA was also assessed, and a PSV was recorded. The VA was identified, and the direction of flow was confirmed. The PSV within the VA was documented.

During the pulse wave measurements, the spectral Doppler angle was maintained between 45-60 degrees. PSV and end-diastolic velocities (EDV) were measured and documented in all vessels mentioned above.

Following the routine Duplex assessment, PIUR t3DUS Infinity CND/EMDN: Z110690 Various Digital Bioimaging Management Instruments were attached to the transducer to produce a 3D image Using the exact pre-set. The product also complies with RoHS directive 2011/65/EU.

The patients were scanned from the proximal CCA to the distal level. Particularly, ICA was scanned, and the stenotic area was recorded. The system automatically produces the report after adjusting the measurement lines.

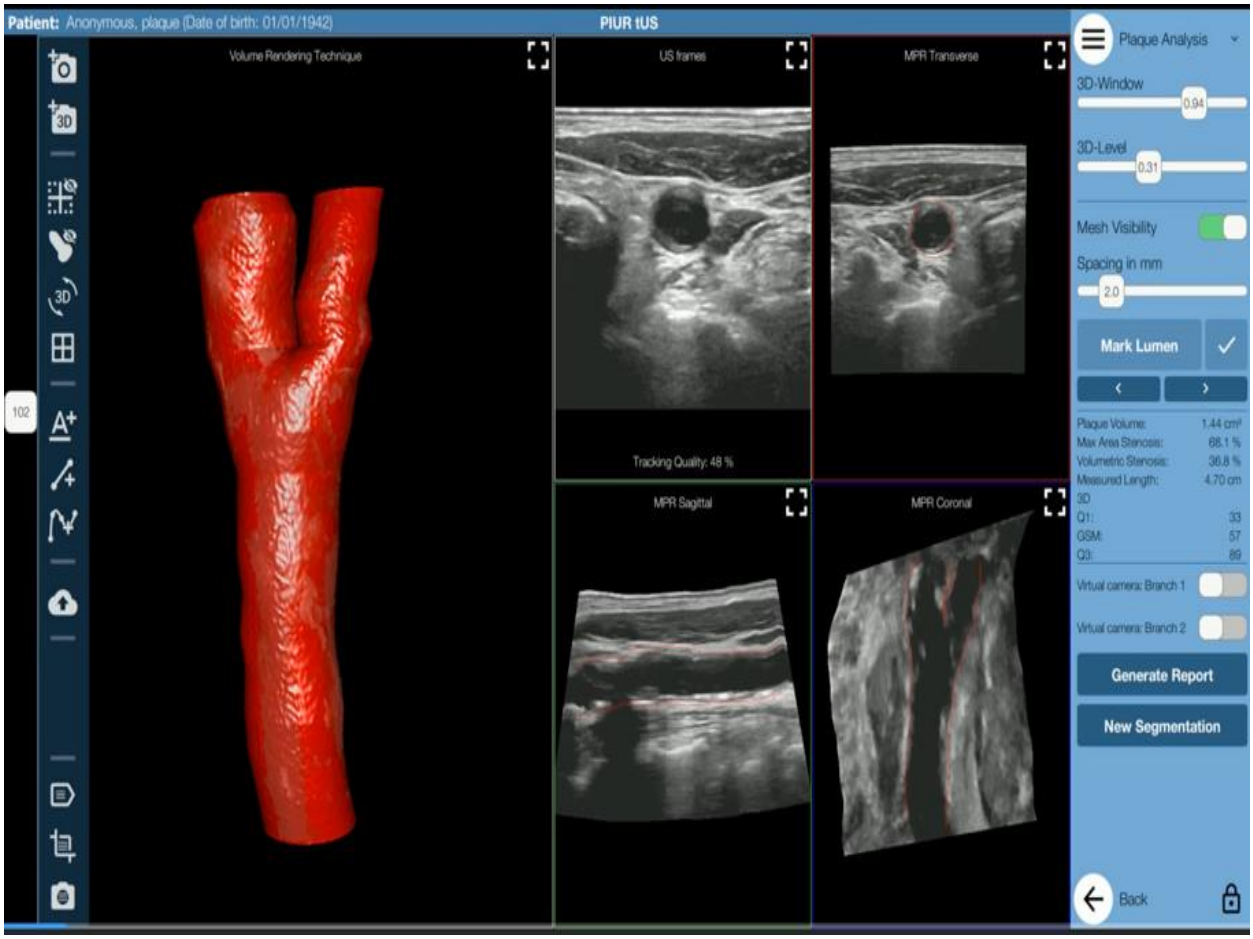

Figure 2. 6 An example of the report generated from PUIR.

The system produces five different parameters, which are:

- Plaque volume.
- Max area stenosis.
- Volumetric stenosis.
- Measured length.
- Grayscale median.

When the patients underwent their CEA within 48 hours of the scan, the surgeon was aware of the research investigation; the researcher was presented to collect the plaque specimen immediately. The specimens were collected and taken in a sterilised medical container (Figure 2.7). Each patient's specimens were measured using ergonomically designed MICROMAN E positive displacement pipettes and compared to the t3DUS plaque volume measurement pre-CEA to assess the accuracy of t3DUS compared to actual plaque volume.

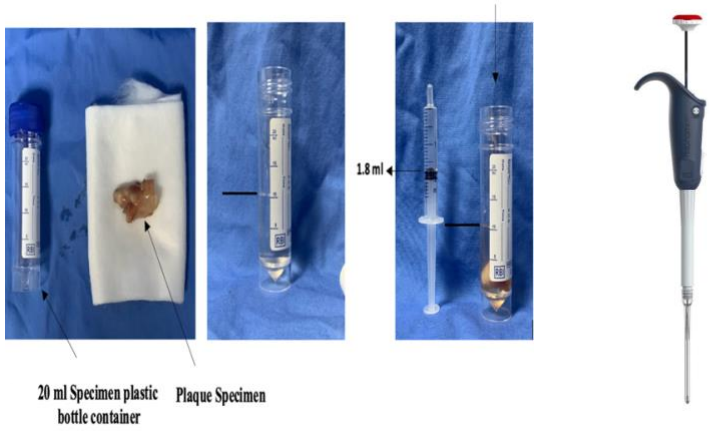

Figure 2. 7 An example of measuring CPV using the displacement method.

2.3.2 Peripheral Arterial Disease Study

Fifty patients were recruited for this study. The patients presented with different arterial symptoms, including intermittent claudication, acute limb ischemia and critical limb ischemia. The patient had their normal Duplex assessment using the same equipment mentioned earlier, followed by t3DUS to scan the SFA.

Nationally approved protocol for assessing the lower limb arterial Duplex followed. In a B mode and transverse view, the Micky mouse view, which consists of the Common Femoral Artery (CFA), long saphenous vein (LSV) and common femoral vein (CFV), was identified as a landmark to start the scan. The colour mode applied to assess CFA, Profunda Femoris Artery (PFA), SFA, Popliteal Artery, Posterior Tibial Artery (PTA), Anterior Tibial Artery (ATA), Peroneal Artery (PL) and Dorsalis Pedis Artery (DPA). Stenosis was graded based on the current Duplex criteria (Table 2.1).

STENOSIS (%)	VR (PSV AT STENOSIS / PSV PROXIMAL TO STENOSIS)
20%–49%	1.5–2
50%–80%	2–4
>80%	>4

Table 2. 1 Current Duplex criteria for grading arterial stenosis (68) .

When the traditional scan was done, t3DUS was used to assess stenosis in the SFA. Using the same pre-set and without moving the patient. The SFA was assessed from the proximal to above the knee level. The stenotic area was recorded, and the grade of stenosis was calculated by the system.

CHAPTER 3

3-DIMENSIONAL ULTRASOUND FOR THE ASSESSMENT OF CAROTID ARTERY DISEASE: LITERATURE REVIEW

3.1 Introduction:

3.1.1 Background

Carotid Artery disease arises due to damage to the endothelium, which mainly develops plaque in carotid arteries. The plaque's nature, as well as its composition and haemodynamic effects, enhances the risk of stroke as well as Transit Ischemic Attach (TIA). Besides this, various other methods like 2DUS is also in use for several years for determining the carotid disease extent with the help of velocity criteria or diameter reduction; however, it is also quite evident that 2DUS possesses a wide range of limitations. Additionally, 3DUS is a new technology that focuses on obtaining as well as assembling 2DUS slices in 3DUS reconstruction with the help of computer software. The aim of the literature review is to gain information from a wide range of scholarly journal articles about the use of 3DUS for the purpose of assessing carotid artery disease.

3.1.2 Method

A literature review was performed using the standard academic database Ovid MEDLINE to collect studies and exclude papers that fail to match eligibility criteria. A total of 102 papers have been reviewed, and only 23 papers have been considered in the review.

3.1.3 Result

The results indicate that 3DUS specificity and sensitivity report high 3DUS pertaining to the detection of high grades of stenosis. Additionally, the variability among observers is relatively

low. 3DUS enables characterising plaques through surface morphology, which is quite beneficial for therapeutics' response and identification of ulcerated plaques. The key advantage associated with 3DUS is fewer scan times. However, using different segmentation techniques might raise the possibility of extending the scan length. Further, no specific guideline related to the plaque using 3DUS for treatment plans exists. 3D reconstruction can be seen as the best and most useful method for visualising carotid disease and eliminating any variability that 2DUS has introduced. This can be favourable for interdisciplinary decisions as it helps provide disease visualisation in a better manner.

Carotid artery plaque prevalence was estimated to be 2.2% in the study carried out in the year 2009 (69). However, the age of 70 has significantly increased in past years. De Weerd et al. (70) also used a meta-analysis in Norway, which showed that the prevalence of carotid stenosis within the general population was 3.1%, with an annual stroke risk of between 2% and 5%. The main causes of such diseases include high cholesterol, diabetes, lack of exercise, smoking, and other factors. Besides this, the atherosclerosis family history can also be seen as one of the key risk factors (69).

The dysfunction in the endothelium is the key reason behind plaque formation. The key risk factors that were attached to such type of damage cover smoke, high cholesterol, hyperglycaemia, and others. Such risk factors are mainly attached to a harmful or unhealthy lifestyle. The plaque occurs at carotid bifurcation as it makes significant changes in blood flow haemodynamic. Additionally, the meeting of laminar blood flow with carotid emerges a new profile, wherein external bifurcation walls are mainly exposed to a high level of shear stress (71). The low shear stress is also attached to increased atherosclerosis. This is because

endothelial cells exposed to reduced shear stress have a more rounded shape (72). The plaque, as well as thrombus formation, are also the most common pathology that are mostly seen at the carotid bifurcation.

The endothelium intima damage mainly causes immune cell migration, like immune cells proliferation to macrophages as well as monocytes. The Oxidised Low-Density Lipoproteins form inside macrophages. Besides this, fatty streaks also formed in the inner intima (73). The development of fatty streaks takes quite a long period to build and thereby causes intima thickening. The tunica smooth muscle cells migrate in endothelium for the purpose of producing collagen that creates a fibrous cap on the plaque. It is also quite evident that the formation of plaque, as well as the thickening of intima-media, increased with increased age. Additionally, it has also been identified that endothelium damage was the key reason for collagen destruction in fibrous caps. Once broken, it releases signals and starts a clotting cascade, forming a thrombus inside the vessel (74).

The plaque also has a different composition, like calcified, fatty, and ulcerative. All such compositions cause vessel stenosis, which results in a reduction in cerebral vessels' blood flow. Besides this, it is also quite vulnerable to rupture of both fatty as well as ulcerative plaques. In case of the formation of a thrombus and rupturing of plaque, clots can travel upstream and shed off cerebral arteries, which can be seen as one of the key causes of blockages (75).

The arterial disease, mainly in the carotid artery, is caused by significant stenosis or occlusion. A partial or complete arterial blockage in one of the cerebral arteries. This is because of

embolism as well as stenotic areas caused by plaque. The data also revealed that carotid artery stenosis and occlusion are the main two aspects responsible for almost 15% of ischemic strokes (76). Hemiparasthesia, amaurosis fugax, hemiparalysis, and others are key symptoms of a stroke. Besides, the TIA, known as mini-stroke, mainly arises due to blockage in cerebral arteries on a temporary basis. The patient, in this case, shows neuralgic symptoms, which can last from a few minutes to a maximum of twenty-four hours (77). Additionally, it has also been identified that TIAs can be seen as solid predictors for strokes. Furthermore, data also revealed that almost 25% of patients that have experienced or faced TIA previously might have a large number of chances of getting a major stroke within a time span of one year (78).

3.2 Search Strategy and Method of Selection:

A literature review was performed using the standard academic database Ovid MEDLINE to fulfil objective 1 of this study. Relevant papers that effectively track the application and disease visualisation outcomes of using 3DUS in assessing CAD compared to 2DUS and other angiography techniques were retrieved from 1998 to 2017. The search strategies were conducted following Boolean Algorithm and were assessed by a subject librarian (Table 3.1).

#	SEARCH STRATEGY	RESULTS
1	exp Ultrasonography/	436859
2	"ultraso*".m_titl.	146484
3	"sonograph*".m_titl.	21401
4	1 or 2 or 3	485847
5	three dimensional.m_titl.	48313
6	three-dimensional.m_titl.	48313
7	3D.m_titl.	42379
8	5 or 6 or 7	90095
9	exp Carotid Arteries/	58694
10	carotid.m_titl.	55949
11	9 or 10	85204
12	exp Carotid Artery Diseases/	47512
13	exp Carotid Stenosis/	15835
14	(Plaque adj5 volume).m_titl.	157
15	stenosis.m_titl.	54589
16	12 or 13 or 14 or 15	97845
17	4 AND 8 AND 11 AND 16	102

Table 3. 1 Boolean Algorithm used for literature search in Ovid MEDLINE database.

3.3 Criteria for Eligibility:

The search process included human studies and peer-reviewed journal articles. Papers were included if they fulfilled the main objectives of this study which are, plaque volume measurements, comparison of stenosis degree between two different medical imaging modalities and the changes in the carotid plaque morphology. Articles were excluded if they were review articles, not available in full text, or published in languages other than English.

A two-step process has been followed to achieve comprehensive and credible findings, as outlined in (Figure 3.1.) In the first process, the significance of abstracts and titles of the papers have been screened in alignment with the research topic under investigation. In this

process, a total of 73 papers were eliminated, and 29 papers were selected for further screening. Moreover, in the second step, the screening of all 29 papers was done based on the criteria discussed above. Based on this screening, 23 papers were found most authentic and relevant to be included in the present research for review.

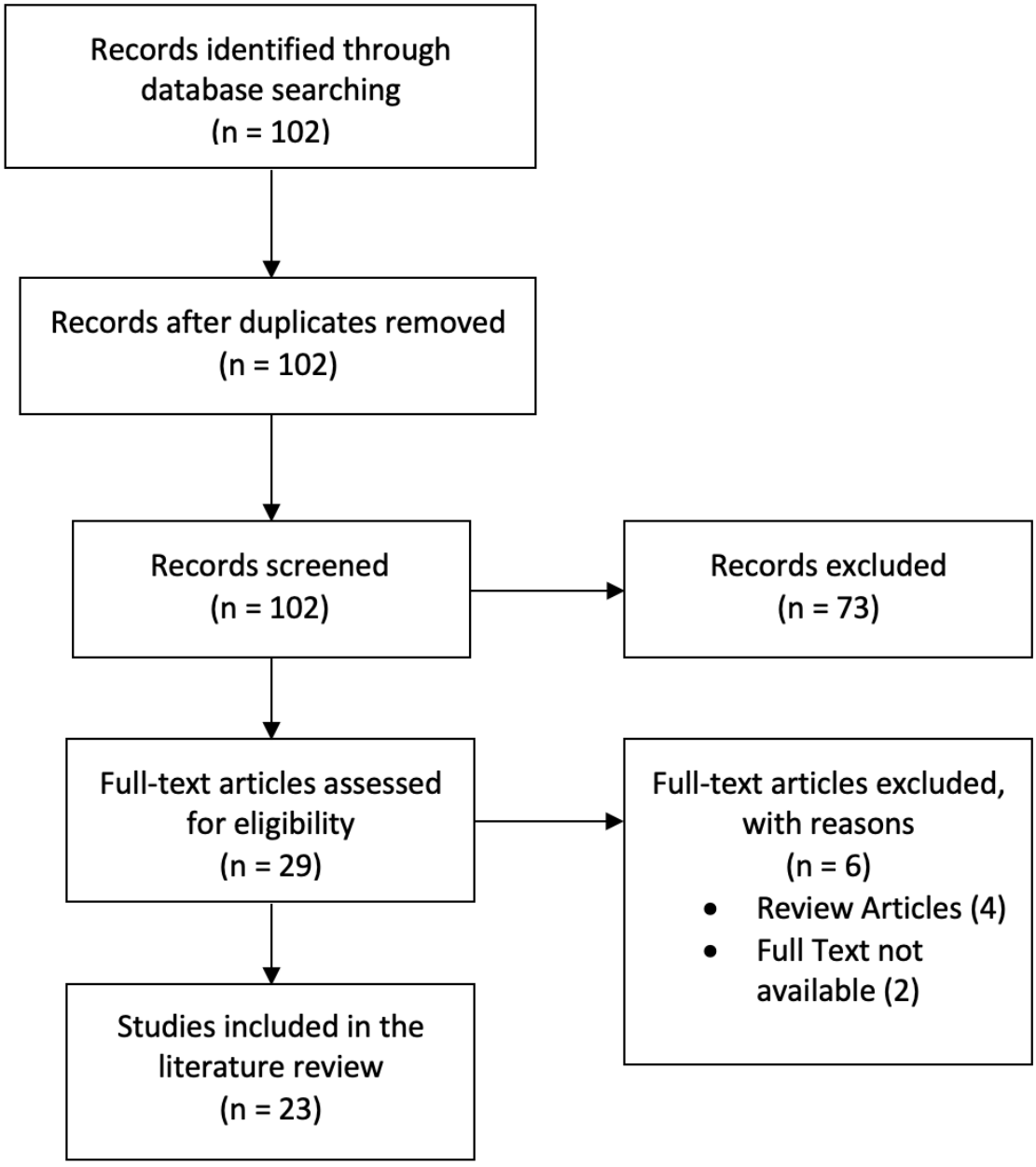

Figure 3. 1 Articles Screening Process.

3.4 Results:

The database search identified a total of 102 papers relevant to the present research. The search has not identified duplicate papers. Twenty-three studies were included in the literature review and are listed in table 3.2.

Table 3.2 Results of literature search.

REFERENCE	TITLE	3D TECHNOLOGY	OBJECTIVE
(Palombo et al., 1998)(79)	Ultrafast three-dimensional ultrasound: application to carotid artery imaging.	Motorised linear array 7.5/10 MHz, swept up to 65°	Plaque volume measurement by 3DUS in phantoms compared with true volume.
(Yao et al., 1998) (80)	Three-dimensional ultrasound study of carotid arteries before and after endarterectomy; analysis of stenotic lesions and surgical impact on the vessel.	Motorised linear array 7.5/10 MHz, swept up to 65°	Carotid stenosis measured by 3DUS compared with angiography results.
(Schminke et al., 2000) (81)	Three-dimensional ultrasound observation of carotid artery plaque ulceration.	Motorised linear array 5MHz – TOMTEC 'Echoscan'	Ulcerative plaque progression/regression.
(Kozakova et al., 2001) (82)	Quantification of extracranial carotid artery stenosis by ultrafast three-dimensional ultrasound.	Motorised linear array 7.5/10 MHz, swept up to 6°	Area reduction and diagnostic value by 3DUScompared with carotid angiography.
(Tetickovic et al., 2001) (43)	Three-dimensional ultrasonography for the evaluation of atherosclerotic stenoses of the carotid trunk.	Mechanical linear array 5-10 MHz	3DUS and angiography comparison.

Continue: Table 3. 3

REFERENCE	TITLE	3D TECHNOLOGY	OBJECTIVE
(Landry and Fenster, 2002) (83)	Theoretical and experimental quantification of carotid plaque volume measurements made by three-dimensional ultrasound using test phantoms.	Motorised linear array 4-7MHz	Accuracy of 3DUS plaque volume measurements using plaque phantoms
(Bucek et al, 2003) (84)	Three-dimensional colour Doppler sonography in carotid artery stenosis.	Freehand Linear array 5-10MHz fitted with electromagnetic tracking system -'Echotech'	Percentage stenosis and diagnostic value 3DUS and angiographic comparison.
(Wessels et al., 2004) (85)	Three-dimensional assessment of extracranial Doppler sonography in carotid artery stenosis compared with digital subtraction angiography.	Freehand linear array 5-10MHz fitted with electromagnetic tracking system – 'Echotech'	Comparing stenotic degree by 3DUS and DSA
(Ainsworth et al., 2005) (86)	3D ultrasound measurement of change in carotid plaque volume: a tool for rapid evaluation of new therapies.	Motorised linear array 5-12MHz – 'Life Imaging Systems'.	Change in plaque volume in response to antiatherosclerotic therapy measured by 3DUS
(Landry et al., 2005) (87)	Quantification of carotid plaque volume measurements using 3D ultrasound imaging.	Motorised linear array 5-12MHz – 'Life Imaging Systems'.	Inter and intra-observer variability of 3DUS plaque volume measurements.

Continue Table 3. 4

REFERENCE	TITLE	3D TECHNOLOGY	OBJECTIVE
(Egger et al., 2007) (88)	Validation of 3D ultrasound vessel wall volume: an imaging phenotype of carotid atherosclerosis.	Motorised linear array 5-12MHz.	Inter and intra-observer variability of 3DUS plaque volume measurements.
(Chiu et al., 2008) (89)	Quantification of carotid vessel wall and plaque thickness change using 3D ultrasound images.	-	Analyse changes in morphology of carotid plaque.
(Krasinski et al., 2009) (90)	Magnetic resonance imaging and three-dimensional ultrasound of carotid atherosclerosis: mapping regional differences.	Mechanical linear array 5-12MHz – 'ATL-HDI 5000 Philips'	VWV measured by 3DUS and MRI comparison.
(Krasinski et al., 2009) (91)	Three-dimensional ultrasound quantification of intensive statin treatment of carotid atherosclerosis.	Mechanical linear array 5-12MHz – 'ATL-HDI 5000 Philips'	VWV changes in response to statin treatment measured by 3DUS.
(Kalashyan et al., 2013) (92)	Comprehensive and rapid assessment of carotid plaques in acute stroke using a new single sweep method for three-dimensional carotid ultrasound.	Volumetric single sweep linear transducer 5-13MHz.	Plaque volume accuracy case study with new single sweep technology

Continue Table 3. 5

REFERENCE	TITLE	3D TECHNOLOGY	OBJECTIVE
(Kalashyan et al., 2014) (93)	Single sweep three-dimensional carotid ultrasound: reproducibility in plaque and artery volume measurements	Volumetric single sweep linear transducer 5-13MHz	Reproducibility of new single sweep technology
(Van engelen et al., 2014) (94)	Three-dimensional carotid ultrasound plaque texture predicts vascular events	Freehand Linear array 5-12MHz – '3DEchotech'	Changes in plaque volume and texture after one year measured by 3DUS
(Almhanna et al., 2015) (95)	Carotid plaque morphometric assessment with three-dimensional ultrasound imaging.	Motorised linear array 5-14MHz	Inter and intra-observer variability of 3DUS measurement of VWV.
(Kumar et al., 2016) (96)	Plaque Volume of Carotid Endarterectomy Specimens Measured by 3D Ultrasound Technology	Freehand Linear array fitted with electromagnetic tracking system.	Comparing plaque volume after CEA by 3DUS with MRI true volume.
(Leong et al., 2016) (97)	Observer performance in characterization of carotid plaque texture and surface characteristics with 3D versus 2D ultrasound.	Motorised linear array 5-13MHz.	Reproducibility of plaque characterisation using 3DUS images.

Continue Table 3. 6

REFERENCE	TITLE	3D TECHNOLOGY	OBJECTIVE
(Kalashyan et al., 2017) (98)	Three-Dimensional and Conventional Carotid Ultrasound for Assessment of Carotid Plaque in a Stroke Patient: A Simple Way to Validate Findings.	Volumetric single sweep linear transducer 5-13MHz	Comparison of 3DUS plaque volume with true volume measured by endarterectomy following CEA.
(Khan et al., 2017) (99)	Semiautomatic quantification of carotid plaque volume with three-dimensional ultrasound imaging.	Motorised linear array 5-14MHz	Accuracy and reliability of semi-automatic segmentation technique for 3DUS.
(Pelz et al., 2017) (100)	Evaluation of Freehand B-Mode and Power-Mode 3D Ultrasound for Visualisation and Grading of Internal Carotid Artery Stenosis.	Freehand Linear array 13MHz – 'Curefab'	Degree of stenosis of 2DUS compared with 3DUS.

3.5 Interobserver and Intraobserver Variability:

The intraobserver and interobserver variability are crucial parameters for the assessment using new technologies for diagnosis. In a Vivo study conducted on a group of 33 patients with more than 50% stenosis plaque to measure carotid plaque volume, an assessment of intraobserver variability was carried out via repeated plaque volume measurements on a monthly basis. Further, interobserver variability was measured among 12 patients. The findings indicate a mean volume of carotid plaque by observer 1 of 109.4mm^3 +/- 101.4$mm^3$and by observer 2 of 109.7 mm^3+/-104.2mm^3 with a correlation of 0.99 and $p<0.01$. Further, the mean difference measured by a similar observer under the study was -1.44+/- 6.2mm^3 for intraobserver variability (79).

A study conducted by Landry et al. (101) with the help of individual and multiple observers in measuring Vivo plaque volumes exhibited new results. The measurement was repeated 5 times by 5 observers concerning 40 carotid plaques. The range of 37.43mm^3-604.10mm^3 concerning plaque volume was determined, and interobserver variance reflected an outcome of 24.1%-2.2% scope, respectively. The same study calculated plaque volumes using intraobserver variability that ranged between 1.9% to 19.2%, respectively, for the research problem (101). The findings of the study suggest that larger plaques can be identified easily as data exhibit an increase in plaque volume as variability decreases. Furthermore, the boundaries can be perceived similarly between repeat scans and observers.

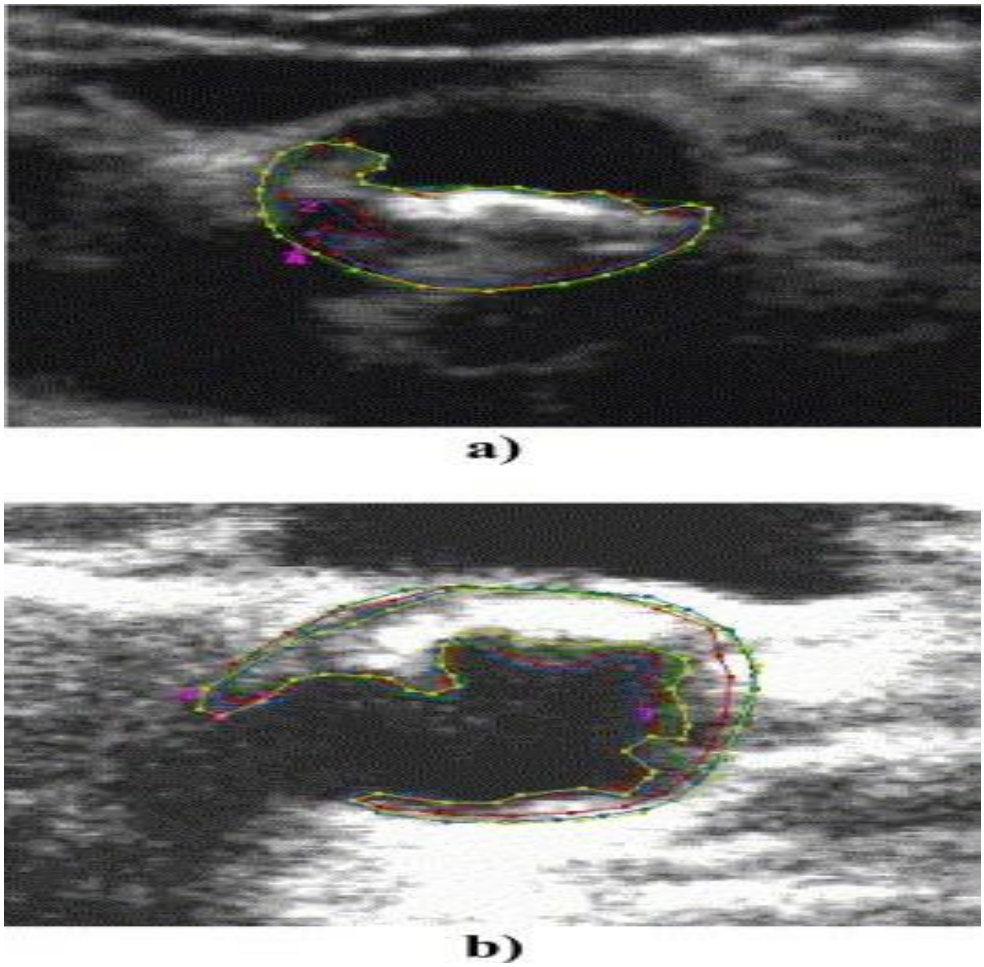

Figure 3. 2 Determining variability of manual plaque outlining technique. a) multiple observer study, each colour represents one of 5 different observers b) single observer study each colour represents a different attempt (87).

Furthermore, the same study conducted a repeated scan; wherein a single observer undertook repeated measurements five times concerning the plaque volume of 10 carotid plaques. This study classified plaque as an intima-media-thickness of <1.0mm. However, the study discussed limitations such as difficulty in determining plaque boundaries due to shadows on the image produced by ultrasound and differences in perceptions of individuals on the image that might explain the very existence of variability. The study concluded that interobserver variability was 6.9%, whereas intraobserver variability was 6.5%, indicating reliable outcomes (101). These outcomes can be supported with the help of other studies that indicate sound plaque volume variability concerning interobserver and intraobserver

methods via 3DUS technology (82,85). Wessels et al. (85) studied 65 patients with ICA stenosis aged between 64 and 75 years to establish the diagnostic effectiveness of 3DUS. The study reconstructed 62 ICA patients with 3DUS. However, as noted in previous studies, extensive calcification and acoustical shadowing hindered reliable 3DUS construction in 2 patients. The results showed reliable interobserver agreement since the K-coefficient was 0.88 (85). The Mean sensitivity of 3DUS was 93%, whereas the mean specificity was 82.5%. The mean positive and negative predictive values were 82% and 98%, respectively. Therefore, the results also show reliable reproducibility of 3DUS technologies.

The findings of Wessels et al. (85) are closely related to those of Kozakova et al. (82) who studied sixty-nine stenotic lesions of the extracranial carotid artery using both carotid angiography and 3DUS technology. Besides showing a high reproducibility and reliable variability between interobserver and intraobserver values, the results also showed that 3DUS exhibited higher values of specificity (77.7%), sensitivity (96.0%), diagnostic accuracy (88.3%), and positive predictive value of ≥70%.

The Vivo study of Kumar et al. (96) also applied 3DUS, MRI, and true volume analyses (TVA) on a sample of 20 CEA patients to assess reproducibility. Reproducibility analysis was undertaken using one observer to assess all volumes, whereas another investigator analysed a subset of 3DUS volumes. The interclass coefficient between observers was 0.98 (95% CI: 0.91 to 0.99). Hence 3DUS reproducibility was reliable. The results also reported higher validity, accuracy, and reliability values for 3DUS compared to MRI and TVA. Compared to other studies assessing volume measurement. The findings of Kumar et al. (96) were reliable because plaque samples irregular and heterogeneous were used instead of phantoms.

Additionally, excellent interobserver and intraobserver variability results were reflected by volume under the Vivo plaque length indicating high reproducibility of the methods (80).

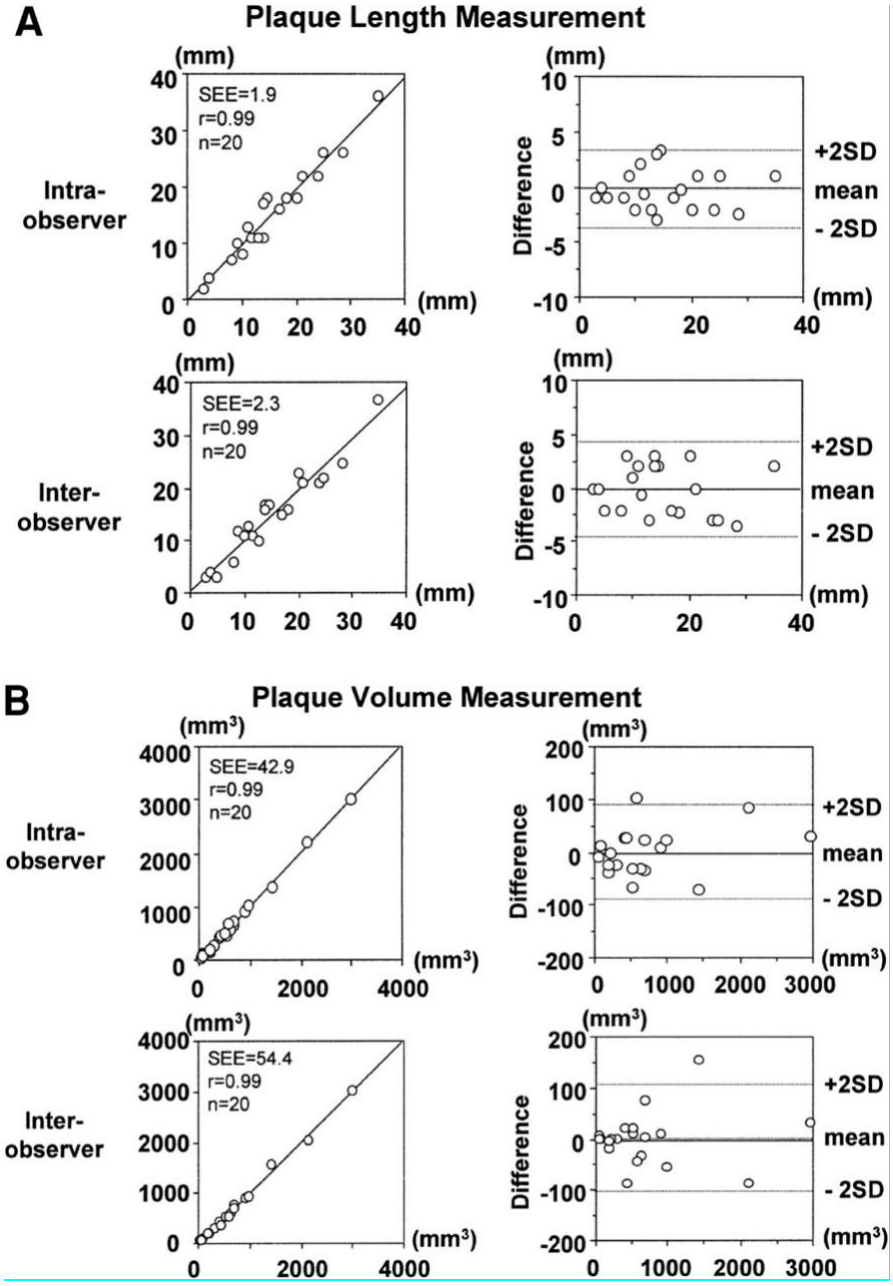

Figure 3. 3 interobserver and intraobserver variability while measuring plaque volume and plaque length.

The disease visualisation efficacy of 3DUS, in comparison to carotid angiography, is also shown by the ability to visualise regression and progression of the plaque, as demonstrated by Yao et al. (80) who applied both carotid angiography and 3DUS to 14 patients to establish regional vessel volume and cross-sectional area changes after endarterectomy. In patients with suture closure, the study concluded that the segmental vessel volume and the cross-sectional area did not exhibit any significant changes. Nevertheless, in patients with polyfluorethylene patches, an increase in the segmental vessel was reported (2227 mm3 (874 to 3240 mm3) and 111 mm2 (44 to 162 mm2) before surgery to 2318 mm3 (1648 to 3368 mm3) and 115 mm2 (82 to 168 mm2).

The studies that use 3DUS for measuring diameter reduction indicate higher reproducibility. One such past empirical study showed a mean diameter measured as 2.4+/-1.2mm and 2.3+/-1.1mm of plaque by 2 observers. This indicates sound interobserver variability, along with excellent intraobserver variability, provided repeated measurements. However, it can be noted that the data presented by this study is merely based on the two investigators and, therefore, could be improved by involving more investigators in the future (81).

The results produced by computing intraobserver and interobserver variability in test phantoms were compared with data mentioned previously under Vivo studies. Hereunder, the plaques simulation was used as phantoms with obtained volumes and agar with water displacement. Low 3DUS values were recorded under the study at approximately 4%, wherein 5% was recorded for both observer measurements (83). The data findings suggest that variability can be reduced by enhancing plaque volume and vice versa, indicating consistency with past studies (101). Thus, phantoms were quite helpful for determining accuracy as well

as variability because water displacement can help in measuring actual plaque volume. Further, a mean accuracy of 3.1% was recorded when actual plaque volume was compared with recorded plaque volume with the help of deploying 3DUS. Although, the variability can be eliminated using phantoms in the probe's anatomical positioning on patients by observers, which explains the high degree of variability in past clinical studies on research problems (83).

Apart from the above, a detectable change in volume at minimum was revealed using statistical analysis under a phantom study. The study suggests that a change of 11.1% is required to be detected as volume change in the true sense instead of the observer variability effect. Despite that, the statistical analysis undertaken in the study was able to demonstrate high reproducibility for every subset of plaque among patients (83). Further, a change of 12.9% was detected in vessel wall volume (VWV) with the help of different observers (95). Additionally, the minimum detectable change in volume explains that significant changes in volume must be observed for the small plaques and vice versa to conclude that changes in plaque volume have attained at least a 95% confidence level (101).

3.6 Discussion:

Carotid plaque and carotid intima-media thickness (CIMT) have been highlighted for responding differently to various therapies, and the burden of plaque is the indicator of the threat of higher cardiovascular events (94). In addition, 2DUS could identify transformations in the thickness of the overall intima-media thickness (IMT) and 3DUS is needed for measuring the changes in the volume of plaque and substantially the burden of plaque. Moreover, the 2DUS IMT computations give no showcasing of regression and progression of the plaque

lengthwise along the overall vessel, which is a critical indicator of transforming the burden of the plaque. Further, Ainsworth et al. (86) highlighted that acoustic and shadowing drops out are resources of variability across different studies because of the loss of an adequate explanation of the boundaries of the plaque. Moreover, the poor machine and contrast frame-up could also decrease the capability of detecting the boundaries correctly. Besides, the reports could highlight systematic under and overestimating of plaque volume. This could be balanced by using a highly clear strategy and a better teaching approach to standardise the placement of the cursor during the process of segmentation.

The study conducted by Landry and Fenster (83) highlighted that the gating with cardiac or respiratory fluctuation decreases the given artefacts when the 2D slices are reconstructed for the 3D image. However, gating enhances the overall scan lengths as one particular slice is gathered within the single cardiac cycle. The time taken for obtaining a complete view of the carotid artery mechanism is currently enhanced and carries fewer threats related to angiography and MRI. In addition, the time is enhanced with the manual segregation tools even further. Still, with such adequate reproducibility outcomes, the shortage of side effects and threats, as well as ease of utilisation, it can be highlighted that further time is adequate for clinic authenticity. Further, it has been found that there is no issue that 3DUS has manufactured adequate outcomes in detecting plaque volumes, accuracy, repeatability, and low variability. Besides, Landry and Fenster (83) and Palombo et al. (79) have also provided adequate evidence which highlights that 3DUS is able to determine the transformation in the volume of plaque in relation to the therapies.

Ultimately, it is also prudent that 3DUS is suitable and efficient for qualitative and quantitative analyses, detection, and quantification of stenosis. Follow-up studies like Yao et al (80) show that the volumetric capacity of 3DUS exhibits significant clinical attributes like visualising the progression and regression of stenotic nature and assessment of the outcomes of other interventions like endarterectomy. In detecting 40% to 70% of carotid artery stenosis, 3DUS reported a higher degree of accuracy compared to other interventional approaches like Carotid angiography. Subsequently, Kozakova et al. (82) concluded that the severity of carotid stenosis was sometimes underestimated by carotid angiography due to inconsistencies between linear measurements and true anatomic situations.

Another merit of 3DUS is that it can be performed easily and conveniently, particularly on critically ill patients. For example, Wessels et al.(85) showed that 3D could be easily performed on patients with stroke and in the intensive care unit. Therefore, for patients who could not withstand invasive imaging techniques due to critical illness, 3DUS was applicable. Kozakova et al. (82) agree that 3DUS was also suitable for non-invasive assessment and detection of extracranial carotid artery stenosis. Further, Kozakova et al., Kumar et al., and Wessels et al. (82,85,96) also agreed that 3DUS exhibited reliable diagnostic accuracy, sensitivity, and specificity compared to Carotid angiography when applied in the detection of carotid artery stenosis. However, on the other hand, it has been highlighted by Almuhanna et al. (95) that the next step will be to detect the way to utilise the volume of plaque as an innovative measure of the high severity of the carotid disease as well as suitability for the surgery.

Furthermore, it will be highly useful for developing an innovative criterion that equates to the ongoing 2D diameter and velocity criteria. Such as the development of ratio plaque volume within the artery and the particular volume of the plaque at which the threat of high vascular events in relation to the burden of plaque is higher than the threat of surgical complications or issues. Therefore, in this case, the studies would require performing both 3DUS and 2DUS approaches for comparing velocity-derived stenosis and plaque volume. In addition, the studies could make the approach earlier in the upcoming time by utilisation innovation and technology, which was highlighted in the review and that has currently been highlighted in relation to reliability and accuracy. In addition, such longitudinal studies must be carried out that detect the volume of plaque in the overall carotid artery as well as integrate this with the incidence or presence of stroke. However, if 2DUS finds symptomatic stenosis is greater than 50%, the surgery must be conducted where reasonable and appropriate.

Van Engelen et al. (94) highlighted that the transformations in the plaque volume must be taken into consideration and the computation from particular time periods. The transformation in the plaque volume is possibly more considerable than plaque volume at the baseline. Besides, relations can also be conducted that completely differentiate between the symptomatic and asymptomatic patients. These can investigate whether the volume of the plaque is considerably distinct across the groups for determining in case the burden of plaque is an adequate technique for identifying the asymptomatic individuals who will get an advantage from the surgery. Therefore, this will be adequately utilised as, in the current period of time, there is little research on the sole treatment for asymptomatic individuals with less than 50% stenosis. Moreover, there will also be a requirement for developing the direct relations between mechanically and free-hand steered transducers in case this is to be more

practically implemented in the total clinical routine. Therefore, this must determine which offers clear outcomes in relation to both presents as well as accuracy for interpretation by the clinicians.

Furthermore, the evidence highlights that when utilised in integrations with 3DUS, 2DUS could enhance the overall diagnostic value of the ultrasound. However, where there exist limitations within the context of 2DUS, utilising the velocity criteria and the modality could be enhanced by adequate visualisation of the 3-D structure of the plaque. In addition, Wessels et al. (85) highlight that the ongoing research is inadequate for replacing the 2DUS as the current guidelines use the overall velocity-derived diameter reduction or stenosis. But 3DUS could be utilised to improve the overall reliability of the scanning related to ultrasound. For example, in case the user carries a lack of experience and understanding as the 3D mechanisms decrease opportunities for the overall variability and highlight exceptional in terms of observer variability. Integrated with greater repeatability, accuracy, good safety levels, low scan times and, this will be an adequate tool for investigating further in relation to growing standardised criteria in terms of the volume of plaque as the predictor of the vascular suitability and events for surgery.

In addition, adequate visualisation of the plaque and a clear image of its regression and progression is adequate for the inter-disciplinary strategy, unlike the 2D data that cannot be adequately compiled into a particular set of data. Therefore, the 3D data could be checked in the digital form that is highly adequate for the inter-disciplinary meeting with the associated clinical for overall decision-making related to the overall treatment plans involving suitability for surgery.

3.7 Conclusion:

The general advantages of 3DUS are related to the overall structure that makes it easier in the overall clinical setting with adequate repeatability, reliability, and accuracy in a highly faster period of time as compared to innovative radiographic technology like angiography and MRI. In addition, a high level of specificity reports in the overall pieces of literature highlights that the 3DUS can be an adequate screening strategy in order to detect those with greater grade stenosis, where angiographic technology can then be used for considering the diagnosis in the patients. Most essentially, 3DUS is capable of tackling the limitation shown by the 2DUS in that a 3-D object is just being highlighted in the 2D scan. Collecting exactly the similar plane in repetition ode for following up the scans is not an issue utilising 3DUS. The operator can view the carotid artery and various other types of plaques as the total image that could be sliced and viewed from any dimension. Furthermore, this is generally useful for seeking transformations in the structure of plaque and texture along with observing regression or progression of plaques in relation to the therapies, and this is critical as the transformations in the structure of plaque and the volume of plaque over the period of time have been displayed for predicting considerable vascular events.

CHAPTER 4

RELIABILITY AND ACCURACY OF TOMOGRAPHIC 3D ULTRASOUND FOR GRADING VESSEL STENOSIS: A PHANTOM STUDY

4.1 Introduction:

CVD is a term used for a number of pathologies affecting the heart and blood vessels, including coronary heart disease, cerebrovascular disease, and peripheral arterial disease (102). CVD is of-ever increasing health concern affecting all ages, genders, races, and ethnicities and is associated with 17.8 million deaths annually worldwide (103). Atherosclerotic plaques in arteries are a major cause of CVD (104). The build-up of large atherosclerosis can lead to severe stenosis or occlusion of arteries influencing blood perfusion to distal tissues (105). The degree of luminal stenosis and features of atherosclerotic plaques are essential when choosing an optimal intervention (106,107). thus, accurate assessment grading of stenosis caused by atherosclerosis is necessary.

Blood vessels and atherosclerosis plaques are 3D structures in nature that can be accurately assessed with 3D imaging (108,109). An attempt to quantify vessel size and volume, luminal stenosis, and plaque morphological features using a 2D imaging method may provide inaccurate outcomes. 2DUS is the current first-line imaging method for demonstrating arterial wall thickness, plaque surface regularity and morphology, and grading of stenosis through diameter reduction (DR) and area reduction (AR). However, ulcerated plaque may be misdiagnosed with irregular plaque surface in addition to the difficulty of detecting echolucent plaque (109). Furthermore, imaging vessel stenosis using a 2D scanning technique can be mis-graded and may result in over or under-estimation of stenosis (44,100,110–113). Several studies that compared the use of 3DUS to 2DUS showed that 3DUS is superior for the quantification of vascular disease and can provide more information on plaque morphology and degree of stenosis (114–119). Other studies assessing the use of 3DUS for the evaluation

of vascular diseases and changes in plaque volume in response to treatments reported that 3DUS imaging has the ability to determine total plaque volume accurately and risk stratification, vessel wall volume, ulceration, echolucency and plaque texture (86,109,120), suggesting that 3DUS can be used as a rapid diagnostic tool for vascular diseases and for treatment evaluation of surgical and medical interventions.

t3DUS is a novel free-hand electromagnetically tracked system that can be coupled to any commercially available ultrasound system. It provides a low-cost, rapid, safe 3D reconstruction of the vasculature (120). A scanned vessel with t3DUS is captured by external software to generate 3D images that can be used for offline analysis to measure several parameters such as plaque volume and maximum stenosis percentage (120). Ultrasound is well-known as an operator-dependent imaging method; thus, the lack of reproducibility and accuracy of t3DUS for grading stenosis in vessels is of concern. Consequently, it is crucial to assess the reproducibility and accuracy of t3DUS for grading stenosis to ensure accurate measurements with low variability between operators pre-clinically. The accuracy of t3DUS for measuring the length, diameter, and volume of an ex-vivo artery and for measuring carotid plaque volume in symptomatic and asymptomatic patients with carotid stenosis has been proven previously (120,121). However, to date, there is no study has been published that specifically addresses the reliability of t3DUS for grading stenosis of peripheral vessels. Therefore, our aims in the present phantom study were to assess the reproducibility and accuracy of t3DUS for grading stenosis.

The aim of this phantom study was to assess the accuracy of tomographic 3D ultrasound (t3DUS) for grading stenosis, using the manufacturer's measurements as a gold standard. The

percentage of maximum stenosis was obtained using 2DUS and t3DUS imaging techniques from a peripheral vascular phantom, including channels with 50%, 75% and 90% stenosis. Inter-observer reproducibility of t3DUS for grading stenosis was assessed using the Intra-class correlation coefficient (ICC) and Bland-Altman. Mean and mean differences were used to evaluate the accuracy of 2DUS and t3DUS in measuring maximum stenosis in all channels. Inter-operator agreement was excellent with ICC value of 0.99 (95% confidence interval (CI) 0.994 – 0.998, p <0.001). Bias in measurements was -0.59±2.01% (95% limit of agreement (LoA) -4.54 – 3.36). The mean difference (MD) of maximum stenosis measurements from reference values for all channels was low in t3DUS than in 2DUS (t3DUS: MD, +1.01%; DR 2DUS: MD, -6.10%; AR 2DUS: MD, +8.20%). t3DUS is a reproducible and accurate imaging method for grading stenosis. The current B-mode 2DUS stenosis grading criteria used in vascular assessment may be under/overestimating the percentage of stenosis. Further phantom and human studies investigating the reliability of t3DUS for grading stenosis and other metrics, including plaque volume, are required. For further reading, the original recently published manuscript is given in *Appendix B.*

4.2 Methods:

4.2.1 Study Design

A high-resolution premium Philips Elite ultrasound imaging system (Philips Healthcare, Bothell, WA, USA) was used to obtain the maximum percentage of stenosis from a peripheral vascular phantom using 2DUS and t3DUS (PIUR imaging GmbH, Vienna, Austria) imaging techniques. Inter-operator reproducibility and accuracy of DR and AR 2DUS and t3DUS in measuring maximum stenosis percentage were assessed. Two experienced certified clinical sonographers with efficient training on t3DUS (operator A and operator B) were asked to measure the maximum percentage of stenosis from all channels with stenosis. Both operators were blinded to each other`s measurements and the reference of the manufacturer's maximum percentage of stenosis of all channels. Ethical approval was not required as animals, or human subjects were not involved in this study.

4.2.2 Phantom

The maximum percentage of stenosis was measured on a peripheral vascular phantom model 525, produced by Computerized Imaging Reference Systems, Inc. (CIRS, Norfolk, Virginia, USA). The phantom is made from urethane rubber tissue-mimicking materials, including four channels (channel 1 with no stenosis, channel 2 with 50% stenosis, channel 3 with 75% stenosis, and channel 4 with 90% stenosis) at a depth of approximate 1.5 cm from the scan surface, simulating superficial vasculature. The acoustic properties of tissue-mimicking materials can be affected by temperature variations. According to the phantom operating manual, the tissue-mimicking material has a sound velocity of 1450 m/s at 0.5 dB/cm/MHz at

room temperature (≈23°C). Our measurements were taken at a temperature of 22-24°C based on the thermometer affixed to the phantom and a hand-held thermometer to ensure measurement accuracy (Figure 4.1).

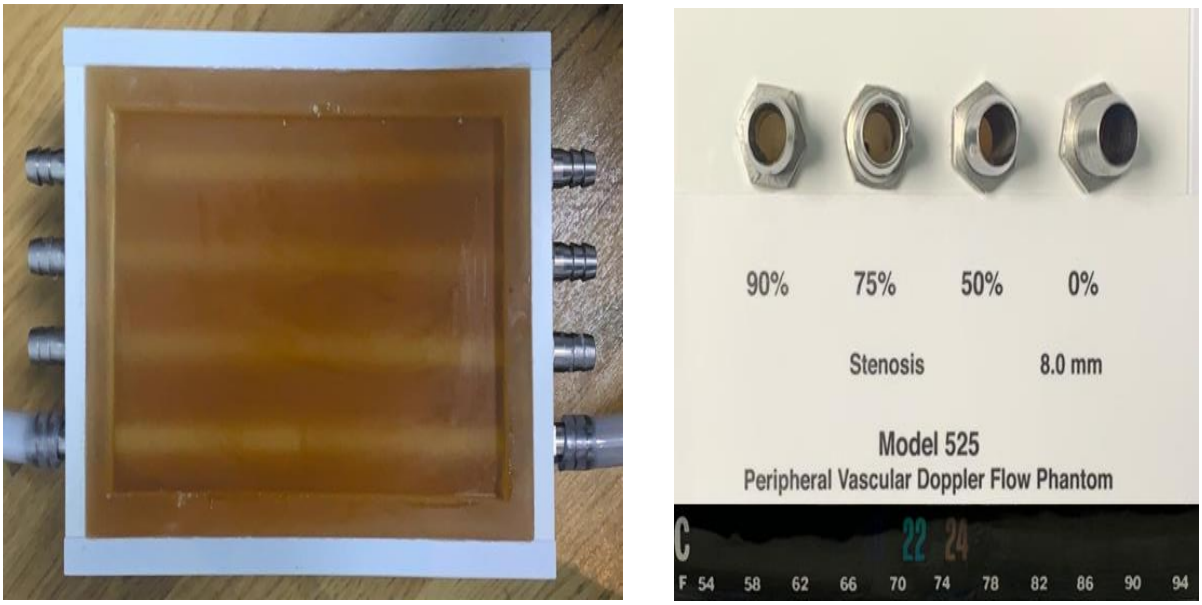

Figure 4. 1 Peripheral vascular phantom (Model 525, Computerized Imaging Reference Systems).

The fluid in channels was Doppler fluid model 769DF which mimics the acoustic and physical properties of human blood. The formulation of Doppler fluid is based on published standards (122).

4.2.3 Data Acquisition

Each operator was asked to take the maximum percentage of stenosis from all channels with stenosis (i.e., channels 2, 3, and 4) in a single visit. Thirty DR and AR in 2DUS and t3DUS measurements of the maximum percentage of stenosis were obtained from each channel with stenosis using a linear-array transducer (12-3MHz) of the Philips Elite ultrasound imaging

system. The data were acquired in longitudinal scanning for DR and in transverse scanning for AR and t3DUS with the transducer lifted and repositioned between acquisitions. The minimum residual luminal diameter in each channel with stenosis was defined using conventional 2D B-mode ultrasound imaging of carotid pre-setting in longitudinal view. Once the minimum residual luminal diameter was located, the ultrasound system control settings were optimised for good image quality. For the DR, original channel diameter (outer-to-outer) and residual lumen were measured using electronic callipers (Figures 4.2A, D and G).

For the AR, the outer channel area and residual lumen were outlined using ellipse and continue trace, respectively (Figures 4.2B, E and H). The degree of stenosis was then determined using t3DUS, in which a semi-automated method was used for measuring the stenosis in all channels by attaching an electromagnetic sensor to the transducer used in the 2D scans with the exact ultrasound same control settings and was swept over the channel 1-2 cm before and after the site where the minimum residual lumen is depicted. Then 2D images were captured and reconstructed into 3D images by tUS external software for offline analysis. Manual multi-planimetry was used at the outer channel area free of stenosis before and after the stenotic site. The maximum stenotic site in the channel was automatically calculated (Figures 4.2C, F and I).

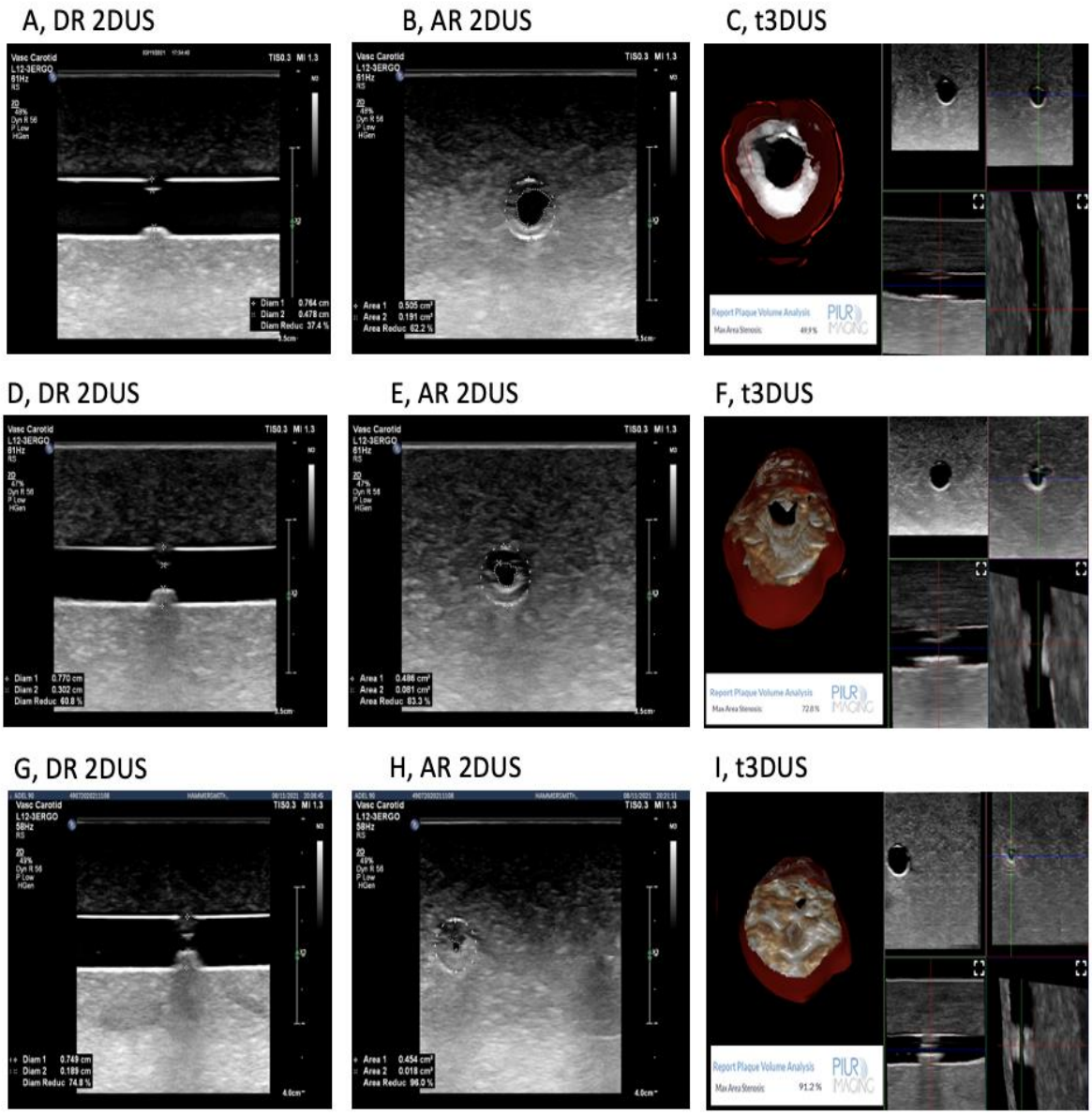

Figure 4. 2 Measurements of the maximum percentage of channels with 50% stenosis (A-C), 75% stenosis (D-F) and 90% stenosis (G-I) using DR 2DUS, AR 2DUS and t3DUS in peripheral vascular phantom (Model 525, Computerized Imaging Reference Systems). AR: area reduction, DR: Diameter reduction, 2DUS: 2D ultrasound, t3D: tomographic 3D ultrasound.

4.2.4 Statistical Analysis

Intraclass correlation coefficient (ICC), Bland-Altman plot and coefficient of determination variance around the fitted regression line were used for assessing inter-observer reproducibility of stenosis measurements using DR and AR 2DUS and t3DUS. The mean

coefficient of variation (CV) from each channel was used to determine inter-operator variability. Mean difference was used to assess the accuracy of imaging techniques (i.e., DR 2DUS, AR 2DUS and t3DUS) in measuring maximum stenosis in all channels with stenosis. Mann-Whitney U test was used to compare stenosis measurements in all techniques. The level of significance was set at < 0.05. Statistical analysis was performed using IBM SPSS Statistics version 21 (Armonk, NY: IBM Corp) and GraphPad PRISM 7 (La Jolla, CA, USA).

4.3 Results:

A total of 540 measurements of maximum stenosis percentage were obtained using DR and AR 2DUS, and t3DUS imaging techniques. On a visit, each operator acquired 270 stenosis percentage measurements from three channels simulating superficial vasculature (90 and 30 measures per technique and channel, respectively).

4.4 Reproducibility of 2DUS and t3DUS:

Inter-operator reproducibility of DR and AR 2DUS and t3DUS maximum stenosis measurements between operator A and B (number (n)=90 for each operator per technique) were excellent (DR 2DUS, ICC value of 0.96 (95% confidence interval (CI) 0.90 – 0.98, p <0.001, Figure 3A; AR 2DUS, ICC value of 0.96 (95% CI 0.93 – 0.97, p <0.001, Figure 4.4A; t3DUS, ICC value of 0.99 (95% CI 0.994 – 0.998, p <0.001, Figure 5A). The percentage of variance in 2DUS and t3DUS measurements was excellent, with 96%, 87% and 98% of DR 2DUS, AR 2DUS and t3DUS measurements around the fitted regression line, respectively (Figure 4.3A, 4.4A and 4.5A). Bias in DR 2DUS measurements was -3.66±5.92% (95% limit of agreement (LoA) -15.28

– 7.94, Figure 4.3B), and in AR 2DUS measurements was 1.89±0.48% (95% LoA -7.68 – 11.47, Figure 4.4B). Bias in t3DUS measurements was -0.59±2.01% (95% LoA -4.54 – 3.36, Figure 5B). Mean of CV for stenosis measurements using 2DUS and t3DUS (n=60 per technique per channel) was low (DR 2DUS, channel with 50% stenosis, CV 4.85%; 75% stenosis, CV 3.93%; 90% stenosis, CV 7.03%; AR 2DUS, channel with 50% stenosis, CV 6.41%; 75% stenosis, CV 4.93%; 90% stenosis, CV 2.62%; t3DUS, channel with 50% stenosis, CV 2.86%; 75% stenosis, CV 3.90%; 90% stenosis, CV 0.87%, see Table 4.1

Ref	DR 2DUS				AR 2DUS				t3DUS			
	Mean	SD	MD*	CV	Mean	SD	MD*	CV	Mean	SD	MD*	CV
50%	43.63	2.11	-6.37	4.85	63.41	4.06	13.41	6.41	50.49	1.44	0.49	2.8
75%	68.83	2.70	-6.16	3.93	81.88	4.03	6.88	4.93	77.25	3.01	2.25	3.90
90%	84.24	5.92	-5.76	7.03	94.80	2.49	4.80	2.62	90.27	0.79	0.27	0.87

*Table 4. 1 Accuracy and coefficient of variation in B-mode 2DUS and t3DUS for grading of stenosis. Abbreviation: 2DUS: 2D ultrasound, AR: area reduction, CV: coefficient of variation, DR: diameter reduction, MD: mean difference, Ref: reference, SD: standard deviation, t3DUS: tomographic 3D ultrasound. * Mean difference of stenosis between imaging technique and reference value.*

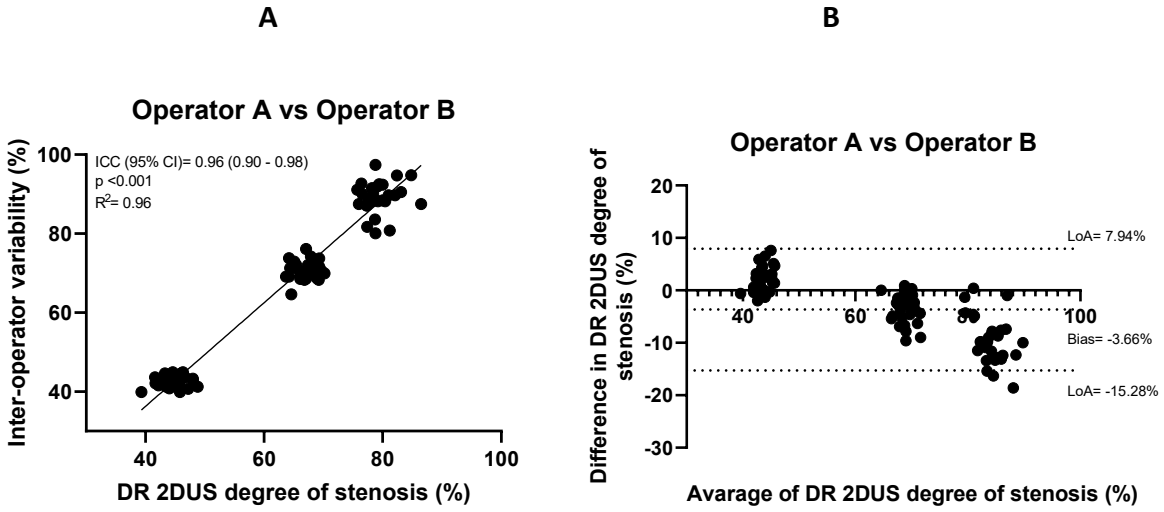

Figure 4. 3 Inter-operator and Bland-Altman agreement. Linear regression (A) and Bland-Altman agreement (B) of DR 2DUS maximum stenosis measurements between operators A and B. CI: confidence interval; DR: diameter reduction; ICC: Intraclass correlation; LOA= limit of agreement.

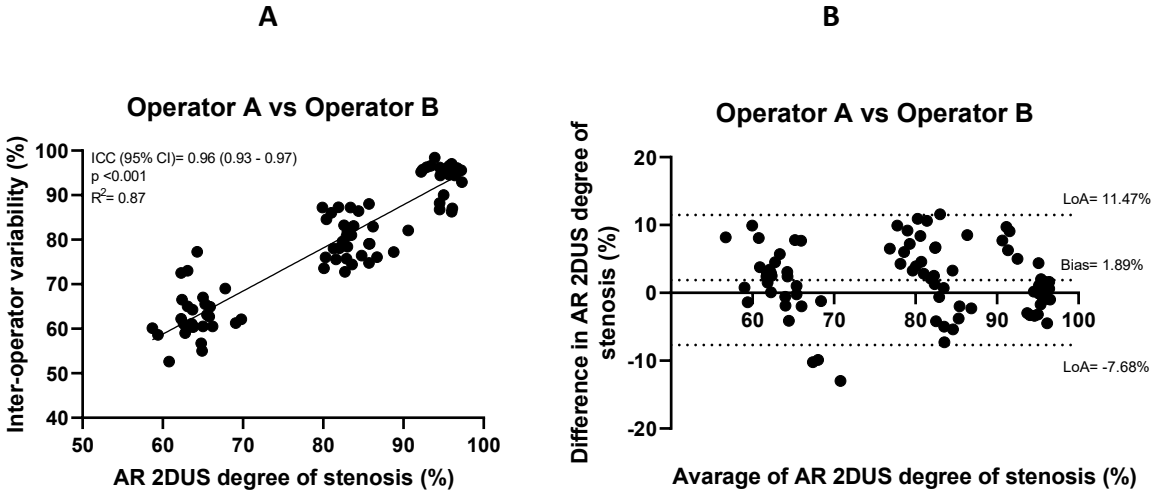

Figure 4. 4 Inter-operator and Bland-Altman agreement. Linear regression (A) and Bland-Altman agreement (B) of AR 2DUS maximum stenosis measurements between operators A and B. AR: area reduction, CI: confidence interval; ICC: Intraclass correlation; LOA = limit of agreement.

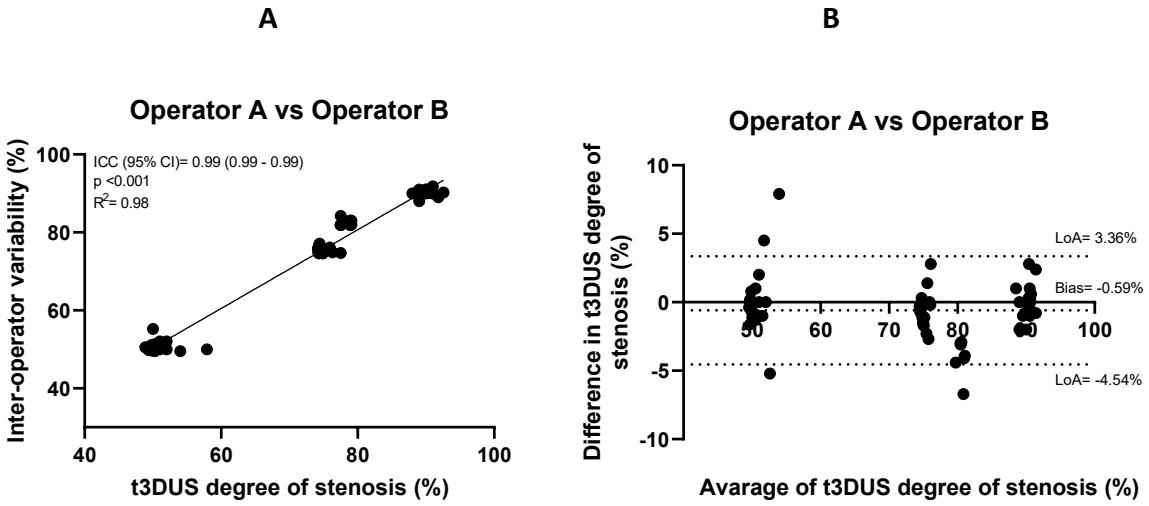

Figure 4. 5 Inter-operator and Bland-Altman agreement. Linear regression (A) and Bland-Altman agreement (B) of t3DUS maximum stenosis measurements between operators A and B. CI: confidence interval; ICC: Intraclass correlation; LOA = limit of agreement; t3D: tomographic three-dimension ultrasound.

4.5 Accuracy of 2DUS and t3DUS:

The mean of repeated measures taken by the two operators of maximum stenosis for each channel (n=60 per technique) was as follows: t3DUS: channel with 50% stenosis, 50.49±1.44%, a channel with 75% stenosis, 77.25±3.01%, a channel with 90% stenosis, 90.27±0.79%; DR 2DUS: channel with 50% stenosis, 43.63±2.11%, a channel with 75% stenosis, 68.83±2.70%, a channel with 90% stenosis, 84.24±5.92%; AR 2DUS: channel with 50% stenosis, 63.41±4.06%, a channel with 75% stenosis, 81.88±4.03%, a channel with 90% stenosis, 94.80±2.49%, Figure 4.6).

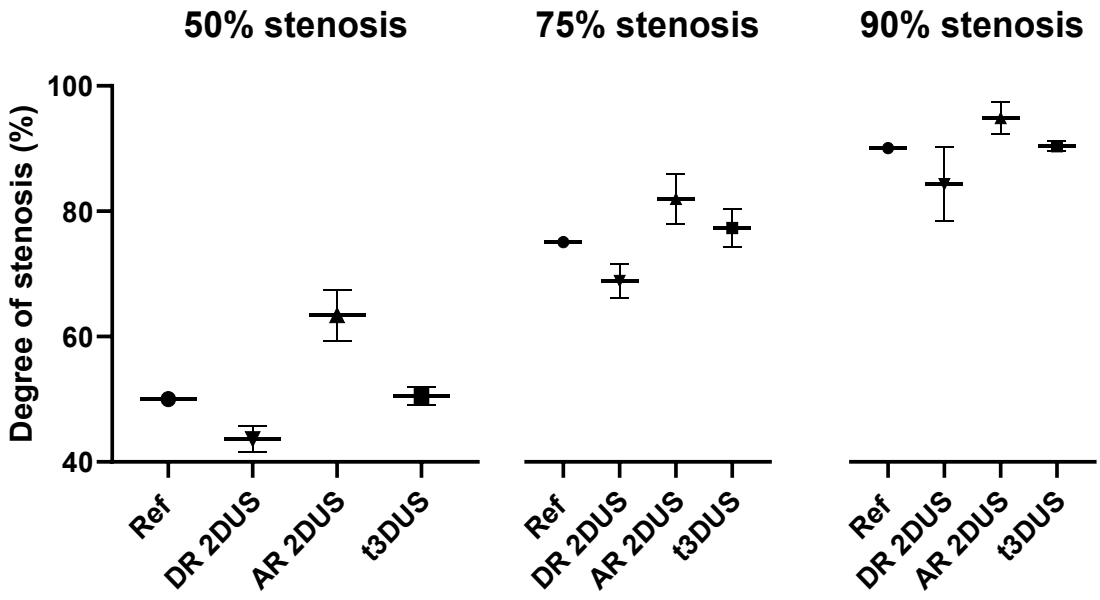

Figure 4. 6 Accuracy of DR and AR 2DUS and t3DUS in grading stenosis in channels with 50%, 75% and 90% stenosis (mean ± SD). AR: area reduction; DR: diameter reduction, 2DUS: 2D ultrasound; t3D: tomography 3D ultrasound.

There was a significant difference between t3DUS and 2DUS in measuring maximum stenosis in all channels, with under and over-estimation of 2D DR and AR, respectively (t3DUS vs DR 2DUS: channel with 50%, z= -9.45, p<0.001, channel with 75%, z= -9.27, p<0.001, channel with 90%, z= -5.86, p<0.001; t3DUS vs AR 2DUS: channel with 50%, z= -9.39, p<0.001, channel with 75%, z= -5.94, p<0.001, channel with 90%, z= -7.94, p<0.001, Figure 4.7).

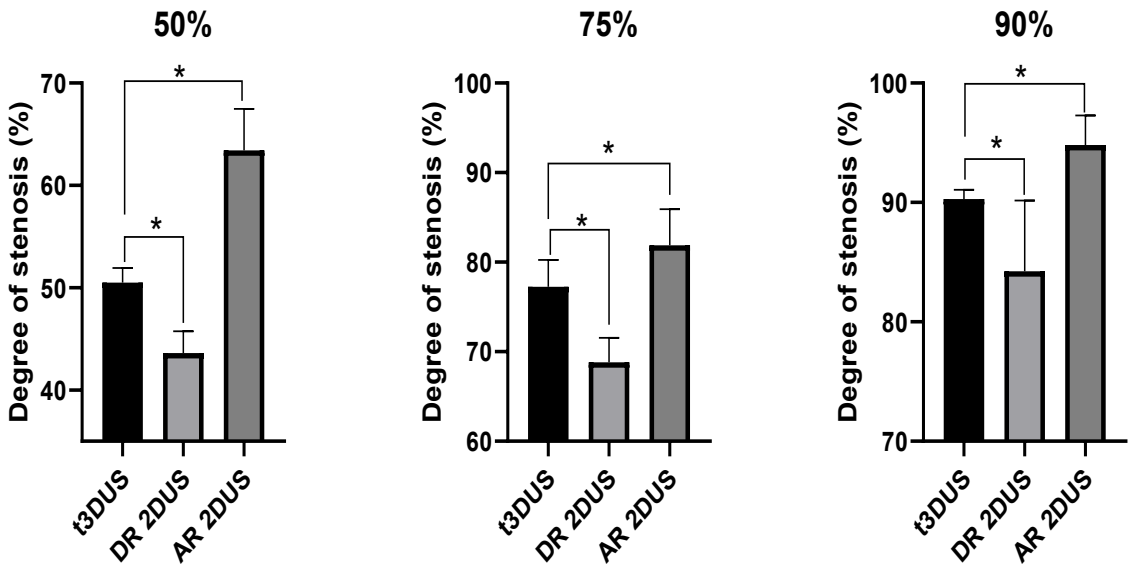

*Figure 4. 7 Comparison between t3DUS and DR and AR 2DUS in measuring stenosis in channels with 50%, 75% and 90% stenosis (mean ± SD). * p≤0.05 using Mann Whitney-U test between imaging techniques. AR: area reduction, DR: diameter reduction, 2DUS: 2D ultrasound, t3D: Tomographic 3D ultrasound.*

The mean difference of maximum stenosis measurements from reference values for all channels was lower in t3DUS than in 2DUS (t3DUS: mean difference for reference value (MD) in the channel with 50% stenosis, 0.49%, MD in the channel with 75% stenosis, 2.25%, MD in the channel with 90% stenosis, 0.27%; DR 2DUS: MD in the channel with 50% stenosis, -6.37%, MD in the channel with 75% stenosis, -6.16%, MD in the channel with 90% stenosis, -5.76%; AR 2DUS: MD in the channel with 50% stenosis, 13.41%, MD in the channel with 75% stenosis, 6.88%, MD in the channel with 90% stenosis, 4.80%) (Table 4.1).

4.6 Discussion:

To the best of our knowledge, this is the first study that specifically addresses the reproducibility and accuracy of t3DUS for grading stenosis pre-clinically, using a phantom with channels simulating superficial vasculature with a range of stenosis. The analysis demonstrated that t3DUS has an excellent inter-operator agreement with low variability and is more accurate than 2DUS for grading stenosis compared to manufacturer reference values. These findings suggest that t3DUS is a reliable and reproducible method for grading vessel stenosis. Further work investigating the reliability of t3DUS in grading vessel stenosis in patients with vascular diseases is required.

The degree of stenosis in vessels is a crucial parameter in management decisions. The findings from the present study demonstrated that t3DUS provides accurate and reproducible measurements of the degree of stenosis pre-clinically with the potential to improve working circumstances for vascular scientists in clinical practice considerably. Besides ultrasound, the current imaging modalities for assessing vessel stenosis include X-ray angiography, CTA, and MRA. X-ray angiography and CTA involve ionising radiation, and MRA is a costly imaging tool that may not be available in health centres with limited funds. Using ultrasound to assess vascular disease has a secure place in modern medicine for being a safe and cost-effective diagnostic tool. The promising development of t3DUS, with its potentially accurate and detailed information, may significantly impact patient's medical and surgical interventions and reduce the use of other imaging modalities such as X-ray angiography, CTA and MRA, which are being used to determine the uncertainty that 2DUS provides.

The excellent inter-operator reproducibility of t3DUS seen in our study was also reported in a study that used t3DUS for length and diameter with good agreement for volume measurements of an ex-vivo artery (123). Our analysis also showed that the mean difference of maximum stenosis measurements was lower in t3DUS than in 2DUS compared to manufacturer reference values for all channels with stenosis. The study done by Rogers et al. (120) also reported that t3DUS has a minor error of B-mode, CT and MRI at calculating volume compared to the gold standard (i.e. water suspension volume). The degree of stenosis of fixed tubular geometry was used to assess the reliability of t3DUS in our *in-vitro* phantom study. This could differ from *ex-vivo* or *in-vivo* vasculature assessment, in which vessel and plaque geometry may be more complex and can alter the reproducibility of t3DUS. Further studies investigating the reliability of t3DUS in patients with vascular diseases are required.

t3DUS is a freehand scanning technique that is operator-dependent; therefore, the operator`s experience level in scanning and using t3DUS will reduce error in calibration and image reconstruction and reduce the variability in the grading stenosis (88,124,125). For this reason, in our present study, a semi-automated method developed by PIUR imaging was used, and operators were only asked to outline the outer channel area. The maximum stenotic site through the scanned region is calculated automatically, making it less operator-dependent. The reproducibility of t3DUS for grading stenosis can also be affected by morphological characteristics of plaque (e.g., smooth vs irregular plaque surface) (110). These factors should be considered in future research investigating the reproducibility of t3DUS for grading stenosis in patients.

We also identified a significant difference between t3DUS and 2DUS in measuring maximum stenosis in all channels, with under and over-estimating 2D DR and AR, respectively. It has been reported that in severe stenosis, haemodynamic and velocity criteria are more prevalent than 2D DR and AR as they are more challenging to generate and are dependent on the type of stenosis that may lead to variations in grading stenosis (126). The North American symptomatic carotid endarterectomy trial (NASCET) and European carotid surgery trial (ESCT) methods are used for quantifying the degree of stenosis developed for angiography. Thus, 2DUS B-mode ultrasound is prone to over and under-estimating the actual severity of stenosis (108,126).

There are limitations to consider in clinical practice when using t3DUS. t3DUS relies on the conventional 2DUS B-mode US; thus, resolution errors that may affect the precession of measurements in 2DUS images, including the type of transducer and ultrasound system software level used, will be translated into t3DUS and may affect the manual planimetry for grading the stenosis. Therefore, a premium ultrasound system with appropriate control optimisation of 2D B-mode US is necessary to ensure high-quality 3D images (123). Also, unavoidable artefacts such as acoustic shadowing in the 2DUS images will be present in the reconstructed 3D images (123), limiting the use of t3DUS in grading vessel stenosis with calcified plaques in the near wall. Furthermore, the reconstruction of t3DUS images may be time-consuming, especially when using manual segmentation through the entire length of the scanned vessel for calculating the degree of stenosis. It has been reported that reconstructing diseased carotid bifurcation using a freehand 3D ultrasound system may take up to 40 minutes depending on the extent and geometric complexity of plaque, suggesting the use of a smart-based tool for fast scanning, and making t3DUS more feasible in practice

(108,123). This suggestion has been considered in our present study with the use of a semi-automated tool, as described earlier, which remarkably reduces the time required for calculating the degree of stenosis in t3DUS images.

4.7 Conclusion:

Free-hand t3DUS is a reproducible and accurate imaging method for grading stenosis. Interoperator reproducibility of t3DUS for grading stenosis was excellent, with a low coefficient of variation. The mean difference of stenosis measurements from manufacturer reference values for all channels was low in t3DUS than in 2DUS. There was a significant under and over-estimation of 2D DR and AR, respectively, compared to t3DUS. Other phantom and human studies investigating the reliability of t3DUS for grading stenosis and additional metrics, including plaque volume, are required. In the next chapter, the use of 3D ultrasound for the measurement of carotid plaque volume is presented.

CHAPTER 5

RELIABILITY OF TOMOGRAPHIC 3D ULTRASOUND IN MEASURING CAROTID PLAQUE VOLUME

5.1 Introduction:

Stroke is a known leading cause of mortality and disability globally (127). Extracranial stroke is usually an embolisation from carotid plaque and haemodynamic compromise due to carotid artery stenosis (128,129). ICA atherosclerosis is a cause of up to 15% of ischemic strokes (130). The severity of carotid stenosis defined using the North American Symptomatic Carotid Endarterectomy Trial (NASCET) and European Carotid Surgery Trial (ESCT) methods remain the primary parameter for surgical or endovascular interventions (131,132). A recent review performed by Paraskevas et al. (133) included 1,121 asymptomatic patients with ≥50% carotid stenosis and reported that ultrasonic plaque features, including carotid plaque echogenicity and area, could independently predict future ipsilateral cerebrovascular events (133). The European Society for Vascular Surgery guidelines recommended that carotid plaque area and stenosis progression be considered for medical treatment in asymptomatic patients (134,135).

It has been shown that Carotid Plaque Volume (CPV) is an independent predictor of recurrent ischemic stroke and cardiovascular events (136,137) progression of carotid plaque volume in symptomatic patients with 30–69% stenosis was associated with an increased chance of recurrent ischemic stroke (138). It has been proposed that the progression of CPV is related to a decrease in fibrous cap thickness and an increase in the lipid composition of plaque, indicating its involvement in plaque vulnerability (139). These suggest that CPV may be a useful prediction indicator of stroke risk in symptomatic and asymptomatic patients.

Duplex ultrasound is the first-line imaging tool for assessing carotid diseases (140). The use of 3D ultrasound for the quantification of vascular disease can provide more information on plaque morphology and the degree of stenosis (116,118), accurately assess changes in plaque volume in response to anti-atherosclerotic therapies and determine stroke risk stratification (141,142). t3DUS is a novel free-hand electromagnetically tracked system that can be coupled to an ultrasound system and used for offline analysis to measure several parameters, including arterial lumen diameter and length, wall volume and percentage of maximum stenosis (143,144) with only one study found that investigated the accuracy of t3DUS for measuring CPV (145). Therefore, this study aimed to assess the reproducibility and accuracy of t3DUS for measuring CPV in patients undergoing CEA.

5.1.1 Background

t3DUS is a promising imaging technique for quantifying carotid plaque by measuring the degree of stenosis and plaque volume. CPV could add benefit in predicting the potential risk of stroke. Therefore, this study aimed to assess the reproducibility and accuracy of t3DUS for measuring CPV within the ICA in patients undergoing CEA.

5.1.2 Methods

t3DUS was used to obtain CPV *in-vivo* from 25 symptomatic patients before surgery. *Ex-vivo* CPV from the CEA specimen was then measured using a validated water displacement method as a reference standard. CPV for each patient was measured twice using both

methods (total n=50 per technique). ICC and Bland-Altman plots were used to establish bias and limit agreement between CPV measurements.

5.1.3 Results

There was an excellent agreement between t3DUS and the reference test in measuring CPV with an ICC value of 0.98 (95% CI 0.97 – 0.99, p <0.001). Bias in measurements was 0.02±0.11 cm^3 (95% limit of agreement (LoA) -0.19 – 0.25). Intra-observer agreement of t3DUS CPV measurements was excellent with an ICC value of 0.95 (95% confidence interval (CI) 0.92 – 0.97, p <0.001). Bias in measurements was 0.004±0.07 cm^3 (95% limit of agreement (LoA) -0.14 – 0.15).

5.2 Materials and Methods:

5.2.1 Study Design and Participants

This pilot trial was conducted by the Declaration of the Health Research Authority (HRA) and Health and Care Research Wales (HCRW) (20/LO/0814) and approved by the Imperial College London Ethics Committee. For this study, written informed consent was taken from recruited patients with severe internal carotid artery stenosis (i.e., >70%) undergoing CEA. Patients with calcified plaque causing acoustic shadowing or unable to give informed consent were excluded. Measuring CPV *in-vivo* using t3DUS was performed twice in a single visit 48 before surgery with 1-2 hours apart. *Ex-vivo* CPV was calculated using the water displacement method immediately following the CEA procedure and 24 hours after surgery. *In-vivo* and *ex-*

vivo CPV was measured by two experienced vascular scientists blinded to the patient`s ID and each other's results.

5.3 Study Assessments:

5.3.1 CPV Measurement Using t3DUS

This study performed a complete carotid ultrasound examination using a high-resolution premium Philips Elite ultrasound imaging system (Philips Healthcare, Bothell, WA, USA) with a 9-4MHz ultrasound transducer. The stenosed carotid was defined using conventional 2D Duplex ultrasound of carotid pre-setting, and the PSV at the most stenotic site was measured (146,147) (Figure 5.1 A).

The CPV, atherosclerotic burden within a defined length of the ICA and DoS was then determined using free-hand t3DUS in which a semi-automated method by attaching an electromagnetic sensor to the transducer used in the 2DUS transverse scanning and swept over the carotid artery 1-2 cm before and after the site where the plaque is depicted. Then 2D images were captured and reconstructed into 3D images by tUS external software for offline analysis. Manual multi-planimetry was used at the outer layer of the ICA walls, and the CPV and Dos were automatically calculated (143,145) (Figure 5.1B).

A B

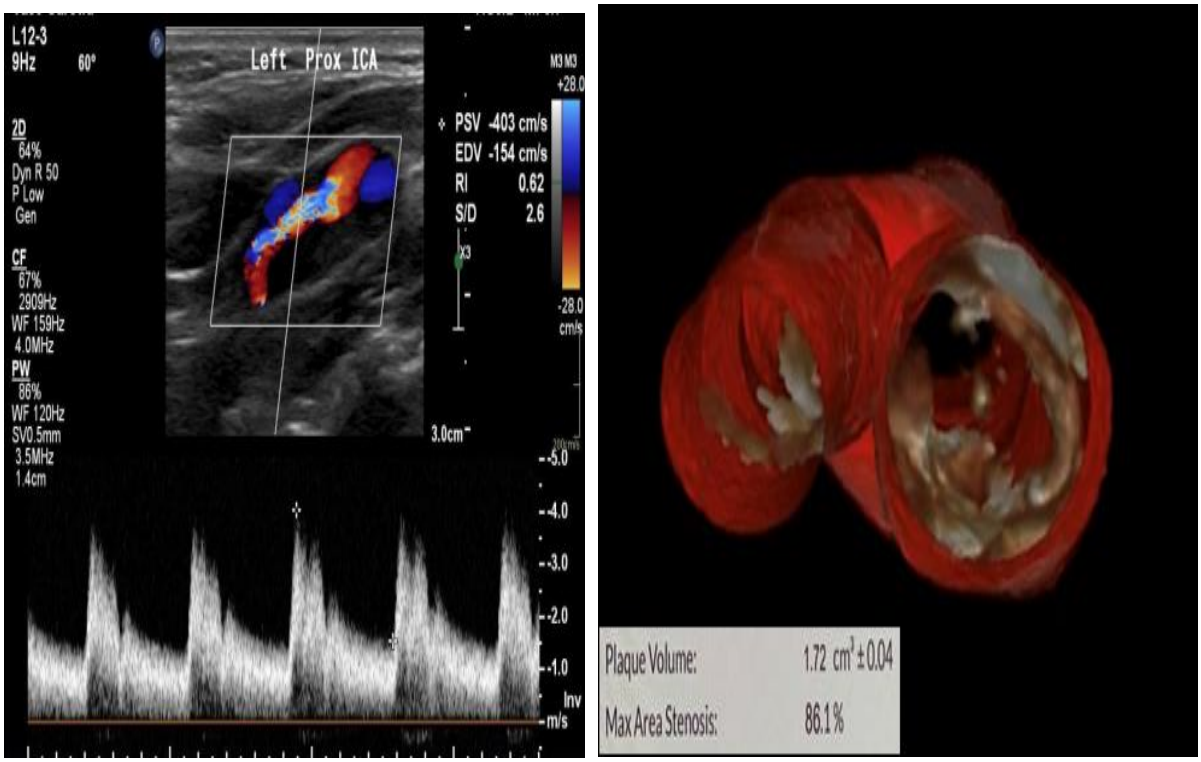

Figure 5. 1 Measurements of peak systolic velocity in 2DUS (A), plaque volume and maximum percentage of stenosis in t3DUS (B) in the internal carotid artery. 2DUS: 2D ultrasound; t3DUS: tomography 3D ultrasound.

The surgeon was asked to provide the entire carotid plaque specimen (Figure 5.2 A). Once removed from the patient, it was placed in a universal container filled with normal saline and taken immediately to the vascular laboratory for volume measurement using ergonomically designed MICROMAN E positive displacement pipettes (Figure 5.2 B).

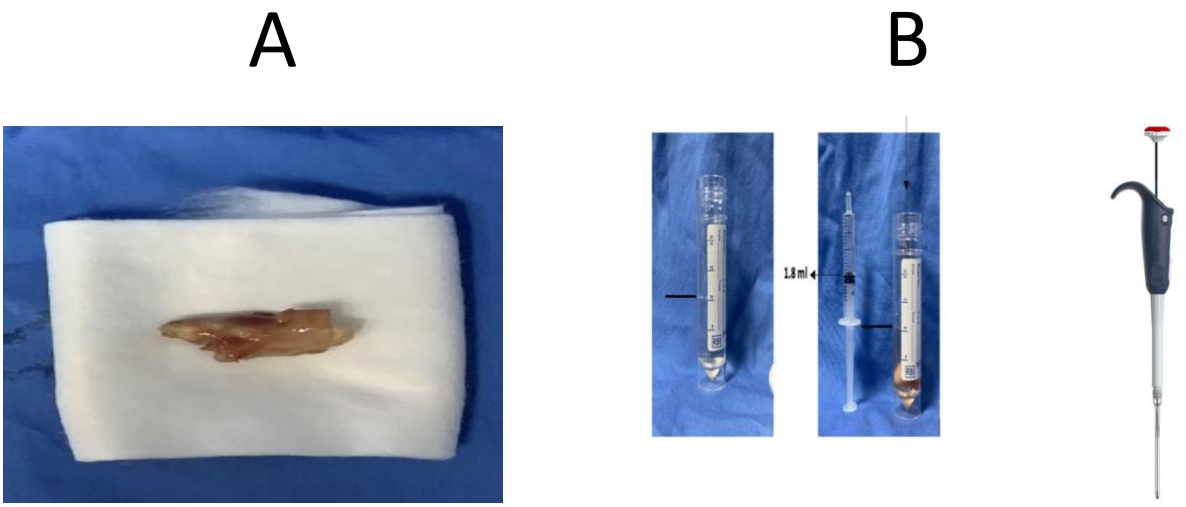

Figure 5. 2 Measurements of plaque volume from ICA post-CEA using water displacement method (reference test). Carotid plaque specimen (A). (B) MICROMAN E positive displacement pipettes, CEA: Carotid endarterectomy; ICA: Internal Carotid artery.

5.4 Statistical Analysis:

The accuracy of t3DUS in measuring CPV against reference standard test (i.e., water displacement method) and intra-observer reproducibility of t3DUS were assessed using Intraclass correlation coefficient (ICC); ICC <0.50 poor agreement; ICC 0.50-0.75 moderate agreement; ICC 0.76-0.90 good agreement; ICC >0.90 excellent agreement (148). Coefficient of determination (R^2, ranges 0-100%) was used to determine proportion percentage of variance in plaque volume measurements around the fitted regression line; R^2 < 50% poor variance; R^2 50-70% moderate variance; R^2 >70% excellent variance (149). Bland-Altman plot was used to establish bias and limit of agreement between CPV measured with t3DUS and reference standard test and betweent3DUS measurements (150). Mann Whitney U test was used to determine whether there is a significant difference in CPV measured using t3DUS and reference standard. Spearman's rank correlation coefficient (*r*) was used to determine the

relationship between CPV and PSV, and between CPV and DoS; *r* < 0.1 no correlation; *r* 0.1-0.39-week correlation; *r* 0.40-0.69 moderate correlation; *r* > 0.70 strong correlation (151). The level of significance was set at < 0.05. Statistical analysis was performed using IBM SPSS Statistics version 21 (Armonk, NY: IBM Corp) and GraphPad PRISM 7 (La Jolla, CA, USA).

5.5 Results:

5.5.1 Patient Characteristics

A total of 25 symptomatic patients with severe carotid stenosis (i.e., >70%) undergoing CEA were recruited. Patient demographics and clinical information is shown below.

CHARACTERISTICS	NUMBER OF PATIENTS n (%)
Gender	
Male	23 (92%)
Female	2 (8%)
Age (Years)	
Mean ±SD	72.4 ±6.2
Weight (Kg)	
mean ±SD	87.5 ±18.4
Comorbidities (n (%))	
Hypertension	12 (48%)
Diabetes	15 (60%)
Currently smoking	10 (40%)

Abbreviations: kg: kilogram, n: number of patients, SD: standard deviation.

Table 5. 1 Patients' demographics and clinical information (n=25).

5.5.2 Agreement between t3DUS and Reference Standards in Measuring CPV

There was an excellent agreement between t3DUS and reference standard (i.e., water displacement) in measuring CPV with an ICC value of 0.98 (95% confidence interval (CI) 0.97 – 0.99, p <0.001, number (n)=50 per technique, Figure 5.3A).

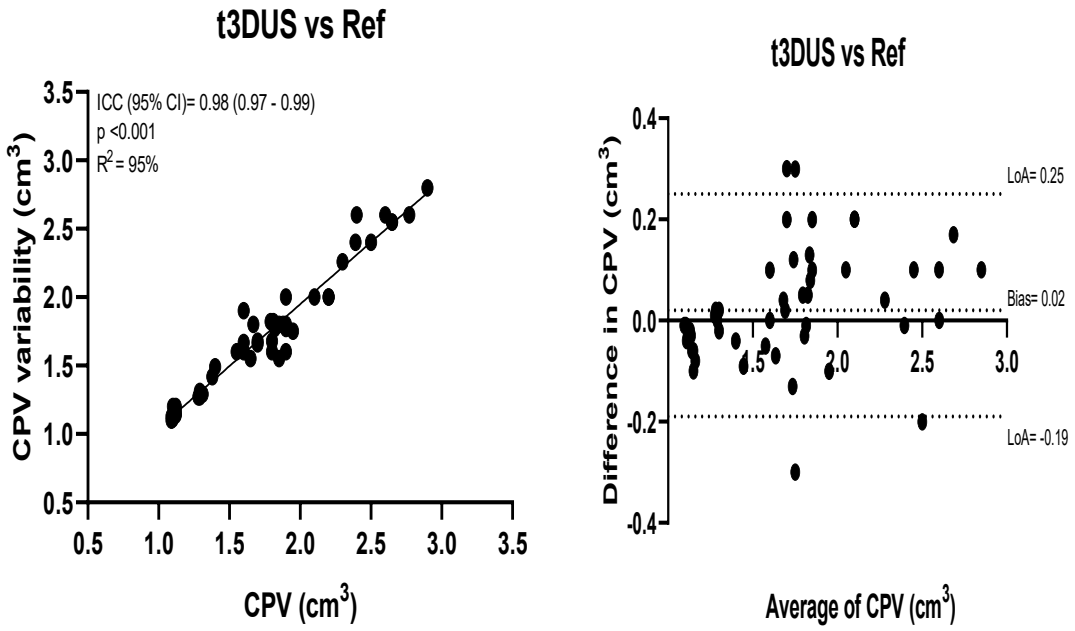

Figure 5. 3 Linear regression (A) and Bland-Altman agreement (B) of carotid plaque volume (CPV) measurements (n=50) between tomographic 3D ultrasound (t3DUS) and reference test (Ref). CI: confidence interval; ICC: Intraclass correlation; LOA = limit of agreement.

Bias in measurements was 0.02±0.11 cm^3 (95% limit of agreement (LoA) -0.19 – 0.25, n= 25, Figure 5.3B). The percentage of variance in CPV measurements between t3DUS and reference *standard* was excellent, with R^2= 95% around the fitted regression line (Figure 5.3A). Mann Whitney U test showed no significant difference between t3DUS and reference standard in measuring CPV (Z= -0.4, p = 0.68, Figure 5.4).

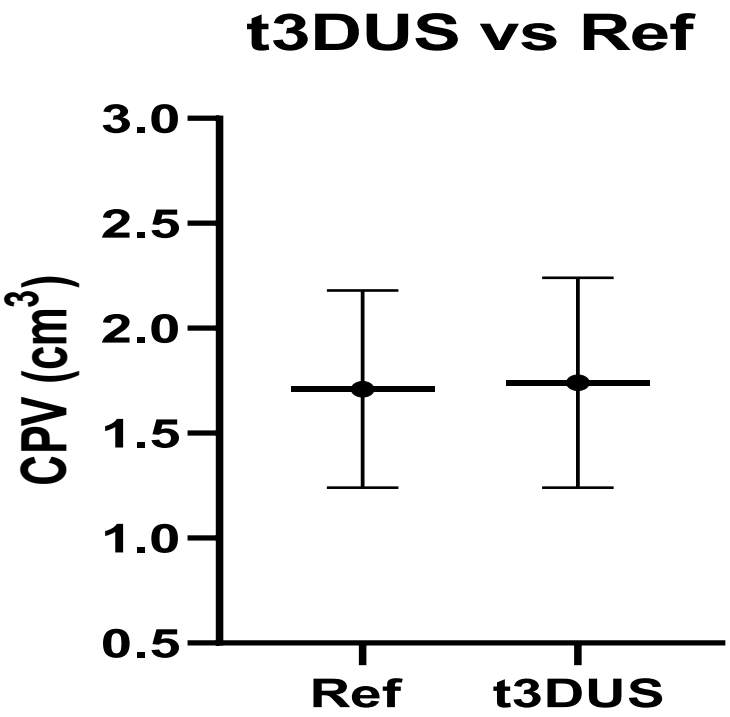

Figure 5. 4 Comparison of carotid plaque volume measurements (CPV) between tomographic 3D ultrasound (t3DUS) and reference test (Ref) (n=50). Mean ± SD, p=0.68 using Mann Whitney-U test.

5.6 Reproducibility of t3DUS in Measuring CPV:

Intra-observer agreement of *in-vivo* CPV measured using t3DUS in two different visits (n=50 in each visit) was excellent, with an ICC value of 0.95 (95% CI 0.92 – 0.97, p <0.001, Figure 5A). Bias in measurements was 0.004±0.07 cm^3 (95% limit of agreement (LoA) -0.14 – 0.15, Figure 5.5B). The percentage of variance in CPV measured by the same operator in two different visits using t3DUS was excellent, with R^2= 94% around the fitted regression line (Figure 5.5 A).

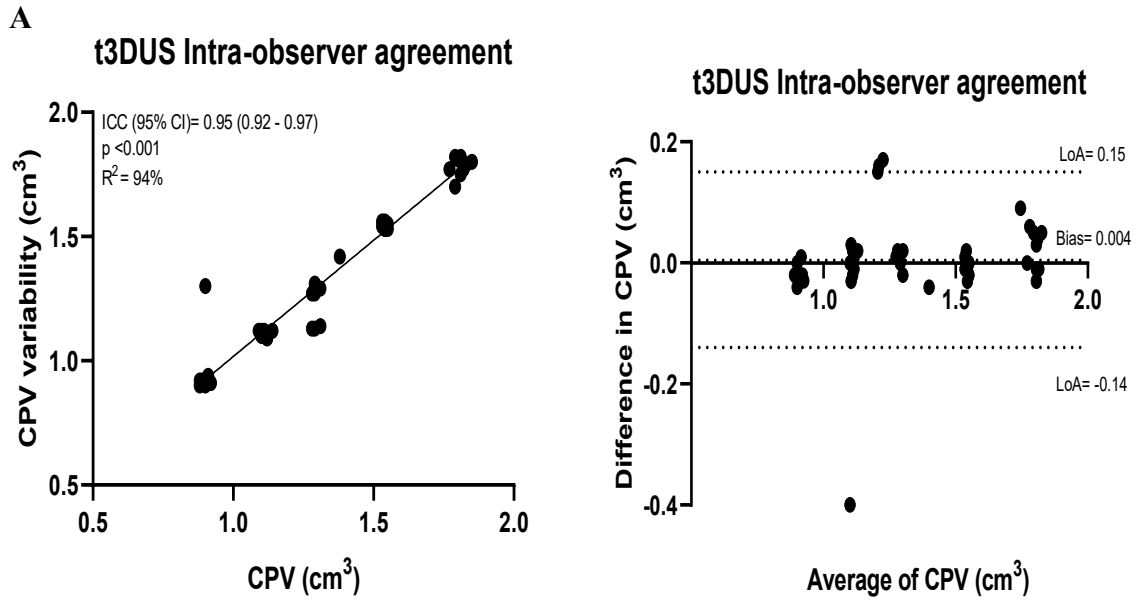

Figure 5. 5 Intra-observer and Bland-Altman agreement. Linear regression (A) and Bland-Altman agreement (B) of tomographic 3D ultrasound carotid plaque volume measurements (n=50). CI: confidence interval; ICC: Intraclass correlation; LOA = limit of agreement.

There is no correlation between CPV measured using t3DUS and PSV (*r* −0.031, p=0.88, Figure 5.6 A). Similarly, there is no correlation between CPV and DoS (*r* −0.026, p=0.90, Figure 5.6 B). There is a strong correlation between DoS and PSV (*r* 0.82, p<0.001, Figure 5.6 C).

A. B. C

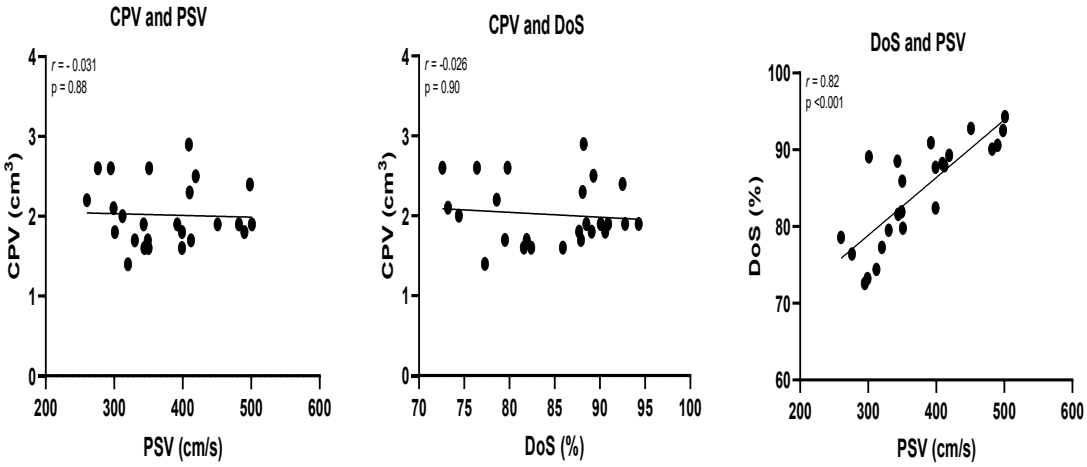

Figure 5. 6 Relationship between CPV measured using t3DUS and PSV and DoS.

5.7 Discussion:

CPV has gained interest as a predictor of recurrent ischemic stroke and cardiovascular events in symptomatic and asymptomatic patients and for assessing response to anti-atherosclerotic therapy. Due to the limited studies that investigated the accuracy of t3DUS for measuring CPV, we aimed to evaluate the reproducibility and accuracy of t3DUS for measuring CPV in patients undergoing CEA. There was an excellent agreement between t3DUS and reference test (i.e., water displacement method of *ex-vivo* plaque specimen post-CEA) and excellent intra-observer agreement of t3DUS in measuring CPV. No relationship between CPV and PSV or DoS. Similar findings were seen in a study done by Ball et al. (145) in which CPV was measured in 34 patients using t3DUS. The same study reported a significantly higher CPV in symptomatic than asymptomatic populations. These findings suggest that t3DUS is a reliable and reproducible method for measuring CPV and that CPV measured using t3DUS could be a valuable indicator for cerebral ischemic symptoms.

Reproducible and precise CPV quantification would require an accurate assessment of the cardiovascular system. Studies evaluating carotid stenosis using the freehand 3DUS imaging technique reported excellent reproducibility (Khan et al., 2017; Sandholt et al., 2018; Iommi et al., 2020). The range of reproducibility levels seen with the freehand scanning technique could be related to being operator-dependent. In our study, a semi-automated method developed by PIUR Imaging was used, and the operator only outlined the outer wall of the ICA. CPV was calculated automatically through the scanned area. In addition, the average time required for reconstructing 3D images and providing a report that includes the measurements

of CPV and maximum DoS is approximately 10 minutes. These make t3DUS a less operator-dependent and fast imaging tool for accurately assessing CPV.

It is well known that Doppler PSV is proportional to the degree of stenosis (DoS) (155). Our study revealed a strong positive relationship between PSV and Dos but not between CPV and PSV or DoS. Bell et al. (145) also showed no association between CPV and the severity of stenosis and that a decline in CPV over time following cerebral ischemic symptoms was not associated with significant changes in the severity of lumen stenosis. It has been reported that with the progression of CPV, the artery may enlarge to compensate for the reduction in the lumen area to maintain adequate blood flow to distal tissues, indicating that plaques could be present without causing stenosis or haemodynamic changes (139).

5.8 Study Limitations:

Limitations of this study were that patients with calcified plaque causing acoustics shadowing were excluded since t3DUS relies on the conventional B-mode 2DUS and that disadvantages of 2DUS will be translated into t3DUS [see (143) for more details]. In addition, t3DUS doesn't support Doppler features; thus, measuring PSV is not possible, indicating that t3DUS should be used alongside conventional 2DUS for a complete carotid examination. Only symptomatic patients with carotid plaque were included in the present study. Further studies investigating the association between CPV measured using t3DUS alongside severity of stenosis and potential risk of recurrent ischemic stroke and cardiovascular events are required.

5.9 Conclusion:

Free-hand t3DUS is a reproducible and accurate imaging method for measuring CPV. It showed excellent agreement with reference standards in measuring CPV. No relationship between CPV and PSV or DoS. Further studies investigating the reliability of t3DUS in assessing plaque morphological characteristics and composition to predict plaque vulnerability and responses to anti-atherosclerotic treatment in patients with carotid diseases and the association between CPV and measured using t3DUS and the potential risk of recurrent ischemic stroke and cardiovascular events are warranted.

t3DUS emerging technology is proving to be an advancement in the diagnostic accuracy of carotid stenosis; arterial disease is a generalised phenomenon, and lower limb arterial disease also has high morbidity and mortality. The next chapter will investigate the benefit of t3DUS scanning for lower limb arterial occlusive disease.

CHAPTER 6

COMPARISON BETWEEN 2DUS AND t3DUS FOR THE ASSESSMENT OF THE LOWER LIMB ARTERY

6.1 Introduction:

Peripheral Arterial Disease (PAD) is the third leading morbidity caused by atherosclerosis, following coronary heart disease and stroke, affecting more than 2 million adults worldwide (156). It increases cardiovascular morbidity and mortality of up to 10% of the global population (157,158). The risk of PAD increases with age and cardiovascular risk factors, including diabetes, hypertension, and smoking (159). PAD can lead to intermittent claudication (i.e., calf pain resolving with rest) or critical limb ischemia with rest pain (160,161). In severe PAD cases, revascularisation using angioplasty or arterial bypass surgery may be required to improve quality of life and avoid limb loss. For those with less severe PAD, structured walking exercises under conservative treatment or interventions stimulating calf muscle activity improved the patient's outcome (162).

2DUS is a cost-effective and safe imaging method for primary PAD screening and initial treatment planning (163,164). The severity of stenosis in the lower limb using ultrasound is determined through the flow velocity of each arterial segment based on the analysis of the Doppler spectral waveform (165). The velocity ratio is a widely accepted Duplex parameter for grading stenosis. It can eliminate the influence of confounding factors such as hypertension and hyperaemic responses that can lead to a systemic increase in blood flow velocity (166). The current criteria of velocity ratio using Duplex 2DUS for grading iliofemoral and femoral-popliteal segments are shown in Table 6.1 (167). The reported stenosis percentage has wide ranges, which makes it difficult to determine the exact degree of stenosis and if the disease is progressing and causing a greater degree of stenosis in follow-

up scanning. This may be an issue in patients who develop recurrent following intervention procedures.

STENOSIS (%)	VR (PSV AT STENOSIS / PSV PROXIMAL TO STENOSIS)
20%–49%	1.5–2
50%–80%	2–4
>80%	>4

Abbreviation: PSV: peak systolic velocity, VR: velocity ratio

Table 6. 1 Criteria for grading arterial stenosis in lower limbs stenosis using Duplex 2DUS (68)

t3DUS is a novel free-hand electromagnetically tracked system that can be coupled to any commercially available ultrasound machine and can provide a low-cost, rapid 3-D reconstruction of the vasculature (144). Several previous studies have shown the accuracy of t3DUS in measuring the length, diameter, and volume of an *ex-vivo* artery and plaque volume (144,145). A recent phantom study illustrated that semi-automated t3DUS is an accurate and reliable imaging method for grading vessel stenosis (143). This study aimed to provide a more precise measurement of superficial femoral artery (SFA) stenosis using t3DUS in patients with PAD by assessing its correlation with velocity ratio and comparing the measurements of the degree of stenosis using DR 2DUS and t3DUS.

6.1.1 Background

Treatment decision for PAD is governed by the severity of stenosis. t3DUS is a reliable imaging technique for measuring vessel stenosis. This study attempted to precisely measure SFA stenosis using t3DUS in patients with PAD.

6.1.2 Methods

t3DUS was used to measure the maximum stenosis percentage in SFA from 50 patients. Velocity ratio and diameter reduction at the most stenotic segment in SFA were calculated using 2DUS and DUS. The association between blood flow velocity ratio and the degree of stenosis measured using t3DUS was assessed using Spearman rank correlation. Paired t-test was used to compare stenosis measured using 2DUS and t3DUS.

6.1.3 Results

There was a strong positive correlation between velocity ratio and degree of stenosis in SFA measured using t3DUS (correlation value *(r)* = 0.99, $p<0.001$). There was a significant difference between t3DUS and DR 2DUS in measuring maximum stenosis in SFA with DR 2DUS under-estimating degree of stenosis (DR 2DUS vs t3DUS: mean difference -5.72%, 95% confidence interval -10.19 – -1.24, $p=0.01$).

6.2 Methods:

6.2.1 Study Design and Participants

This pilot trial was conducted in accordance with the declaration from the Health Research Authority (HRA) and Health and Care Research Wales (HCRW) under number 20/LO/0814 and approved by Imperial College London Ethics Committee. For this study, written informed consent was taken from recruited patients with PAD. Patients with a calcified plaque in SFA causing acoustic shadowing, large thigh circumference or unable to give informed consent were excluded.

This study performed a complete lower limb arterial ultrasound examination using a high-resolution premium Philips Elite ultrasound imaging system (Philips Healthcare, Bothell, WA, USA) with a 9-4MHz ultrasound transducer. The maximum stenotic segment in the SFA was defined using 2DUS Duplex ultrasound of arterial lower extremity pre-setting in which aliasing was noted. The PSV was measured at the maximum stenotic site and 1-2 cm proximal to aliasing, where laminar blood flow was observed for calculating the velocity ratio (VR = PSV within stenosis / PSV proximal to stenosis) (Figure 6.1 A, B).

For the DR measurement using 2DUS, the SFA was scanned in longitudinal view, and the diameter outer-to-outer (OTO) and residual lumen were measured using electronic callipers (Figures 6.1 C). The degree of stenosis was then determined using semi-automated t3DUS (PIUR imaging GmbH, Vienna, Austria) (Figures 6.1 D), following the exact method described

in our previous publication (143). All parameters were measured once by an experienced vascular scientist with efficient training on t3DUS for assessing vascular diseases.

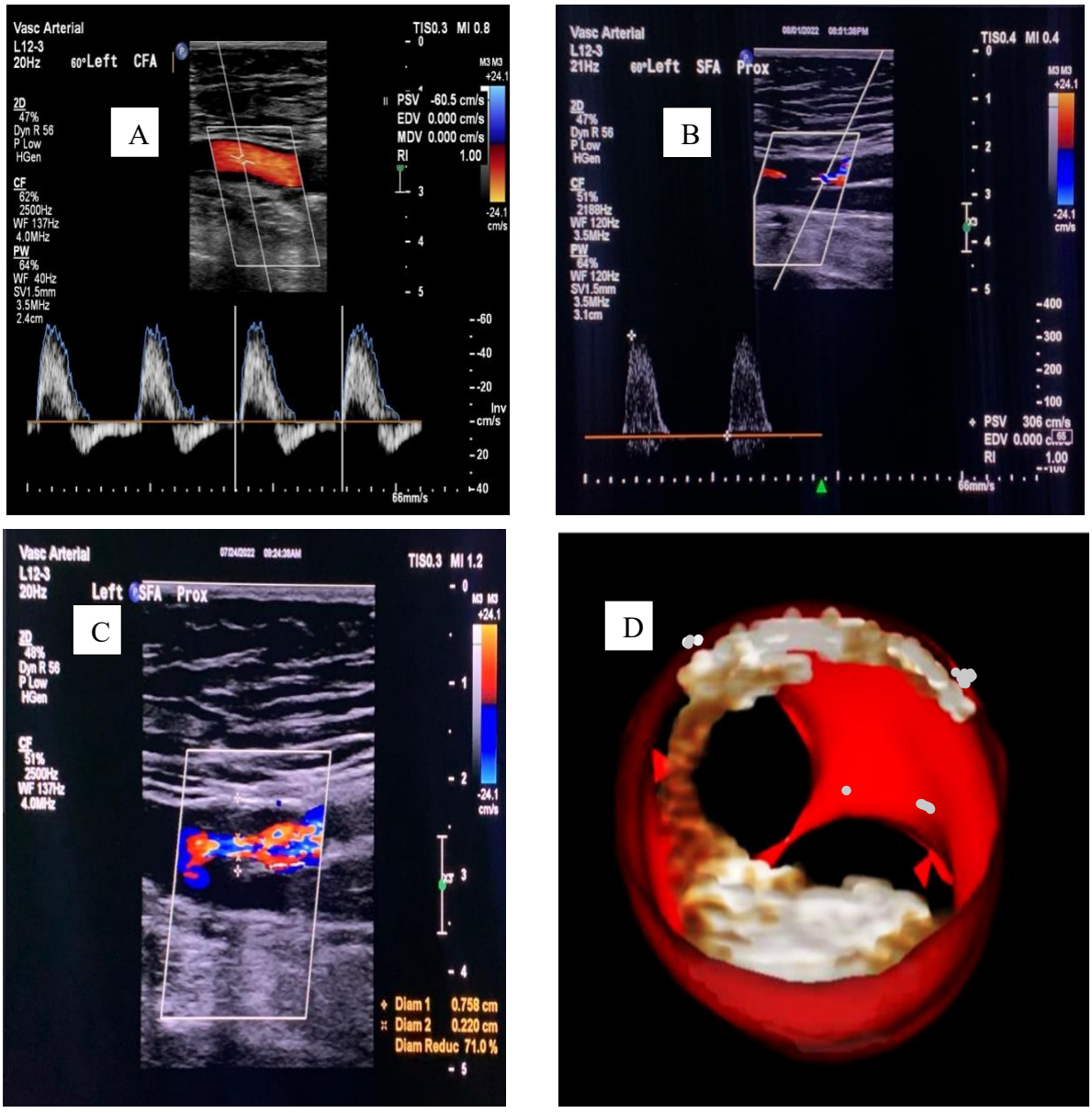

Figure 6. 1 Spectral waveform for measuring PSV pre stenotic area. B: PSV within the stenotic area. C: diameter reduction (DR) measurement using 2DUS. D: virtual t3DUS.

6.3 Statistical Analysis:

Spearman rank correlation was used to assess the association between blood flow velocity ratio and the degree of stenosis measured using t3DUS. Paired t-test was used to compare stenosis measured using 2DUS and t3DUS. The level of significance was set at < 0.05. Statistical analysis was performed using IBM SPSS Statistics version 21 (Armonk, NY: IBM Corp) and GraphPad PRISM 7 (La Jolla, CA, USA).

6.4 Results:

6.4.1 Patient Characteristics

A total of 50 patients with PAD and SFA stenosis were recruited. Patient demographics and clinical information is shown in Table 6.2.

CHARACTERISTICS	NUMBER OF PATIENTS n(%)
Gender	
Male	33 (66%)
Female	17 (34%)
Age (Years)	
Mean, ±SD	70 ±7.7
Height (m)	
Mean, ±SD	1.71 ±0.08
Weight (Kg)	
Mean, ±SD	105.8 ±11.7
Comorbidities	
Hypertension	11 (22%)
Diabetes	25 (50%)
Smoking	36 (72%)

Abbreviations: kg: kilogram, n: number of patients, SD: standard deviation

Table 6. 2 Patient demographics and clinical information (n=50).

6.4.2 Correlation between Velocity Ratio and Degree of Stenosis Measured Using t3DUS

There was a strong positive correlation between velocity ratio and degree of stenosis in SFA measured using t3DUS (correlation value *(r)* = 0.99, p<0.001, Figure 6.2).

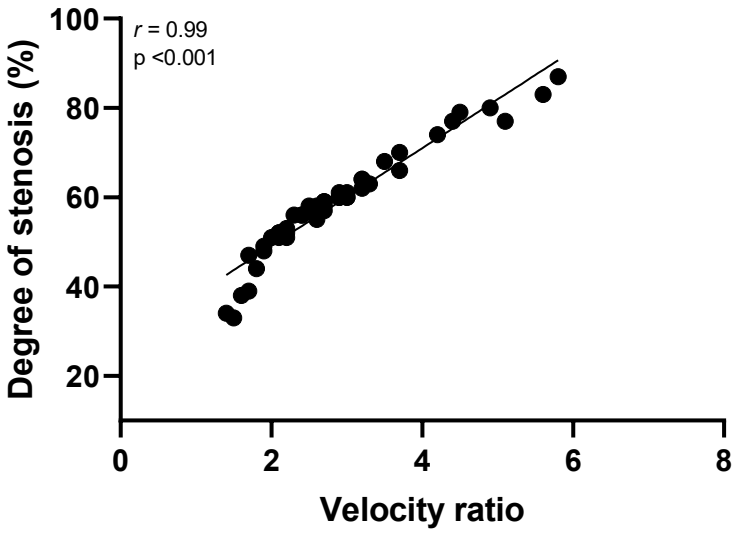

Figure 6. 2 Linear regression between velocity ratio and degree of stenosis in superficial femoral artery measured using tomographic 2D ultrasound (n=50).

6.4.3 Comparison between 2DUS and t3DUS in Measuring the Degree of Stenosis

There was a significant difference in under-estimation of DR 2DUS compared to t3DUS in measuring maximum stenosis of SFA (DR 2DUS vs t3DUS: mean difference -5.72%, 95% confidence interval -10.19 – -1.24, p=0.01, Figure 6.3).

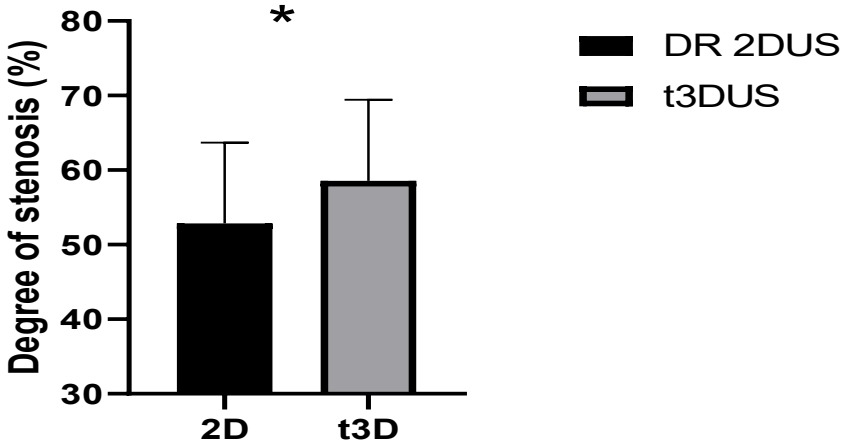

*Figure 6. 3 Comparison between DR 2DUS and t3DUS in measuring superficial femoral artery stenosis (mean ± SD, n=50). * p≤0.05 using Paired t-test between imaging techniques. DR: diameter reduction, 2DUS: 2D ultrasound; t3DUS: tomography 3D ultrasound.*

6.5 Discussion:

To the researcher's knowledge, this is the first study that attempted to precisely measure SFA stenosis using semi-automated t3DUS in patients with PAD. The newly established criteria for grading stenosis in SFA (Table 6.3) show that t3DUS can be used to predict precise measurement of the severity of arterial stenosis in lower extremities with a strong positive correlation with velocity ratio. This criterion can be applied to the current practice of using 2DUS for precise stenosis measurement in SFA, considering that DR 2DUS may underestimate the degree of stenosis. Further studies investigating the sensitivity of t3DUS in assessing patients with lower limb arterial diseases are required.

STENOSIS (%)	VR (PSV AT STENOSIS / PSV PROXIMAL TO STENOSIS)
<50	<2
50-54	2-2.4
55-59	2.5-2.9
60-64	3-3.4
65-69	3.5-3.9
70-74	4-4.4
75-79	4.5-4.9
>80	>5

Abbreviation: PSV: peak systolic velocity, VR: velocity ratio

Table 6. 3 Newly established Criteria for grading stenosis in SFA stenosis measured using t3DUS

PAD compromises blood flow supplying legs caused by atherosclerotic stenosis and occlusion, which can lead to limb ischemia (160). The severity of stenosis governs the treatment decision in patients with PAD. 2DUS is a safe and inexpensive imaging method, making it the first-line tool for assessing PAD (168). It has been reported that DUS has lower sensitivity in detecting stenosis, greater than 50%, compared to CTA and MRA (169). However, CTA involves ionising radiation, and CTA and MRA are more expensive imaging tools than ultrasound. Therefore, developing an accurate, reliable, cost-effective ultrasound imaging method is vital for assessing lower limb arterial stenosis.

A well-known disadvantage of 2DUS is being operator-dependent; thus, the outcome accuracy of 2DUS is highly dependent on the operator's skills and experience. In addition, measuring DR using B-mode 2DUS may under-estimating the degree of stenosis (143,170). This has also been noted in the present study. In addition, in the current Duplex 2DUS criteria, there are wide ranges of degrees of stenosis (reaching up to 25%, see Table 6.1), making it difficult to determine the exact degree of stenosis and to determine recurrent post-intervention, mainly if performed by an inexperienced operator. In the present study, the severity of SFA stenosis measured using semi-automated t3DUS showed a positive correlation with velocity ratio.

The accuracy and reproducibility of the semi-automated t3DUS for measuring stenosis have been investigated pre-clinically using a phantom with channels simulating superficial vasculature with a range of stenosis (i.e., 50%, 70% and 90%), showing that t3DUS has excellent intra-operator reproducibility and accurate stenosis measurements, suggesting that t3DUS is a reliable method for grading vessels stenosis (143). This may indicate that our established criteria for grading SFA stenosis using t3DUS are reliable and can be used by DUS by measuring the velocity ratio of a diseased segment for more precise grading of SFA stenosis. Further studies investigating the sensitivity of t3DUS for grading severe stenosis, near occlusion and occlusion in lower limb arteries are needed.

In this study, the use of t3DUS for grading arterial stenosis in the SFA was only assessed. Future studies are required to determine the infra-inguinal, supra, and infra-popliteal and foot arteries. The limitations of t3DUS for assessing vascular diseases have been addressed in previous studies (143,144), including calcified plaque limiting the 2D images to be

reconstructed into 3D images due to acoustic shadowing artefact. Also, in patients with large thigh circumference (≈45 perimeters) in which SFA is imaged at a depth of 7-8 cm, analysis was not possible with tomographic software. For these reasons, patients with calcified plaque and large thigh circumference were excluded. In addition, t3DUS doesn't support Doppler features, and that DUS is used for the measurements of velocity ratio.

6.6 Conclusion:

t3DUS can measure the severity of SFA in patients with lower extremities arterial disease. Grading of stenosis in SFA measured using t3DUS showed a strong positive correlation with the currently used velocity ratio and can be applied to the current practice using DUS for precise measurement of SFA stenosis. Further studies investigating the sensitivity and specificity of t3DUS in assessing stenosis in lower limb arteries are required. The established criteria for grading stenosis in SFA in this study can be applied to the current practice using 2DUS as it demonstrated a strong positive correlation with velocity ratio. Further studies investigating the sensitivity and specificity of t3DUS in assessing stenosis in lower limb arteries are required.

CHAPTER 7

GENERAL DISCUSSION AND CONCLUSION

The aim of this thesis was to assess the accuracy of the t3DUS. According to the data presented in this thesis, t3DUS can be reliably used for arterial geometry assessment with higher accuracy than traditional Ultrasound. In assessing CPV, it is known that atherosclerotic plaque appears in an irregularly shaped 3D phenomenon, and measurements performed by conventional 2DUS in a 2D plane may miss the true extent of plaque if it is out of visualised plan. In symptomatic patients, 3D evaluation of carotid plaque was more sensitive to clinically significant angiographic stenosis than 2D (171). However, measuring the changes within the plaque in the carotid artery is out of this thesis's scope. It requires a large sample size for more precise results and more time to observe carotid plaque volume changes. A previous study has demonstrated that carotid plaque morphology can change within three months. Progression or regression can be noted and used as a prediction from having further cardiovascular disease (172). A large population-based study conducted by Silleses et al. (171) showed that 3DUS used in their study identified more patients with carotid plaque than others using 2DUS. This indicates the superiority of 3DUS over 2DUS when scanning and assessing carotid disease.

3DUS has proven that it can detect and evaluate the shape and the surface of the carotid plaque (173). Among vascular scientists, there is a significant variation in differentiating between irregular plaque surface and ulcerated plaque. This confusion might be avoided by using 3DUS. Ulcerated plaque can lead to serious cardiovascular consequences; therefore, identifying and accurately diagnosing it would significantly impact a patient's treatment plan. Regardless of the severity of the stenosis, ulcerated plaque can increase the risk of stroke (174).

The other study for SFA grade of stenosis, t3DUS, was used to narrow the current criteria and grade of stenosis. Currently, a PSVR from 2- 4 indicates 50 – 80% stenosis. There is a gap of 30%, and each vascular scientist can use their judgments in quantifying and grading the stenosis >50% based on the PSVR criteria. This leads to significant variation, which may not be helpful for the vascular surgeon or interventional radiologist to make a treatment decision. In this thesis, both 2DUS applying current criteria for grading stenosis and t3DUS computerised degree of stenosis measurement were used to associate the degree of stenosis produced by the t3DUS with the PSV produced by 2DUS. It is essential to assess the stenotic areas accurately and the possibility of developing recurrent post-angiography. A review by Miller et al. (175) showed that out of 96 treated SFA lesions, 28 patients developed recurrent stenosis. This indicates that nearly 27% of treated SFA are likely to develop recurrent stenosis. Using 2DUS with current criteria will not provide any change within the progressions of the stenosis. Hence, it is important to use a more accurate percentage to observe the progression of the stenosis and to determine the need for intervention where required.

This research investigated the utility of t3DUS in diagnosing vascular disease, specifically within ICA and SFA. It has demonstrated the accuracy, repeatability, and precision of non-invasive t3DUS in three different clinical studies, phantom study and two clinical studies in ICA plaque volume measurements accuracy and in comparing the lower limb arterial system 2DUS with t3DUS for grading SFA stenosis. This study has contributed to the published literature whilst also providing the groundwork for future research into transluminal Ultrasound for vascular surgery.

This research argues that t3DUS might be used for carotid screening and assessing atherosclerosis with further research, which will interest the pharmaceutical sector; with tight coordination with contrast and Duplex manufacturers, A combination of ultrasound contrast agent and t3DUS might be the future of non-invasive angiogram without the need for radiological imaging. The applicability of t3DUS will only improve as the technology's hardware, and software continues to develop. One of the t3DUS advantages is that it can be used across many hospital departments and in the community to influence the management of large numbers of patients. It will expand as well as reach across many different medical fields. This is due to its small part sensor and its accessories which can be carried and moved from one machine to another. In addition to the first development, the long-term utility of t3DUS must include interventional and surgical guidance with augmented reality and the original product. Performing endovascular treatments safely by avoiding radiation and nephrotoxic contrast appeals to both the medical workforce and the public.

The use of Ultrasound in the diagnosis, management, and, hopefully, treatment of vascular disease has a secure place in modern medicine. t3DUS has the potential to enhance working circumstances for vascular scientists considerably whilst also highlighting more accurate and appropriate approaches to research and assess vascular disease for cardiovascular patients, which is a promising development.

Limitations and Future Research:

Although the scanning time has not been investigated in this research, t3DUS is likely much faster than the conventional 2DUS in terms of the scanning time. This is because of the time needed to scan the structures being investigated by 2DUS from different angles with a certain angle of insolation degree where the operator needs to obtain an adequate diagnostic image. In t3DUS, the operator needs to move the ultrasound probe, which has the t3DUS sensor attached to it, on the area of interest from the proximal to the distal level to generate a 3D image.

Scanning time is a point for future potential research where both scanning times can be compared. Suppose t3DUS is scientifically proven to provide a shorter scanning time. In that case, this will significantly impact the clinical flow within vascular surgery and the vascular imaging studies or vascular laboratories. Hence, more patients can be scanned with a shorter waiting list; therefore, more patients will be seen in the clinic.

The disparity between t3DUS and other imaging modalities like CTA for in-vivo diameter and volume measurements should be researched. The establishment of thresholds and the premise of application in artery disease screening are critical next steps in developing t3DUS technology. One of the weak points of using t3DUS is that it cannot provide a reasonable image quality when assessing deep vessels. This point is considered an obstacle and should be looked into for a better engineering solution in the future. For example, scanning AAA in slightly high BMI patients would not be achieved using the current version of t3DUS. The system may provide an adequate image with less quality, which may impact the

measurement’s accuracy. Virtual endoscopy is a critical element that will aid in adopting t3DUS; it’s a point of development the manufactories would look at in the future.

Other measures of plaque vulnerability should also be studied using t3DUS, in addition to the ones listed above. It is an excellent chance to design a tool that measures the plaque's morphology, known as Grey Scale Median (GSM). The current t3DUS provides GSM, but this has not been scientifically studied or correlated with other imaging techniques, such as shear wave elastography, to define accuracy for additional medical investigation tools with new criteria. The use of t3DUS histology to validate t3DUS GSM is an innovative approach.

The potential future directions of non-contrast-enhanced t3DUS are planning all forms of vascular procedures while extending the vascular team's reach into the community through screening and remote services.

Another point for future optional research is to compare current 2DUS with t3DUS for vein mapping can be investigated. Scanning the same patients using two different methods with two other images and result along with a questionnaire to the vascular surgeons would help define whether t3DUS can add more medial details with more accuracy. This may change the entire surgical plan and improve current misdiagnosis and measurement accuracy. The planning of radiofrequency ablation of varicose veins, endoscopic vein harvesting, and surgical and endo-AVF formation are some of the other interventional treatments that are now being investigated using t3DUS technology.

Completion imaging EVAR scans from t3DUS and rotational angiography to construct predictive algorithms for delayed endoleak and AAA growth at the intervention location should be focused on in future ultrasound contrast agent research. This could aid in developing individualised surveillance measures for patients at high risk. There is a variation between vascular centres in measuring AAA. Outer to outer and inner to inner measurements may confuse and lead to incorrect measurements.

Another point of research using t3DUS is measuring AAA and correlating it with other imaging modalities such as CT scan images. Future lower limb artery imaging research should investigate if post-reactive hyperaemia can improve the picture quality of tiny arteries in the lower limb. This method effectively depicts patent arteries with a sluggish, low-volume flow that may seem blocked even when there is no hyperaemia in the patient. 3D perfusion studies of muscle perfusion should also be investigated to determine viable perfusion thresholds that may be used to determine the level of amputation.

Because t3DUS is substantially faster than alternative imaging techniques, it should be developed into a portable and wireless technology significantly less expensive than the device employed in this study. However, this is not an essential advancement. Automation devices that are less expensive and more accurate will broaden the range of acceptable equipment and may use t3DUS for planning and intra-operative imaging, negating the necessity of radiographic exposure altogether. On the other hand, another challenging point is using t3DUS with attached software and computer, which may slow the process due to technical errors. The manufacturers must also look into the time post-scanning using t3DUS, which may delay the report's process.

The application of technology to t3DUS guiding within the operating setting with virtual reality is an attractive route to pursue in conjunction with t3DUS-guided interventional work, which is now being investigated. Randomised control trials are currently required to generate evidence to support the more comprehensive clinical implementation of t3DUS technology.

This research has brought many themes that will continue to be explored in future work. It is crucial for the future development of t3DUS that automation and advanced image analysis techniques, such as artificial intelligence (AI), are made available to users. Specifically, it is used for diameter and volume measurements. The usage of artificial intelligence for data gathering should also be explored to find any improvements that may be made in reducing or limiting the effect of image artefacts or other undesirable effects. Technology development using AI may become the best and easiest imaging method in scanning lower limb superficial venous systems for varicose veins. The current protocol for scanning varicose veins has its limitation and variation; in the future, t3DUS, along with AI, can overcome the current limitations by scanning the patient without needing to stand up for an extended period and have their calf muscles squeezed. AI may provide future technology where vascular surgeons can observe a live superficial venous system scan from their clinic and make their treatment plan and decision. This will reduce the scanning time and save recourses such as paper to draw the veins.

As with any other modality, there are some limitations points of both 2DUS and t3DUS. Current t3DUS overcomes some but not all the shortcomings of 2DUS, but it also has its drawbacks. The lack of Doppler information is a critical flaw. Currently, t3DUS imaging does not show a clear presentation of flow information. Although colour Doppler information can

show flow, it is difficult to read in t3DUS due to many colour Doppler artefacts. t3DUS, on the other hand, can be used to demonstrate patency with more accurate medical details. Although t3DUS spectral Doppler for velocity estimation is impossible, it would be beneficial in future if manufacturers consider this point and develop more scanning modes for t3DUS.

Motion artefact is another significant restriction of all methods of t3DUS imaging, including CT and MR, which can be mitigated to some extent. Respiratory motion can be controlled by holding one's breath. However, this is limited to brief, rapid 3D scans, and pulse gating can be used to avoid cardiac and artery wall motion. Physical patient movement on the couch is the most difficult to control, although it can be lowered by informing the patient to remain still. Because patient movement cannot be compensated for within tracking, patients with tremors may not be suitable, yet quick image collections with freehand systems may be limited (176).

Calcification is another issue that contributes to reducing image quality. Both 2DUS and t3DUS calcified arterial walls cause acoustic shadowing, which leads to an inability to assess that particular segment. However, t3DUS can be used to assess the calcified vessel virtually.

Computer science is necessary for t3DUS imaging but can also be a source of error. Most t3DUS systems employ sophisticated software based on complex computer algorithms (176), where faults in the coding of these algorithms might influence reconstruction accuracy. Still, these usually are visible when photos are evaluated. Although the ability to calculate disease volume is an exciting benefit of t3DUS, Fenster et al. (57) state that segmentation algorithms, the most common method for calculating volume, are lacking because they require significant time from experienced users manually calculate the volume slice by slice. The clinical

acceptability of t3DUS may depend on automatic segmentation methods. However, these have previously failed due to artefacts that cannot be read by the computer, such as calcium shadowing. Artefacts are particularly problematic for automatic segmentation methods because they signify a lack of information inside a specific image region that needs to be measured, such as calcium, which has a massive black gap due to acoustic shadowing. This is not correctly read by the computer, resulting in measurement error. Artificial intelligence technology may overcome this problem in the future through prediction.

References:

1. Naghavi M, Abajobir AA, Abbafati C, Abbas KM, Abd-Allah F, Abera SF, et al. Global, regional, and national age-sex specifc mortality for 264 causes of death, 1980-2016: A systematic analysis for the Global Burden of Disease Study 2016. The Lancet. 2017 Sep 16;390(10100):1151–210.
2. Namara KM, Alzubaidi H, Jackson JK. Cardiovascular disease as a leading cause of death: how are pharmacists getting involved? Integr Pharm Res Pract [Internet]. 2019 Feb [cited 2022 May 3];8:1. Available from: /pmc/articles/PMC6366352/
3. Sharma B, Chang A, Red-Horse K. Coronary Artery Development: Progenitor Cells and Differentiation Pathways. Annu Rev Physiol [Internet]. 2017 Feb 10 [cited 2022 Sep 17];79:1–19. Available from: https://pubmed.ncbi.nlm.nih.gov/27959616/
4. He L, Lui KO, Zhou B. The Formation of Coronary Vessels in Cardiac Development and Disease. Cold Spring Harb Perspect Biol [Internet]. 2020 May 1 [cited 2022 Sep 17];12(5). Available from: https://pubmed.ncbi.nlm.nih.gov/31636078/
5. Kuriakose D, Xiao Z. Pathophysiology and Treatment of Stroke: Present Status and Future Perspectives. Int J Mol Sci [Internet]. 2020 Oct 2 [cited 2022 Sep 15];21(20):1–24. Available from: https://pubmed.ncbi.nlm.nih.gov/33076218/
6. Sarikaya H, Ferro J, Arnold M. Stroke prevention--medical and lifestyle measures. Eur Neurol [Internet]. 2015 Apr 25 [cited 2022 Sep 15];73(3–4):150–7. Available from: https://pubmed.ncbi.nlm.nih.gov/25573327/
7. Musuka TD, Wilton SB, Traboulsi M, Hill MD. Diagnosis and management of acute ischemic stroke: speed is critical. CMAJ : Canadian Medical Association Journal

[Internet]. 2015 Sep 9 [cited 2022 Sep 15];187(12):887. Available from: /pmc/articles/PMC4562827/

8. Broughton BRS, Reutens DC, Sobey CG. Apoptotic mechanisms after cerebral ischemia. Stroke [Internet]. 2009 May 1 [cited 2022 Sep 15];40(5). Available from: https://pubmed.ncbi.nlm.nih.gov/19182083/

9. Wang J, Fields J, Zhao C, Langer J, Thimmulappa RK, Kensler TW, et al. Role of Nrf2 in protection against intracerebral hemorrhage injury in mice. Free Radic Biol Med [Internet]. 2007 Aug 1 [cited 2022 Sep 15];43(3):408–14. Available from: https://pubmed.ncbi.nlm.nih.gov/17602956/

10. Flaherty ML, Woo D, Haverbusch M, Sekar P, Khoury J, Sauerbeck L, et al. Racial variations in location and risk of intracerebral hemorrhage. Stroke [Internet]. 2005 May [cited 2022 Sep 15];36(5):934–7. Available from: https://pubmed.ncbi.nlm.nih.gov/15790947/

11. Testai FD, Aiyagari V. Acute hemorrhagic stroke pathophysiology and medical interventions: blood pressure control, management of anticoagulant-associated brain hemorrhage and general management principles. Neurol Clin [Internet]. 2008 Nov [cited 2022 Sep 15];26(4):963–85. Available from: https://pubmed.ncbi.nlm.nih.gov/19026899/

12. Kiani S, Aasen JG, Holbrook M, Khemka A, Sharmeen F, Leleiko RM, et al. Peripheral artery disease is associated with severe impairment of vascular function. Vasc Med [Internet]. 2013 Apr [cited 2022 Sep 15];18(2):72–8. Available from: https://pubmed.ncbi.nlm.nih.gov/23509089/

13. Firnhaber JM, Powell CS. Lower Extremity Peripheral Artery Disease: Diagnosis and Treatment. Am Fam Physician [Internet]. 2019 Mar 1 [cited 2022 Sep 15];99(6):362–9. Available from: https://pubmed.ncbi.nlm.nih.gov/30874413/

14. Marso SP, Hiatt WR. Peripheral arterial disease in patients with diabetes. J Am Coll Cardiol [Internet]. 2006 Mar 7 [cited 2022 Sep 15];47(5):921–9. Available from: https://pubmed.ncbi.nlm.nih.gov/16516072/

15. Jude EB, Eleftheriadou I, Tentolouris N. Peripheral arterial disease in diabetes--a review. Diabet Med [Internet]. 2010 Jan [cited 2022 Sep 15];27(1):4–14. Available from: https://pubmed.ncbi.nlm.nih.gov/20121883/

16. Pant S, Deshmukh A, Gurumurthy GS, Pothineni NV, Watts TE, Romeo F, et al. Inflammation and Atherosclerosis-Revisited.

17. Atherosclerosis: Causes, Symptoms, Risks & Tests [Internet]. [cited 2022 May 3]. Available from: https://my.clevelandclinic.org/health/diseases/16753-atherosclerosis-arterial-disease

18. Fujiwara K, Abe J, Heo KS, Abe JI. Shear Stress and Atherosclerosis. Mol Cells [Internet]. 2014 [cited 2022 May 3];37(6):435–40. Available from: http://dx.doi.org/10.14348/molcells.2014.0078http://creativecommons.org/licenses/by-nc-sa/3.0/.

19. Zhou J, Li YS, Chien S. Shear stress-initiated signaling and its regulation of endothelial function. Arterioscler Thromb Vasc Biol [Internet]. 2014 [cited 2022 May 3];34(10):2191–8. Available from: https://pubmed.ncbi.nlm.nih.gov/24876354/

20. Feaver RE, Gelfand BD, Wang C, Schwartz MA, Blackman BR. Atheroprone hemodynamics regulate fibronectin deposition to create positive feedback that

sustains endothelial inflammation. Circ Res [Internet]. 2010 Jun 11 [cited 2022 May 3];106(11):1703–11. Available from: https://pubmed.ncbi.nlm.nih.gov/20378855/

21. Ayer J, Charakida M, Deanfield JE, Celermajer DS. Lifetime risk: childhood obesity and cardiovascular risk. Eur Heart J [Internet]. 2015 Jun 7 [cited 2022 May 3];36(22):1371–6. Available from: https://pubmed.ncbi.nlm.nih.gov/25810456/

22. Mandviwala T, Khalid U, Deswal A. Obesity and Cardiovascular Disease: a Risk Factor or a Risk Marker? Curr Atheroscler Rep [Internet]. 2016 May 1 [cited 2022 May 3];18(5). Available from: https://pubmed.ncbi.nlm.nih.gov/26973130/

23. Balakumar P, Maung-U K, Jagadeesh G. Prevalence and prevention of cardiovascular disease and diabetes mellitus. Pharmacol Res [Internet]. 2016 Nov 1 [cited 2022 May 3];113(Pt A):600–9. Available from: https://pubmed.ncbi.nlm.nih.gov/27697647/

24. Allaire J, Vors C, Couture P, Lamarche B. LDL particle number and size and cardiovascular risk: anything new under the sun? Curr Opin Lipidol [Internet]. 2017 Jun 1 [cited 2022 May 3];28(3):261–6. Available from: https://pubmed.ncbi.nlm.nih.gov/28460374/

25. Sarzani R, Spannella F, Giulietti F, Balietti P, Cocci G, Bordicchia M. Cardiac Natriuretic Peptides, Hypertension and Cardiovascular Risk. High Blood Press Cardiovasc Prev [Internet]. 2017 Jun 1 [cited 2022 May 3];24(2):115–26. Available from: https://pubmed.ncbi.nlm.nih.gov/28378069/

26. Messner B, Bernhard D. Smoking and cardiovascular disease: mechanisms of endothelial dysfunction and early atherogenesis. Arterioscler Thromb Vasc Biol [Internet]. 2014 Mar [cited 2022 May 3];34(3):509–15. Available from: https://pubmed.ncbi.nlm.nih.gov/24554606/

27. S N R H Cl R = H Ticlopidine R = CO 2 CH 3 Clopidogrel.

28. Conte MS, Bradbury AW, Kolh P, White J v., Dick F, Fitridge R, et al. Global Vascular Guidelines on the Management of Chronic Limb-Threatening Ischemia. European Journal of Vascular and Endovascular Surgery [Internet]. 2019 Jul 1 [cited 2022 May 3];58(1):S1-S109.e33. Available from: http://www.ejves.com/article/S1078588419303806/fulltext

29. Viera AJ. Screening for Hypertension and Lowering Blood Pressure for Prevention of Cardiovascular Disease Events. Med Clin N Am [Internet]. 2017;101:701–12. Available from: http://dx.doi.org/10.1016/j.mcna.2017.03.003

30. Näslund U, Ng N, Lundgren A, Fhärm E, Grönlund C, Johansson H, et al. Visualization of asymptomatic atherosclerotic disease for optimum cardiovascular prevention (VIPVIZA): a pragmatic, open-label, randomised controlled trial. Lancet [Internet]. 2019 Jan 12 [cited 2022 May 3];393(10167):133–42. Available from: https://pubmed.ncbi.nlm.nih.gov/30522919/

31. Pomposelli F. Arterial imaging in patients with lower extremity ischemia and diabetes mellitus. J Vasc Surg [Internet]. 2010 [cited 2022 Sep 19];52(3 Suppl):81S-91S. Available from: https://pubmed.ncbi.nlm.nih.gov/20804938/

32. Kreitner KF, Kunz RP, Herber S, Martenstein S, Dorweiler B, Dueber C. MR angiography of the pedal arteries with gadobenate dimeglumine, a contrast agent with increased relaxivity, and comparison with selective intraarterial DSA. J Magn Reson Imaging [Internet]. 2008 Jan [cited 2022 Sep 19];27(1):78–85. Available from: https://pubmed.ncbi.nlm.nih.gov/18058929/

33. Iglesias J, Peña C. Computed tomography angiography and magnetic resonance angiography imaging in critical limb ischemia: an overview. Tech Vasc Interv Radiol

[Internet]. 2014 [cited 2022 Sep 19];17(3):147–54. Available from: https://pubmed.ncbi.nlm.nih.gov/25241315/

34. Eshed I, Rimon U, Novikov I, Goitein O, Konen E. Time-resolved MR angiography of the calf arteries using a phased array cardiac coil: comparison of visibility with standard three-step bolus chase MR angiography. Acta Radiol [Internet]. 2011 Nov [cited 2022 Sep 19];52(9):973–7. Available from: https://pubmed.ncbi.nlm.nih.gov/21982849/

35. Kaufmann TJ, Kallmes DF. Utility of MRA and CTA in the evaluation of carotid occlusive disease. Semin Vasc Surg [Internet]. 2005 [cited 2022 Sep 19];18(2):75–82. Available from: https://pubmed.ncbi.nlm.nih.gov/15986324/

36. U-King-Im JM, Trivedi RA, Graves MJ, Higgins NJ, Cross JJ, Tom BD, et al. Contrast-enhanced MR angiography for carotid disease: diagnostic and potential clinical impact. Neurology [Internet]. 2004 Apr 27 [cited 2022 Sep 19];62(8):1282–90. Available from: https://pubmed.ncbi.nlm.nih.gov/15111663/

37. lower legs arteries | MRA lower legs arteries anatomy [Internet]. [cited 2022 Sep 23]. Available from: https://mrimaster.com/anatomy%20lower%20leg%20arteries%20%20.html

38. Standards for intravascular contrast administration to adult patients. [cited 2022 Sep 17]; Available from: www.rcr.ac.uk

39. Sun Z. Diagnostic accuracy of multislice CT angiography in peripheral arterial disease. J Vasc Interv Radiol [Internet]. 2006 [cited 2022 Sep 17];17(12):1915–21. Available from: https://pubmed.ncbi.nlm.nih.gov/17185686/

40. Isaka Y, Hayashi H, Aonuma K, Horio M, Terada Y, Doi K, et al. Guideline on the use of iodinated contrast media in patients with kidney disease 2018. Clin Exp Nephrol

[Internet]. 2020 Jan 1 [cited 2022 Sep 12];24(1):1. Available from: /pmc/articles/PMC6949208/

41. Iwan E, Yang J, Enders J, Napp AE, Rief M, Dewey M. Patient preferences for development in MRI scanner design: a survey of claustrophobic patients in a randomized study. Eur Radiol [Internet]. 2021 Mar 1 [cited 2022 Sep 12];31(3):1325. Available from: /pmc/articles/PMC7880963/

42. Charlton PH, Harana JM, Vennin S, Li Y, Chowienczyk P, Alastruey J. Vascular Biology and Microcirculation: Modeling arterial pulse waves in healthy aging: a database for in silico evaluation of hemodynamics and pulse wave indexes. Am J Physiol Heart Circ Physiol [Internet]. 2019 Nov 11 [cited 2022 Sep 12];317(5):H1062. Available from: /pmc/articles/PMC6879924/

43. Teti~kovi~ E, Gaj{ek-Marchetti M, Matela J, Flis V. Three-Dimensional Ultrasonography for the Evaluation of Atherosclerotic Stenoses of the Carotid Trunk. Coll Antropol. 2001;25:511–20.

44. Wessels T, Harrer JU, Stetter S, Mull M, Klötzsch C. Three-dimensional assessment of extracranial Doppler sonography in carotid artery stenosis compared with digital subtraction angiography. Stroke. 2004 Aug;35(8):1847–51.

45. [Digital radiography--clinical application of digital subtraction angiography] - PubMed [Internet]. [cited 2022 Sep 15]. Available from: https://pubmed.ncbi.nlm.nih.gov/6355554/

46. Thomas AMK, Banerjee AK, Busch U. Classic papers in modern diagnostic radiology. Classic Papers in Modern Diagnostic Radiology. 2005;1–672.

47. Donald I, Macvicar J, Brown TG. Investigation of abdominal masses by pulsed ultrasound. Lancet [Internet]. 1958 Jun 7 [cited 2022 May 3];1(7032):1188–95. Available from: https://pubmed.ncbi.nlm.nih.gov/13550965/

48. Holmes JH, Howry DH. Ultrasonic diagnosis of abdominal disease. Am J Dig Dis [Internet]. 1963 Jan [cited 2022 May 3];8(1):12–32. Available from: https://pubmed.ncbi.nlm.nih.gov/13961407/

49. Barber FE, Baker DW, Nation AWC, Strandness DE, Reid JM. Ultrasonic duplex echo-Doppler scanner. IEEE Trans Biomed Eng [Internet]. 1974 [cited 2022 May 3];21(2):109–13. Available from: https://pubmed.ncbi.nlm.nih.gov/4818795/

50. Oglat AA, Matjafri MZ, Suardi N, Oqlat MA, Abdelrahman MA, Oqlat AA. A Review of Medical Doppler Ultrasonography of Blood Flow in General and Especially in Common Carotid Artery. J Med Ultrasound [Internet]. 2018 Jan 1 [cited 2022 Sep 12];26(1):3. Available from: /pmc/articles/PMC6029191/

51. Umemura S. Multi-element ultrasonic transducer. J Acoust Soc Am [Internet]. 1998 Jun 4 [cited 2022 May 4];82(5):1865. Available from: https://asa.scitation.org/doi/abs/10.1121/1.395737

52. Shahi F, Murali K. Variations in ultrasound scanning protocols in the UK for suspected deep vein thrombosis in outpatients. Phlebology [Internet]. 2013 Dec 1 [cited 2022 May 4];28(8):397–403. Available from: https://pubmed.ncbi.nlm.nih.gov/23969490/

53. Fenster A, Downey DB. Three-dimensional ultrasound imaging. Annu Rev Biomed Eng. 2000;2(2000):457–75.

54. ten Kate GL, van Dijk AC, van den Oord SCH, Hussain B, Verhagen HJM, Sijbrands EJG, et al. Usefulness of Contrast-Enhanced Ultrasound for Detection of Carotid Plaque Ulceration in Patients With Symptomatic Carotid Atherosclerosis. American Journal of

Cardiology [Internet]. 2013 Jul 15 [cited 2022 May 8];112(2):292–8. Available from: http://www.ajconline.org/article/S0002914913008254/fulltext

55. Fenster A, Downey DB, Cardinal HN. Three-dimensional ultrasound imaging. Phys Med Biol [Internet]. 2001 May [cited 2022 May 4];46(5). Available from: https://pubmed.ncbi.nlm.nih.gov/11384074/

56. Prager RW, Ijaz UZ, Gee AH, Treece GM. Three-dimensional ultrasound imaging. Proc Inst Mech Eng H [Internet]. 2010 Feb 1 [cited 2022 May 4];224(2):193–223. Available from: https://journals.sagepub.com/doi/10.1243/09544119JEIM586

57. Fenster A, Parraga G, Bax J. Three-dimensional ultrasound scanning. Interface Focus [Internet]. 2011 [cited 2022 May 4];1(4):503–19. Available from: https://pubmed.ncbi.nlm.nih.gov/22866228/

58. Smith WL, Lewis C, Bauman G, Rodrigues G, D'Souza D, Ash R, et al. Prostate volume contouring: A 3D analysis of segmentation using 3DTRUS, CT, and MR. Int J Radiat Oncol Biol Phys [Internet]. 2007 Mar 15 [cited 2022 May 4];67(4):1238–47. Available from: http://www.redjournal.org/article/S0360301606035115/fulltext

59. Downey DB, Fenster A, Williams JC. Clinical Utility of Three-dimensional US1. https://doi.org/101148/radiographics202.g00mc19559 [Internet]. 2000 Mar 1 [cited 2022 May 4];20(2):559–71. Available from: https://pubs.rsna.org/doi/epdf/10.1148/radiographics.20.2.g00mc19559

60. Vascular Ultrasound Machine Portfolio | Philips Healthcare [Internet]. [cited 2022 May 4]. Available from: https://www.usa.philips.com/healthcare/resources/landing/ultrasound-article-pages/vascular

61. Savord B, Solomon R. Fully sampled matrix transducer for real time 3D ultrasonic imaging. Proceedings of the IEEE Ultrasonics Symposium. 2003;1:945–53.

62. Bredahl K, Sandholt B, Lönn L, Rouet L, Ardon R, Eiberg JP, et al. Three-Dimensional Ultrasound Evaluation of Small Asymptomatic Abdominal Aortic Aneurysms. European Journal of Vascular and Endovascular Surgery [Internet]. 2015 Mar 1 [cited 2022 May 4];49(3):289–96. Available from: http://www.ejves.com/article/S1078588414006996/fulltext

63. Gargiulo M, Gallitto E, Serra C, Freyrie A, Mascoli C, Bianchini Massoni C, et al. Could four-dimensional contrast-enhanced ultrasound replace computed tomography angiography during follow up of fenestrated endografts? Results of a preliminary experience. Eur J Vasc Endovasc Surg [Internet]. 2014 Nov 1 [cited 2022 May 4];48(5):536–42. Available from: https://pubmed.ncbi.nlm.nih.gov/25023904/

64. Downey DB, Fenster A, Williams JC. Clinical Utility of Three-dimensional US1. https://doi.org/101148/radiographics202.g00mc19559 [Internet]. 2000 Mar 1 [cited 2022 May 4];20(2):559–71. Available from: https://pubs.rsna.org/doi/abs/10.1148/radiographics.20.2.g00mc19559

65. Kot BCW, Sin DMH, Ying M. Evaluation of the accuracy and reliability of two 3-dimensional sonography methods in volume measurement of small structures: an in vitro phantom study. J Clin Ultrasound [Internet]. 2009 Feb [cited 2022 May 4];37(2):82–8. Available from: https://pubmed.ncbi.nlm.nih.gov/18803314/

66. PIUR tUS Infinity - piur imaging [Internet]. [cited 2022 Sep 21]. Available from: https://piurimaging.com/piur-tus-infinity/

67. Doppler Flow Pump - CIRS [Internet]. [cited 2022 Sep 25]. Available from: https://www.cirsinc.com/products/ultrasound/zerdine-hydrogel/doppler-flow-pump/

68. Arterial Duplex Ultrasonography – The Society for Vascular Medicine [Internet]. [cited 2022 Sep 25]. Available from: https://myperipheralarterydisease.com/health-care-providers/algorithmic-approach-and-pathway-to-pad-diagnosis/arterial-duplex-ultrasonography/

69. de Weerd M, Greving JP, de Jong AWF, Buskens E, Bots ML. Prevalence of asymptomatic carotid artery stenosis according to age and sex: systematic review and metaregression analysis. Stroke [Internet]. 2009 Apr 1 [cited 2022 Sep 20];40(4):1105–13. Available from: https://pubmed.ncbi.nlm.nih.gov/19246704/

70. de Weerd M, Greving JP, Hedblad B, Lorenz MW, Mathiesen EB, O'Leary DH, et al. Prevalence of asymptomatic carotid artery stenosis in the general population: an individual participant data meta-analysis. Stroke [Internet]. 2010 Jun [cited 2022 Sep 20];41(6):1294–7. Available from: https://pubmed.ncbi.nlm.nih.gov/20431077/

71. Hoskins PR, Martin K, Thrush A. Diagnostic ultrasound, third edition: Physics and equipment. Diagnostic Ultrasound, Third Edition: Physics and Equipment. 2019 Apr 29;1–387.

72. Dhawan SS, Nanjundappa RPA, Branch JR, Taylor WR, Quyyumi AA, Jo H, et al. Shear stress and plaque development. Expert Rev Cardiovasc Ther [Internet]. 2010 Apr [cited 2022 Sep 20];8(4):545–56. Available from: https://pubmed.ncbi.nlm.nih.gov/20397828/

73. Medical sciences | WorldCat.org [Internet]. [cited 2022 Sep 20]. Available from: https://www.worldcat.org/title/863854665

74. Saxena A, Ng EYK, Lim ST. Imaging modalities to diagnose carotid artery stenosis: progress and prospect. Biomed Eng Online [Internet]. 2019 May 28 [cited 2022 Sep 20];18(1). Available from: https://pubmed.ncbi.nlm.nih.gov/31138235/

75. Finn A v., Nakano M, Narula J, Kolodgie FD, Virmani R. Concept of vulnerable/unstable plaque. Arterioscler Thromb Vasc Biol [Internet]. 2010 Jul [cited 2022 Sep 20];30(7):1282–92. Available from: https://pubmed.ncbi.nlm.nih.gov/20554950/

76. Carotid artery stenosis - Symptoms, diagnosis and treatment | BMJ Best Practice [Internet]. [cited 2022 Sep 20]. Available from: https://bestpractice.bmj.com/topics/en-gb/1205

77. Kheiri B, Osman M, Abdalla A, Haykal T, Swaid B, Ahmed S, et al. Clopidogrel and aspirin after ischemic stroke or transient ischemic attack: an updated systematic review and meta-analysis of randomized clinical trials. J Thromb Thrombolysis. 2019 Feb 15;47(2):233–47.

78. Overview | Carotid artery stent placement for asymptomatic extracranial carotid stenosis | Guidance | NICE [Internet]. [cited 2022 Sep 20]. Available from: https://www.nice.org.uk/guidance/ipg388

79. Palombo C, Kozakova M, Morizzo C, Andreuccetti F, Tondini A, Palchetti P, et al. Ultrafast three-dimensional ultrasound: application to carotid artery imaging. Stroke [Internet]. 1998 [cited 2022 Sep 20];29(8):1631–7. Available from: https://pubmed.ncbi.nlm.nih.gov/9707205/

80. Yao J, van Sambeek MRHM, Dall'Agata A, van Dijk LC, Kozakova M, Koudstaal PJ, et al. Three-dimensional ultrasound study of carotid arteries before and after endarterectomy; analysis of stenotic lesions and surgical impact on the vessel. Stroke [Internet]. 1998 [cited 2022 Sep 20];29(10):2026–31. Available from: https://pubmed.ncbi.nlm.nih.gov/9756576/

81. Schminke U, Motsch L, Hilker L, Kessler C. Three-dimensional ultrasound observation of carotid artery plaque ulceration. Stroke [Internet]. 2000 [cited 2022 Sep 20];31(7):1651–5. Available from: https://pubmed.ncbi.nlm.nih.gov/10884468/

82. Kozàkovà M, Morizzo C, Andreucetti F, Palchetti P, Parenti G, Palombo C. Quantification of extracranial carotid artery stenosis by ultrafast three-dimensional ultrasound. Journal of the American Society of Echocardiography [Internet]. 2001 [cited 2022 Sep 20];14(12):1203–11. Available from: https://pubmed.ncbi.nlm.nih.gov/11734788/

83. Landry A, Fenster A. Theoretical and experimental quantification of carotid plaque volume measurements made by three-dimensional ultrasound using test phantoms. Med Phys [Internet]. 2002 [cited 2022 May 5];29(10):2319–27. Available from: https://pubmed.ncbi.nlm.nih.gov/12408306/

84. Bucek RA, Reiter M, Dirisamer A, Haumer M, Fritz A, Minar E, et al. Three-Dimensional Color Doppler Sonography in Carotid Artery Stenosis. AJNR Am J Neuroradiol [Internet]. 2003 Aug [cited 2022 May 6];24(7):1294. Available from: /pmc/articles/PMC7973656/

85. Wessels T, Harrer JU, Stetter S, Mull M, Klötzsch C. Three-dimensional assessment of extracranial Doppler sonography in carotid artery stenosis compared with digital subtraction angiography. Stroke [Internet]. 2004 Aug [cited 2022 Sep 20];35(8):1847–51. Available from: https://pubmed.ncbi.nlm.nih.gov/15205489/

86. Ainsworth CD, Blake CC, Tamayo A, Beletsky V, Fenster A, Spence JD. 3D ultrasound measurement of change in carotid plaque volume: a tool for rapid evaluation of new therapies. Stroke [Internet]. 2005 Sep [cited 2022 May 6];36(9):1904–9. Available from: https://pubmed.ncbi.nlm.nih.gov/16081857/

87. Landry A, Spence JD, Fenster A. Quantification of carotid plaque volume measurements using 3D ultrasound imaging. Ultrasound Med Biol [Internet]. 2005 Jun [cited 2022 Sep 20];31(6):751–62. Available from: https://pubmed.ncbi.nlm.nih.gov/15936491/

88. Egger M, Spence JD, Fenster A, Parraga G. Validation of 3D ultrasound vessel wall volume: an imaging phenotype of carotid atherosclerosis. Ultrasound Med Biol [Internet]. 2007 Jun [cited 2022 May 6];33(6):905–14. Available from: https://pubmed.ncbi.nlm.nih.gov/17445962/

89. Chiu B, Egger M, Spence JD, Parraga G, Fenster A. Quantification of carotid vessel wall and plaque thickness change using 3D ultrasound images. Med Phys [Internet]. 2008 [cited 2022 May 6];35(8):3691–710. Available from: https://pubmed.ncbi.nlm.nih.gov/18777929/

90. Krasinski A, Chiu B, Fenster A, Parraga G. Magnetic resonance imaging and three-dimensional ultrasound of carotid atherosclerosis: mapping regional differences. J Magn Reson Imaging [Internet]. 2009 Apr [cited 2022 May 6];29(4):901–8. Available from: https://pubmed.ncbi.nlm.nih.gov/19306431/

91. Krasinski A, Chiu B, Spence JD, Fenster A, Parraga G. Three-dimensional ultrasound quantification of intensive statin treatment of carotid atherosclerosis. Ultrasound Med Biol [Internet]. 2009 Nov [cited 2022 May 6];35(11):1763–72. Available from: https://pubmed.ncbi.nlm.nih.gov/19647921/

92. Kalashyan H, Saqqur M, Shuaib A, Romanchuk H, Nanda NC, Becher H. Comprehensive and Rapid Assessment of Carotid Plaques in Acute Stroke Using a New Single Sweep Method for Three-Dimensional Carotid Ultrasound. Echocardiography [Internet]. 2013 Apr 1 [cited 2022 May 6];30(4):414–8. Available from: https://onlinelibrary.wiley.com/doi/full/10.1111/echo.12128

93. Kalashyan H, Shuaib A, Gibson PH, Romanchuk H, Saqqur M, Khan K, et al. Single sweep three-dimensional carotid ultrasound: reproducibility in plaque and artery volume measurements. Atherosclerosis [Internet]. 2014 [cited 2022 May 5];232(2):397–402. Available from: https://pubmed.ncbi.nlm.nih.gov/24468154/

94. A van E, T W, G P, WJ N, A F, JD S, et al. Three-dimensional carotid ultrasound plaque texture predicts vascular events. Stroke [Internet]. 2014 Sep 1 [cited 2022 Sep 20];45(9):2695–701. Available from: https://pubmed.ncbi.nlm.nih.gov/25034714/

95. Almuhanna K, Hossain MM, Zhao L, Fischell J, Kowalewski G, Dux M, et al. Carotid plaque morphometric assessment with three-dimensional ultrasound imaging. J Vasc Surg [Internet]. 2015 Mar 1 [cited 2022 May 5];61(3):690–7. Available from: https://pubmed.ncbi.nlm.nih.gov/25499716/

96. Kumar A, Yang EY, Brunner G, Murray TO, Virani SS, Garami Z, et al. Plaque Volume of Carotid Endarterectomy Specimens Measured by 3D Ultrasound Technology. JACC Cardiovasc Imaging [Internet]. 2016 Sep 1 [cited 2022 May 5];9(9):1118–9. Available from: https://pubmed.ncbi.nlm.nih.gov/26684968/

97. Leong SS, Vijayananthan A, Yaakup NA, Shah N, Ng KH, Acharya UR, et al. Observer performance in characterization of carotid plaque texture and surface characteristics with 3D versus 2D ultrasound. Comput Biol Med [Internet]. 2016 Nov 1 [cited 2022 May 6];78:58–64. Available from: https://pubmed.ncbi.nlm.nih.gov/27658262/

98. Kalashyan H, Saqqur M, Becher H, O'Kelly C, Romanchuk H, Khan K, et al. Three-Dimensional and Conventional Carotid Ultrasound for Assessment of Carotid Plaque in a Stroke Patient: A Simple Way to Validate Findings. Can J Cardiol [Internet]. 2017 Mar 1 [cited 2022 May 6];33(3):412.e1-412.e3. Available from: https://pubmed.ncbi.nlm.nih.gov/28232021/

99. Khan AA, Koudelka C, Goldstein C, Zhao L, Yokemick J, Dux M, et al. Semiautomatic quantification of carotid plaque volume with three-dimensional ultrasound imaging. J Vasc Surg [Internet]. 2017 May 1 [cited 2022 May 6];65(5):1407–17. Available from: https://pubmed.ncbi.nlm.nih.gov/28274755/

100. Pelz JO, Weinreich A, Karlas T, Saur D. Evaluation of Freehand B-Mode and Power-Mode 3D Ultrasound for Visualisation and Grading of Internal Carotid Artery Stenosis. PLoS One [Internet]. 2017 Jan 1 [cited 2022 May 8];12(1). Available from: https://pubmed.ncbi.nlm.nih.gov/28045903/

101. Landry A, Spence JD, Fenster A. Measurement of carotid plaque volume by 3-dimensional ultrasound. Stroke [Internet]. 2004 Apr [cited 2022 Sep 20];35(4):864–9. Available from: https://pubmed.ncbi.nlm.nih.gov/15017019/

102. SS V, A A, HJ A, EJ B, MS B, CW C, et al. Heart Disease and Stroke Statistics-2021 Update: A Report From the American Heart Association. Circulation [Internet]. 2021 [cited 2022 May 8];143(8):E254–743. Available from: https://pubmed.ncbi.nlm.nih.gov/33501848/

103. Roth GA, Abate D, Abate KH, Abay SM, Abbafati C, Abbasi N, et al. Global, regional, and national age-sex-specific mortality for 282 causes of death in 195 countries and territories, 1980–2017: a systematic analysis for the Global Burden of Disease Study 2017. The Lancet [Internet]. 2018 Nov 10 [cited 2022 May 8];392(10159):1736–88. Available from: http://www.thelancet.com/article/S0140673618322037/fulltext

104. Frostegård J. Immunity, atherosclerosis and cardiovascular disease. BMC Med [Internet]. 2013 May 1 [cited 2022 May 8];11(1):1–13. Available from: https://bmcmedicine.biomedcentral.com/articles/10.1186/1741-7015-11-117

105. Cole JW. Large Artery Atherosclerotic Occlusive Disease. Continuum (Minneap Minn) [Internet]. 2017 Feb 1 [cited 2022 May 8];23(1, Cerebrovascular Disease):133–57. Available from: https://pubmed.ncbi.nlm.nih.gov/28157748/

106. Naylor AR, Ricco JB, de Borst GJ, Debus S, de Haro J, Halliday A, et al. Editor's Choice - Management of Atherosclerotic Carotid and Vertebral Artery Disease: 2017 Clinical Practice Guidelines of the European Society for Vascular Surgery (ESVS). Eur J Vasc Endovasc Surg [Internet]. 2018 Jan 1 [cited 2022 May 8];55(1):3–81. Available from: https://pubmed.ncbi.nlm.nih.gov/28851594/

107. Zamani M, Skagen K, Scott H, Russell D, Skjelland M. Advanced ultrasound methods in assessment of carotid plaque instability: a prospective multimodal study. BMC Neurol [Internet]. 2020 Jan 29 [cited 2022 May 8];20(1). Available from: https://pubmed.ncbi.nlm.nih.gov/31996153/

108. Barratt DC, Ariff BB, Humphries KN, McG Thom SA, Hughes AD. Reconstruction and quantification of the carotid artery bifurcation from 3-D ultrasound images. IEEE Trans Med Imaging [Internet]. 2004 May [cited 2022 May 8];23(5):567–83. Available from: https://pubmed.ncbi.nlm.nih.gov/15147010/

109. Calogero E, Fabiani I, Pugliese NR, Santini V, Ghiadoni L, di Stefano R, et al. Three-Dimensional Echographic Evaluation of Carotid Artery Disease. J Cardiovasc Echogr [Internet]. 2018 Oct 1 [cited 2022 May 8];28(4):218–27. Available from: https://pubmed.ncbi.nlm.nih.gov/30746325/

110. Heliopoulos J, Vadikolias K, Piperidou C, Mitsias P. Detection of carotid artery plaque ulceration using 3-dimensional ultrasound. J Neuroimaging [Internet]. 2011 Apr [cited 2022 May 8];21(2):126–31. Available from: https://pubmed.ncbi.nlm.nih.gov/19888925/

111. Pelz JO, Weinreich A, Fritzsch D, Saur D. Quantification of Internal Carotid Artery Stenosis with 3D Ultrasound Angiography. Ultraschall Med [Internet]. 2015 Oct 1 [cited 2022 May 8];36(5):487–93. Available from: https://pubmed.ncbi.nlm.nih.gov/25607630/

112. Pelz JO, Weinreich A, Schob S, Saur D. Multiparametric 3D Contrast-Enhanced Ultrasound to Assess Internal Carotid Artery Stenosis: A Pilot Study. J Neuroimaging [Internet]. 2020 Jan 1 [cited 2022 May 8];30(1):82–9. Available from: https://pubmed.ncbi.nlm.nih.gov/31498524/

113. Yuan J, Usman A, Das T, Patterson AJ, Gillard JH, Graves MJ. Imaging Carotid Atherosclerosis Plaque Ulceration: Comparison of Advanced Imaging Modalities and Recent Developments. AJNR Am J Neuroradiol [Internet]. 2017 Apr 1 [cited 2022 May 8];38(4):664–71. Available from: https://pubmed.ncbi.nlm.nih.gov/28007772/

114. Wessels T, Harrer JU, Stetter S, Mull M, Klötzsch C. Three-dimensional assessment of extracranial Doppler sonography in carotid artery stenosis compared with digital subtraction angiography. Stroke. 2004;35(8):1847–51.

115. Heliopoulos J, Vadikolias K, Piperidou C, Mitsias P. Detection of Carotid Artery Plaque Ulceration Using 3-Dimensional Ultrasound. Journal of Neuroimaging. 2011 Apr;21(2):126–31.

116. Yuan J, Usman A, Das T, Patterson AJ, Gillard JH, Graves MJ. Imaging carotid atherosclerosis plaque ulceration: Comparison of advanced imaging modalities and recent developments. American Journal of Neuroradiology. 2017.

117. Pelz JO, Weinreich A, Fritzsch D, Saur D. Quantification of internal carotid artery stenosis with 3D ultrasound angiography. Ultraschall in der Medizin. 2015;

118. Pelz JO, Weinreich A, Karlas T, Saur D. Evaluation of freehand B-Mode and power-Mode 3D ultrasound for visualisation and grading of internal carotid artery stenosis. PLoS One. 2017;12(1):1–11.

119. Pelz JO, Weinreich A, Schob S, Saur D. Multiparametric 3D Contrast-Enhanced Ultrasound to Assess Internal Carotid Artery Stenosis: A Pilot Study. J Neuroimaging. 2020 Jan 1;30(1):82–9.

120. Rogers SK. Evaluation of Tomographic 3D Ultrasound in Vascular Disease. 2019;

121. Ball S, Rogers S, Kanesalingam K, Taylor R, Katsogridakis E, McCollum C. Carotid plaque volume in patients undergoing carotid endarterectomy. Br J Surg [Internet]. 2018 Feb 1 [cited 2022 May 8];105(3):262–9. Available from: https://pubmed.ncbi.nlm.nih.gov/29315509/

122. Ramnarine K v., Nassiri DK, Hoskins PR, Lubbers J. Validation of a new blood-mimicking fluid for use in Doppler flow test objects. Ultrasound Med Biol [Internet]. 1998 [cited 2022 May 8];24(3):451–9. Available from: https://pubmed.ncbi.nlm.nih.gov/9587999/

123. Rogers S, Carreira J, Thompson R, Morais A, Miller C, Wein W, et al. An Ex Vivo Evaluation of Tomographic 3-D Ultrasound, B-Mode Ultrasound, CT And MR Imaging to Measure Artery Diameter, Length and Wall Volume. Ultrasound Med Biol [Internet]. 2019 Oct 1 [cited 2022 May 8];45(10):2819–29. Available from: https://pubmed.ncbi.nlm.nih.gov/31375217/

124. Huang Q, Zeng Z. A Review on Real-Time 3D Ultrasound Imaging Technology. Biomed Res Int [Internet]. 2017 [cited 2022 May 8];2017. Available from: https://pubmed.ncbi.nlm.nih.gov/28459067/

125. Wen T, Li L, Zhu Q, Qin W, Gu J, Yang F, et al. GPU-accelerated Kernel Regression Reconstruction for Freehand 3D Ultrasound Imaging. Ultrason Imaging [Internet]. 2017

Jul 1 [cited 2022 May 8];39(4):240–59. Available from: https://pubmed.ncbi.nlm.nih.gov/28627330/

126. von Reutern GM, Goertler MW, Bornstein NM, Sette M del, Evans DH, Hetzel A, et al. Grading carotid stenosis using ultrasonic methods. Stroke [Internet]. 2012 Mar [cited 2022 May 5];43(3):916–21. Available from: https://pubmed.ncbi.nlm.nih.gov/22343647/

127. Katan M, Luft A. Global Burden of Stroke. Semin Neurol. 2018 Apr 1;38(2):208–11.

128. Doonan RJ, Abdullah A, Steinmetz-Wood S, Mekhaiel S, Steinmetz OK, Obrand DI, et al. Carotid Endarterectomy Outcomes in the Elderly: A Canadian Institutional Experience. Ann Vasc Surg. 2019 Aug 1;59:16–20.

129. Savardekar AR, Narayan V, Patra DP, Spetzler RF, Sun H. Timing of Carotid Endarterectomy for Symptomatic Carotid Stenosis: A Snapshot of Current Trends and Systematic Review of Literature on Changing Paradigm towards Early Surgery. Neurosurgery. 2019 Aug 1;85(2):E214–25.

130. Bonati LH, Jansen O, de Borst GJ, Brown MM. Management of atherosclerotic extracranial carotid artery stenosis. Lancet Neurol. 2022 Mar 1;21(3):273–83.

131. North American Symptomatic Carotid Endarterectomy Trial Collaborators. Beneficial Effect of Carotid Endarterectomy in Symptomatic Patients with High-Grade Carotid Stenosis. http://dx.doi.org/101056/NEJM199108153250701. 1991 Jan 14;325(7):445–53.

132. European Carotid Surgery Trialists' Collaborative Group. Randomised trial of endarterectomy for recently symptomatic carotid stenosis: final results of the MRC European Carotid Surgery Trial (ECST). The Lancet. 1998 May 9;351(9113):1379–87.

133. Paraskevas KI, Nicolaides AN, Kakkos SK. Asymptomatic Carotid Stenosis and Risk of Stroke (ACSRS) study: what have we learned from it? Ann Transl Med. 2020 Oct;8(19):1271–1271.

134. Naylor AR, Ricco JB, de Borst GJ, Debus S, de Haro J, Halliday A, et al. Editor's Choice - Management of Atherosclerotic Carotid and Vertebral Artery Disease: 2017 Clinical Practice Guidelines of the European Society for Vascular Surgery (ESVS). Eur J Vasc Endovasc Surg. 2018 Jan 1;55(1):3–81.

135. Naylor AR, Rantner B, Ancetti S, De Borst GJ, De Carlo M, Halliday A, et al. Journal Pre-proof European society for vascular surgery (ESVS) 2023 clinical practice guidelines on the management of atherosclerotic carotid and vertebral artery disease. European Journal of Vascular & Endovascular Surgery. 2022;

136. Wannarong T, Parraga G, Buchanan D, Fenster A, House AA, Hackam DG, et al. Progression of carotid plaque volume predicts cardiovascular events. Stroke. 2013 Jul;44(7):1859–65.

137. Nies KPH, Smits LJM, Kassem M, Nederkoorn PJ, Oostenbrugge RJ van, Kooi ME. Emerging Role of Carotid MRI for Personalized Ischemic Stroke Risk Prediction in Patients With Carotid Artery Stenosis. Front Neurol. 2021 Aug 3;12:1327.

138. Lu M, Peng P, Cui Y, Qiao H, Li D, Cai J, et al. Association of Progression of Carotid Artery Wall Volume and Recurrent Transient Ischemic Attack or Stroke: A Magnetic Resonance Imaging Study. Stroke. 2018;49(3):614–20.

139. Rozie S, Weert TT, Monyé C, Homburg PJ, Tanghe HLJ, Dippel DWJ, et al. Atherosclerotic plaque volume and composition in symptomatic carotid arteries assessed with multidetector CT angiography; relationship with severity of stenosis and cardiovascular risk factors. Eur Radiol. 2009 Apr 22;19(9):2294–301.

140. Sprynger M, Rigo F, Moonen M, Aboyans V, Edvardsen T, De Alcantara ML, et al. Focus on echovascular imaging assessment of arterial disease: complement to the ESC guidelines (PARTIM 1) in collaboration with the Working Group on Aorta and Peripheral Vascular Diseases. Eur Heart J Cardiovasc Imaging. 2018 Nov 1;19(11):1195–221.

141. Ainsworth CD, Blake CC, Tamayo A, Beletsky V, Fenster A, Spence JD. 3D ultrasound measurement of change in carotid plaque volume: A tool for rapid evaluation of new therapies. Stroke. 2005 Sep 1;36(9):1904–9.

142. Calogero E, Fabiani I, Pugliese NR, Santini V, Ghiadoni L, Di Stefano R, et al. Three-Dimensional Echographic Evaluation of Carotid Artery Disease. J Cardiovasc Echogr. 2018 Oct 1;28(4):218.

143. Alzahrani A, Alotaibi SA, Aslam M, Sultan SR. Reliability and Accuracy of Tomographic 3-D Ultrasound for Grading Vessel Stenosis: A Phantom Study. Ultrasound Med Biol. 2022 Jun 14;

144. Rogers S, Carreira J, Thompson R, Morais A, Miller C, Wein W, et al. An Ex Vivo Evaluation of Tomographic 3-D Ultrasound, B-Mode Ultrasound, CT And MR Imaging to Measure Artery Diameter, Length and Wall Volume. Ultrasound Med Biol. 2019 Oct 1;45(10):2819–29.

145. Ball S, Rogers S, Kanesalingam K, Taylor R, Katsogridakis E, McCollum C. Carotid plaque volume in patients undergoing carotid endarterectomy. Br J Surg. 2018 Feb 1;105(3):262–9.

146. Hathout GM, Fink JR, El-Saden SM, Grant EG. Sonographic NASCET Index: A New Doppler Parameter for Assessment of Internal Carotid Artery Stenosis. AJNR Am J Neuroradiol. 2005;26(1):68.

147. Oates CP, Naylor AR, Hartshorne T, Charles SM, Fail T, Humphries K, et al. Joint recommendations for reporting carotid ultrasound investigations in the United Kingdom. Eur J Vasc Endovasc Surg. 2009 Mar;37(3):251–61.

148. Koo TK, Li MY. A Guideline of Selecting and Reporting Intraclass Correlation Coefficients for Reliability Research. J Chiropr Med. 2016 Jun 1;15(2):155–63.

149. Moore DS, William IN, Flinger MA. The Basic Practice of Statistics. 6th ed. New York: Freeman and Company; 2013. 138 p.

150. Giavarina D. Understanding Bland Altman analysis. Biochem Med (Zagreb). 2015;25(2):141–51.

151. Schober P, Schwarte LA. Correlation coefficients: Appropriate use and interpretation. Anesth Analg. 2018 May 1;126(5):1763–8.

152. Sandholt B V., Collet-Billon A, Entrekin R, Sillesen HH. Inter-Scan Reproducibility of Carotid Plaque Volume Measurements by 3-D Ultrasound. Ultrasound Med Biol. 2018;44(3):670–6.

153. Khan AA, Koudelka C, Goldstein C, Zhao L, Yokemick J, Dux M, et al. Semiautomatic quantification of carotid plaque volume with three-dimensional ultrasound imaging. J Vasc Surg. 2017;65(5):1407–17.

154. Iommi D, Hummel J, Figl ML. Evaluation of 3D ultrasound for image guidance. PLoS One. 2020;15(3).

155. Alexandrov A V., Brodie DS, McLean A, Hamilton P, Murphy J, Burns PN. Correlation of Peak Systolic Velocity and Angiographic Measurement of Carotid Stenosis Revisited. Stroke. 1997;28(2):339–42.

156. Criqui MH, Matsushita K, Aboyans V, Hess CN, Hicks CW, Kwan TW, et al. Lower Extremity Peripheral Artery Disease: Contemporary Epidemiology, Management Gaps,

and Future Directions: A Scientific Statement From the American Heart Association. Circulation. 2021 Aug 31;144:E171–91.

157. Caro J, Migliaccio-Walle K, Ishak KJ, Proskorovsky I. The morbidity and mortality following a diagnosis of peripheral arterial disease: long-term follow-up of a large database. BMC Cardiovasc Disord. 2005 Jun 22;5.

158. Dua A, Lee CJ. Epidemiology of Peripheral Arterial Disease and Critical Limb Ischemia. Tech Vasc Interv Radiol. 2016 Jun 1;19(2):91–5.

159. Firnhaber JM, Powell CS. Lower Extremity Peripheral Artery Disease: Diagnosis and Treatment. Am Fam Physician. 2019;99(6):362–9.

160. Gerhard-Herman MD, Gornik HL, Barrett C, Barshes NR, Corriere MA, Drachman DE, et al. 2016 AHA/ACC guideline on the management of patients with lower extremity peripheral artery disease: A report of the American college of cardiology/American Heart Association Task Force on Clinical Practice Guidelines. Circulation. 2017;135(12):e726–79.

161. Conte MS, Pomposelli FB, Clair DG, Geraghty PJ, McKinsey JF, Mills JL, et al. Society for Vascular Surgery practice guidelines for atherosclerotic occlusive disease of the lower extremities: management of asymptomatic disease and claudication. J Vasc Surg. 2015 Mar 1;61(3 Suppl):2S-41S.e1.

162. Bolton L. Peripheral arterial disease: Scoping review of patient-centred outcomes. Int Wound J. 2019 Dec 1;16(6):1521.

163. Wong TH, Tay KH, Sebastian MG, Tan SG. Duplex ultrasonography arteriography as first-line investigation for peripheral vascular disease. Singapore Med J. 2013;54(5):271–4.

164. Franz R, Jump M, Spalding MC, Jenkins J. Accuracy of duplex ultrasonography in estimation of severity of peripheral vascular disease. Int J Angiol. 2013 Sep;22(3):155–8.

165. Hwang JY. Doppler ultrasonography of the lower extremity arteries: anatomy and scanning guidelines. Ultrasonography. 2017 Apr 1;36(2):111.

166. Gao M, Hua Y, Zhao X, Jia L, Yang J, Liu B. Optimal Ultrasound Criteria for Grading Stenosis of the Superficial Femoral Artery. Ultrasound Med Biol. 2018 Feb 1;44(2):350–8.

167. Cossman D V., Ellison JE, Wagner WH, Carroll RM, Treiman RL, Foran RF, et al. Comparison of contrast arteriography to arterial mapping with color-flow duplex imaging in the lower extremities. J Vasc Surg. 1989 Nov 1;10(5):522–9.

168. Olinic DM, Stanek A, T A Taru DA, Homorodean C, Olinic M. Acute Limb Ischemia: An Update on Diagnosis and Management. J Clin Med. 2019 Aug 1;8(8).

169. Collins R, Burch J, Cranny G, Aguiar-Ibáñez R, Craig D, Wright K, et al. Duplex ultrasonography, magnetic resonance angiography, and computed tomography angiography for diagnosis and assessment of symptomatic, lower limb peripheral arterial disease: systematic review. BMJ. 2007 Jun 16;334(7606):1257–61.

170. Guo Z, Fenster A. Three-dimensional power Doppler imaging: A phantom study to quantify vessel stenosis. Ultrasound Med Biol. 1996 Jan 1;22(8):1059–69.

171. Sillesen H, Muntendam P, Adourian A, Entrekin R, Garcia M, Falk E, et al. Carotid plaque burden as a measure of subclinical atherosclerosis: comparison with other tests for subclinical arterial disease in the High Risk Plaque BioImage study. JACC Cardiovasc Imaging [Internet]. 2012 Jul [cited 2022 Oct 1];5(7):681–9. Available from: https://pubmed.ncbi.nlm.nih.gov/22789936/

172. Spence JD. Time course of atherosclerosis regression. Atherosclerosis [Internet]. 2014 Aug 1 [cited 2022 Oct 1];235(2):347–8. Available from: http://www.atherosclerosis-journal.com/article/S0021915014011794/fulltext

173. Levin DC, Fallon JT. Significance of the angiographic morphology of localized coronary stenoses: histopathologic correlations. Circulation [Internet]. 1982 [cited 2022 Oct 1];66(2):316–20. Available from: https://pubmed.ncbi.nlm.nih.gov/7094243/

174. Homburg PJ, Rozie S, van Gils MJ, van den Bouwhuijsen QJA, Niessen WJ, Dippel DWJ, et al. Association between carotid artery plaque ulceration and plaque composition evaluated with multidetector CT angiography. Stroke [Internet]. 2011 Feb [cited 2022 Oct 1];42(2):367–72. Available from: https://www.ahajournals.org/doi/abs/10.1161/STROKEAHA.110.597369

175. Miller AJ, Takahashi EA, Harmsen WS, Mara KC, Misra S. Treatment of superficial femoral artery restenosis. J Vasc Interv Radiol [Internet]. 2017 Dec 1 [cited 2022 Oct 1];28(12):1681. Available from: /pmc/articles/PMC5718379/

176. Downey DB, Fenster A, Williams JC. Clinical Utility of Three-dimensional US1. https://doi.org/101148/radiographics202.g00mc19559 [Internet]. 2000 Mar 1 [cited 2022 May 4];20(2):559–71. Available from: https://pubs.rsna.org/doi/abs/10.1148/radiographics.20.2.g00mc19559

177. The Physics and Technique of Ultrasound | Radiology Key [Internet]. [cited 2022 May 3]. Available from: https://radiologykey.com/the-physics-and-technique-of-ultrasound/

178. Thrush A, Hartshorne T, Deane CR. Vascular ultrasound : how, why and when.

179. Physics of Ultrasound | Radiology Key [Internet]. [cited 2022 May 3]. Available from: https://radiologykey.com/physics-of-ultrasound-2/

180. Vascular Ultrasound - 9780443069185 | Elsevier Health [Internet]. [cited 2022 May 3]. Available from: https://www.uk.elsevierhealth.com/vascular-ultrasound-9780443069185.html?gclid=Cj0KCQjwpcOTBhCZARIsAEAYLuVbvZ5Pmtq8Tq1ne6NaupdXigE_ARzgnll8ZBM89PzkVbsTz-J7DCgaAp_FEALw_wcB&gclsrc=aw.ds

181. Ultrasound color Doppler imaging of the right subclavian vein (SV) with... | Download Scientific Diagram [Internet]. [cited 2022 May 4]. Available from: https://www.researchgate.net/figure/Ultrasound-color-Doppler-imaging-of-the-right-subclavian-vein-SV-with-mirror-image_fig15_328349648

182. EPOS™ - C-0879 [Internet]. [cited 2022 May 4]. Available from: https://epos.myesr.org/poster/esr/ecr2019/C-0879

183. General Imaging Ultrasound Systems - M9 - Mindray Global [Internet]. [cited 2022 May 4]. Available from: https://www.mindray.com/en/products/ultrasound/cardiology/m9

184. Uitleg transducers [Internet]. [cited 2022 Oct 2]. Available from: https://www.utwente.nl/nl/techmed/onderwijs/techmed-academy/Scholingen/cash3vasculair/Archief/CASH3Vasc2011/E-materialen%20CASH%203/Uitleg%20transducers.pdf

185. Minami Y, Kudo M. Contrast-enhanced ultrasonography with Sonazoid in hepatocellular carcinoma diagnosis. Hepatoma Res [Internet]. 2020 Aug 7 [cited 2022 May 4];6:46. Available from: https://hrjournal.net/article/view/3579

List of Appendices:

Appendix A: Phantom specifications

Appendix B: Principles of Ultrasound Physics

The fundamental physics of ultrasound and its instruments are essential physical principles. Longitudinal ultrasound waves are classified as infra and audible sound as it is transmitted in cycles of high and low oscillation pressure. To understand this theory, the probe produces a pulse wave which penetrates the anatomical structure within the area being scanned and receives echoes back to formulate the image. Figure A. 1 illustrates the compression (high-level pressure) and rarefaction (low-level pressure) of the sound wave that occurs as it travels through tissue in response to sound source movement (177).

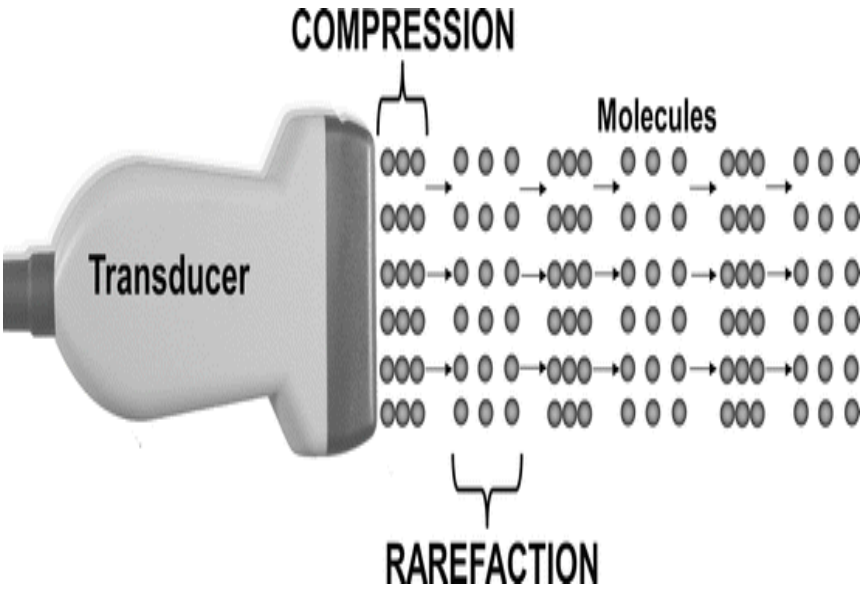

Figure A. 1 A longitudinal sound wave is driven from a transducer into the soft tissue with areas of compression and rarefaction (177).

The characteristics of sound waves involve the number of cycles, wavelengths, amplitude, and frequency (177). One cycle per second (CPS) is how the sound wave changes from high to low pressure. The number of CPS in a sound wave affects its frequency, governed by the sound source. Amplitude is the distance above or below zero at which the highest or minimum pressure occurs and can be thought of as the amount of energy contained inside

the sound wave. This force is proportional to the amount of electrical energy necessary to generate a sound wave of this magnitude. The distance between the peaks of two consecutive cycles is called the wavelength of sound. These properties affect how sound travels through the human body and how sound is used in diagnostic imaging (Figure A.2).

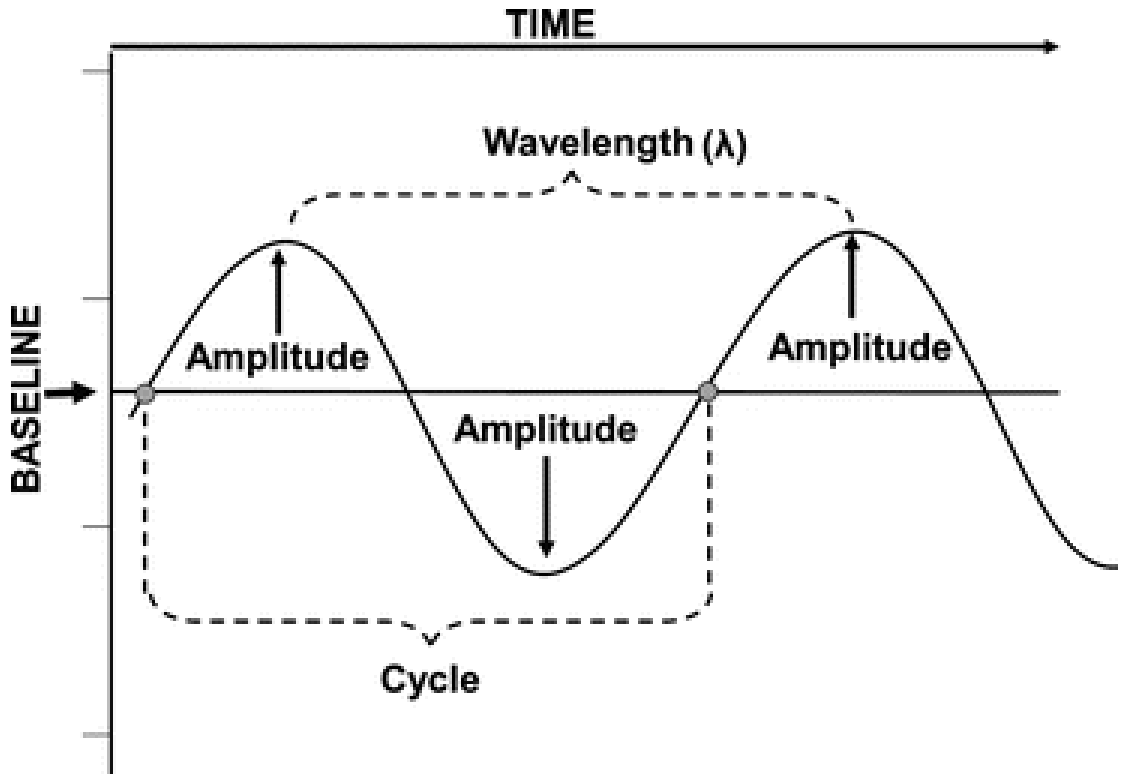

Figure A. 2 Characteristics of a sound wave, including wavelength, amplitude, and cycle (177).

To travel through a distance, sound must pass through a medium. This is because the sound is transmitted from medium particle to another via the oscillation or vibration of the medium particle itself. Therefore, the sound cannot travel in a vacuum. This is also true for air and soft tissues (178).

The higher the sound frequency, the more energy is required to carry it over a long distance. Ultrasound cannot pass through the air due to its extremely high frequency and short

wavelength, as air particles are too close together. As a result, ultrasonography necessitates coupling gel to ensure that sound from the transducer is transmitted into the soft tissue (178).

Infra-sound is assessed in terms of frequency in the unit of Hertz (Hz) when applied to imaging which is any sound with a frequency less than 20 Hz, with an audible range of 20 Hz to 20 kilohertz (kHz). On the other hand, ultrasound is defined as any sound frequency greater than 2. The following formula is used to determine the acoustic impedance:

$$Acoustic\ impedance\ (z) = density\ (\frac{kg}{m3}) \times 1540\ (\frac{\mathrm{m}}{\mathrm{s}})$$

The magnitude of the returning echo is governed by the ratio of reflected transmitted sound, which varies between tissue types due to their varied acoustic impedance. The ratio used to compute the amplitude is as follows:

$$R = \frac{(Z2 - Z1)}{(Z2 + Z1)}$$

Dynamic Range and Reflection

The acoustic impedance ratio and the transmission angle determine the echo amplitude. Reflection has an equal angle to soundwave transmission. This can significantly lose ultrasonic energy if the transmission angle is too shallow, as the ultrasound transducer misses the reflected echo. This is referred to as oblique insonation and is illustrated in (Figure A.3).

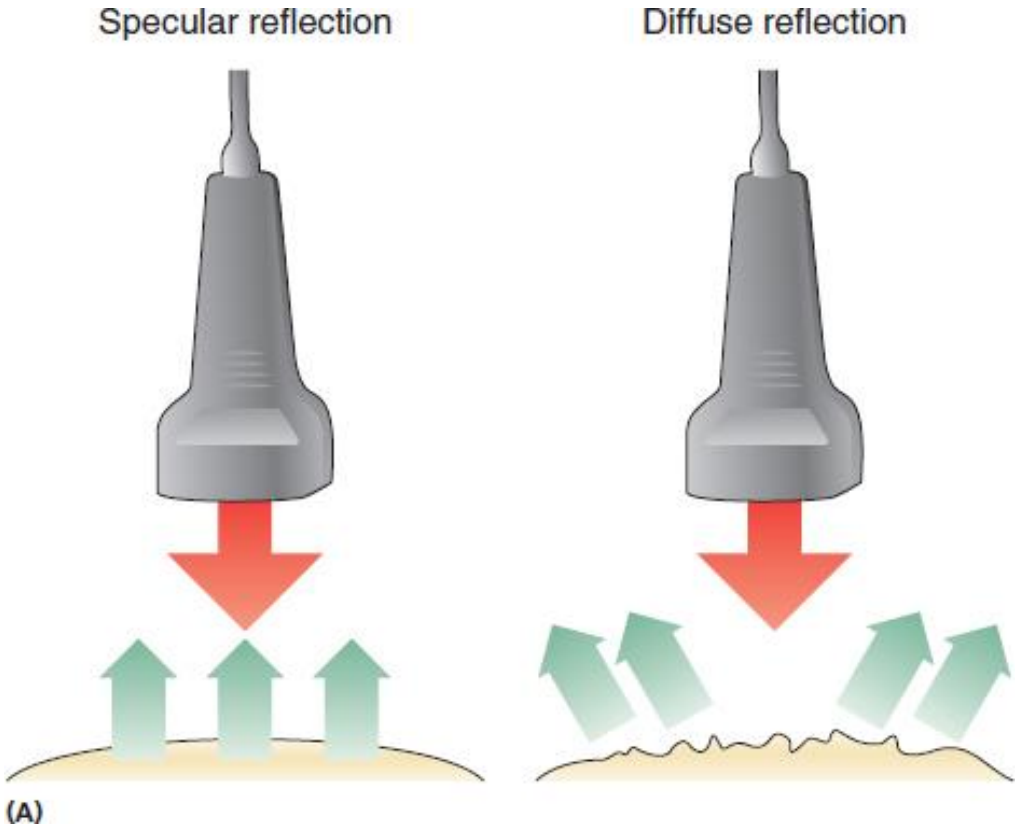

Figure A. 3 Right A, specular reflection Left: oblique insonation (179).

To detect the maximum echos back, the transmission angle must be vertical to the surface of the skin or tissue border. (Figure A.3) This phenomenon is referred to as specular reflection (179,180). Any echo's amplitude has an intensity as a function of the angles and impedance discussed previously. Ultrasound scanners use a logarithmic scale to assign a specific intensity to a particular shade of grey (179). The capacity of the scanner to distinguish two distinct structures is consequently contingent upon the different acoustic impedances and shades of grey. The greyscale ranges from total black (echolucent) to bright white (echogenic). The dynamic range refers to the content of intensities that the scanner can display. Filters can modify the dynamic range of an image to reduce spurious low-intensity artefactual echoes (179).

Ultrasound Image Formation

The process of image generation is intricate, requiring large number of ultrasonic crystals. The ultrasonic machine stimulates a single crystal, which generates a sound pulse transmitted into the tissue (179). The system can determine the maximum length of time required for a sound pulse to travel to and from the maximum depth depends on the given required settings by the operator. The following pulse cannot be transmitted until this time has passed. There are more reflections from a single pulse transmission line than the image. The following pulse will be driven after the allocated time for listening has expired (177).

Slices are created from the ultrasound image or frame based on the number of ultrasonic crystals. Each crystal generates a single picture strip that serves as the ultrasonic frame. If each crystal were operated sequentially, it would take excessive time and produce images at an inordinately slow rate. As a result, ultrasound machine can transmit numerous crystals simultaneously, separated by a distance that prevents nearby crystals from detecting echoes. This reduces frame generation time and may increase frame rate which is the required time to produce a single image in one second per hertz (180).

Additionally, ultrasound industries can save time by utilising a frame averaging tool. Rather than driving alternate crystals, this approach generates the image by averaging a narrow slice of the frame from surrounding slices. Due to the short size of each frame slice, significant inaccuracy is avoided, allowing for a greater frame rate (179). The advantage of these systems is that the cables connecting the machine to the probe may be shortened, resulting in a light transducer cable. A single wire can be linked to many crystals, and sequencing ensures that

no two crystals transmit data simultaneously over the same cable. This is called multiplexing in matrix 3DUS (180).

Artefact

Ultrasound artefact is the appearance on the ultrasound screen that does not represent the reality of the structure scanned. When an anatomical structure is being scanned, a sound reflector returns only a single echo from the transducer. However, ultrasound bounces around the anatomical structure or between the transducer and the reflector numerous times. This results in false echoes being detected as actual data by the ultrasound machine. Thus, ultrasound machine cannot distinguish between the two scans. Some are more problematic than others in 3DUS imaging (180).

Attenuation

Attenuation is proportional to the transmission frequency. High frequency leads to greater attenuation which result in a shallower depth being portrayed (178). Poor ultrasound waves transition leads to energy loss when traveling from one particle to another through soft tissue. This means that when the sound travels deeper, the echoes become weaker.

Reverberation

If the reflector is powerful enough to provide a high-energy echo, the reflected sound wave can bounce off the transducer's surface, return to the reflector, and then back to the scanner. This can occur several times. The PZT crystal registers some energy and generates

an image each time. Multiple reflections at the same depths equal to the distance from the probe will be exhibited in the image due to reverberation (178).

Acoustic Shadowing

When a dense structure has a strong reflector, sound cannot penetrate through it and is instead reflected to the scanner. The reflector's front edge appears dazzling white with a black stripe behind it posteriorly and no other echoes. No sound is present in that anatomical region to generate an echo. This is evident in severely calcified plaque (178).

Perpendicular Transmission and Posterior Enhancement

Oblique insonation occurs when objects are not vertical to the angle of transmission. This is particularly true with blood vessels. While the front and posterior walls are predominantly parallel, the medial and lateral walls are not. This results in poor definition as a result of the oblique insonation. This justifies why the medial-lateral or maximal orthogonal dimensions of aortic aneurysms are inaccurate due to the poor description of the wall (178,180).

Additionally, blood vessels present another form of artefact. Since blood is usually homogeneous and has a high-water concentration, sound easily flows through it. As a result, a little amount of sound energy is lost when it passes through a blood artery, resulting in a high-energy echo. As a result, the posterior vessel wall is brightly depicted. This process is referred to as posterior edge augmentation (178,180).

Mirror Image and Multipath

Mirror image artefact is a phenomenon known as an indirect sound return to the probe via multipath transition of the ultrasound wave, which occurs commonly in the subclavian arteries. (178,180) If the echo bounces off a reflector, then another dense structure, and finally returns to the reflector before reaching the transducer, this might result in the formation of two structures if not every echo follows this path. Hence, the actual depth and position of the object may be incorrectly registered.

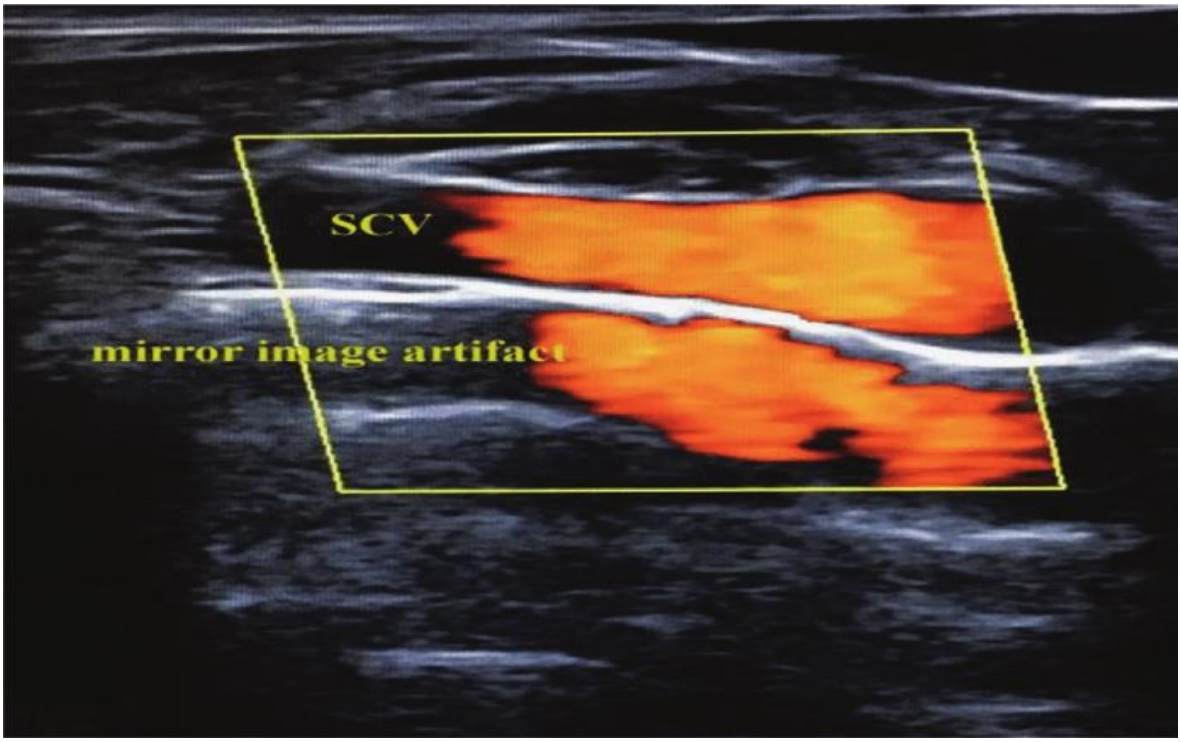

Figure A. 4 Duplex image demonstrating mirror image artefact (181).

Refraction

Refraction occurs when the ultrasound beam tilts from the primary direction as it travels between tissues with different speeds of sound. A soundwave will penetrate the new

tissue and causes acceleration to one edge of the sound and bending the sound wave resulting in feeble echoes and an inaccurate depiction of the reflector's true position (178). Snell's law describes this mechanism and can be calculated as follows:

$$Transmission\ angle = insonation\ angle \times \left[\frac{tissue\ 2\ speed}{tissue\ 1\ speed}\right]$$

Scatter

Rayleigh scatterer occurs when the energy of the dispersed sound is proportional to the fourth power of the frequency. (178) Often, reflector particles do not have flat surfaces and are more similar to spheres. When sound is insonated, this might result in sound reflecting in numerous directions rather than travel back to the transducer. This spreads the sound throughout the tissue, resulting in many faint echoes which can result in blurry photos (i.e., red blood cell). (178)

Time Gain Compensation

Time gain is a process of amplification in which it increases the image's dynamic range, making reflections appear lighter or darker. (178) If an echo is not presented because the returning signal is too weak, the scanner may filter it as artefact information and increase the gain until the signal is powerful enough to pass through the filter and appears on the ultrasound screen. This is referred to as underwriting. On the other hand, If the gain is adjusted too high, artefacts that would normally be filtered out of the image appeared.

This is referred to as excessive writing. As a result, it is critical to select an appropriate gain level (178). The overall ultrasound image may be excessively bright or too dark depending on the ambient light levels in the scan room and the quality of the ultrasound monitor. When evaluating a carotid artery, it is essential to ensure that the vascular lumen is free of plaque. The artefact may be trapped within the vessel if the gain is excessive. It is essential to tune the gain correctly such that the vessel lumen is echolucent and the surrounding tissues may be visualised. (178,180).

Resolution

It is fundamental to acquire the optimal image resolution when ultrasound scanning is performed. The frame rate determines the image quality and resolution. The number of pulses produced per second by a scanner is referred to as the pulse repetition frequency (PRF) or scale, and the amount of time spent creating sound by the scanner is referred to as the duty factor (178,180). The greater the PRF and duty factor, the faster the ultrasonic frame rate will be. The duration of a pulse is referred to as the spatial pulse duration (SPL).

PRF is calculated as $\frac{number\ of\ cycles\ in\ SPL}{frequency}$

Axial resolution

Axial resolution is the ability to distinguish between two identical objects within the same imaging plan along the beam length, which can be displayed as two separate objects. The axial resolution is calculated as half the spatial pulse length; hence it utilises the shortest

possible pulse. The higher the sound frequency, the shorter the spatial pulse length SPL; thus, the greater the axial resolution (178).

$$Axial\ resolution\ (mm) = \frac{SPL\ (mm)}{2} \quad \text{or} \quad Axial\ resolution = 0.77 \times PRF$$

Lateral resolution

Lateral resolution is the ability to distinguish between two identical objects in the same imaging plan across the image which can be displayed as two separated objects. The ultrasonic beam's thickness dictates the length. Higher resolution occurs when higher frequency sound produces a thinner ultrasonic beam. Focusing on the ultrasonic beam becomes thinner and enhances lateral resolution (177).

Elevational resolution

The ultrasound image is a two-dimensional slice of a three-dimensional anatomical structure. The ultrasonic crystal is a small cuboid with a thickness greater than its lateral thickness. This thickness is referred to as slice thickness (Figure A.5). The ultrasound beam must be concentrated in the elevational plane to improve elevational resolution. Focusing will be explored in further detail below, but it can be accomplished using either straight or curved crystals (178).

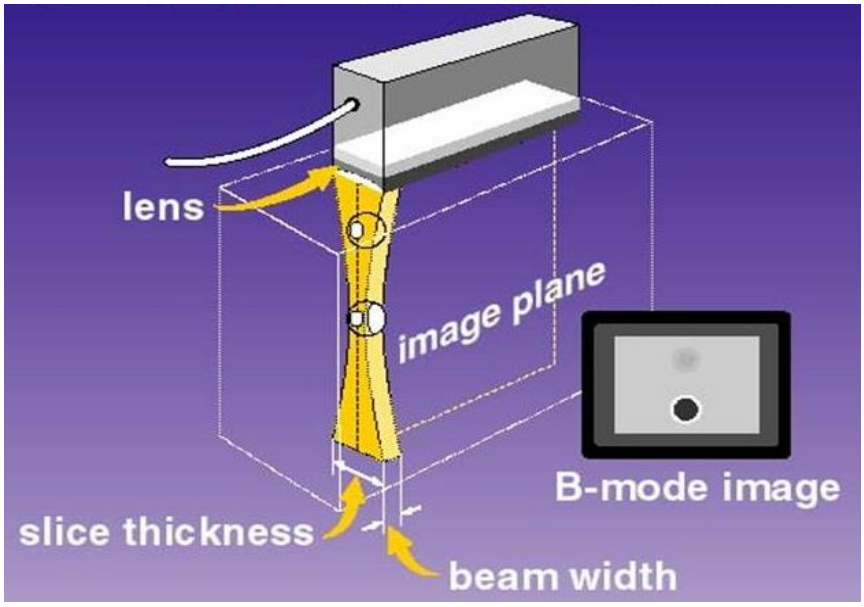

Figure A. 5 ultrasound transducer showing slice thickness (182).

Monitor resolution

Ultrasound scanners of the modern-day provide images on a digital screen separated into individual pixels. The pixel and its corresponding voxel are not covered in detail here; rather, the higher the monitor's resolution, the more defined the image. This is quantified in terms of the multiple pixels per square inch. The more pixels per square inch, the higher image resolution on the screens. (178).

Transducers:

Multi-element array

As illustrated in (Figure A.6), most current ultrasound machines used for vascular assessments are composed of an array of crystals elements, referred to as a multi-element

array. A single array of PZT crystals can include between 128 to many hundreds of them. As a result, the image is formed by several ultrasonic rays. In essence, numerous small ultrasounds interact to generate a single ultrasound beam (178). The Ultrasound's operating frequency is computed as follows:

$$Operating\ frequency\ (Hz) = \frac{speed\ of\ sound\ of\ PZT\ \begin{bmatrix} mm \\ \mu m \end{bmatrix}}{2 \times PZT\ thickness\ (mm)}$$

On the other hand, currently available ultrasound machines do not function at a single frequency due to the electronics. A scanner can work over a very narrow frequency range. This is referred to as bandwidth.

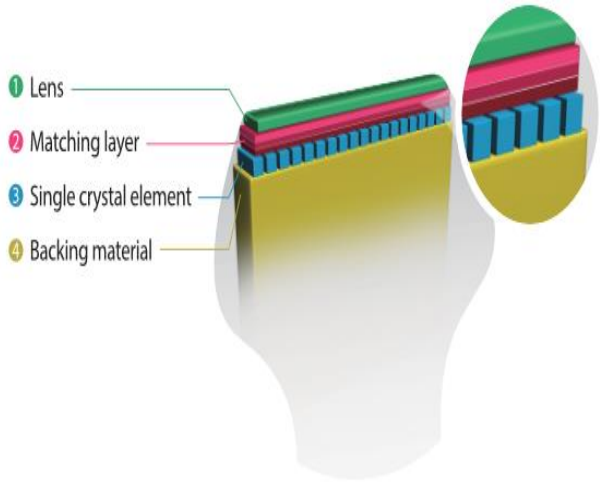

Figure A. 6 multi-element transducer components, including piezoelectric elements that are electrically connected in parallel (183).

Matching Layer

The matching layer is the transducer's end that contacts the skin. It has half the acoustic impedance of the skin layers, which enables optimal sound penetration of the anatomical structure whilst maintaining energy loss. The matching layer's acoustic impedance must be precisely calculated (178).

Acoustic Lens

The acoustic lens focuses the sound before it enters the body. These aid in enhancing lateral resolution. The following section will address electronic focusing. Electrodes are linked via a wire to the scanner via the cable. The alternating current potential is used to apply to the PZT crystal by the acoustic lens.

Piezoelectric Crystal

As mentioned previously, modern crystals are composed of PZT. The crystal is ½ of the thickness of the chosen wavelength at the chosen frequency. Many crystals are linked to a single cable to maintain a reasonable size whilst minimising weight.

Resistor

The resistor enables time delays to be delivered to specific PZT crystals. This will be detailed in further detail below. Additionally, the resistor serves as a filter. When an echo is detected, the resistor functions as a high or low pass filter. This enables the operator to filter out low-energy artefactual echoes, leaving the genuine structures only (178).

Backing material

The backing material isolates the PZT crystals from any sound source, ensuring the signal is not corrupted. PZT will remain to ring whilst producing sound. This is disadvantageous as the bandwidth of a crystal grows as more cycles are produced in the pulse. This lengthens the

spatial pulse and reduces the axial resolution. The crystal is damped to achieve a high axial resolution while maintaining a limited bandwidth and a short spatial pulse length (Figure A.7). This is ensured by the damping substance (178).

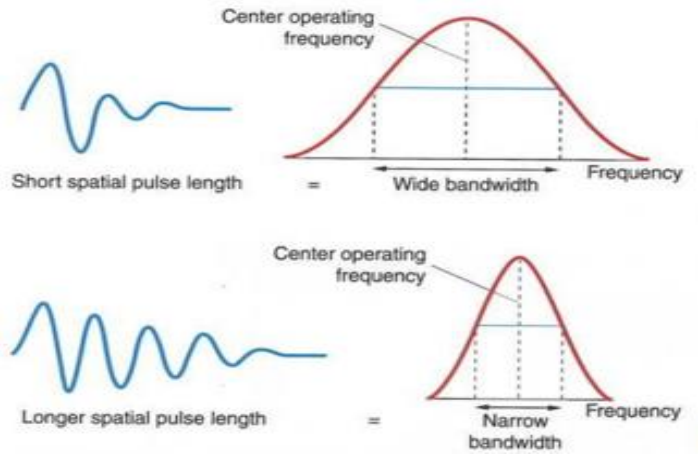

Figure A. 7 The relationship between spatial pulse length and bandwidth (184).

Acoustic Insulator, Transducer Housing, and Cable

The acoustic insulator and transducer housing protects the probe from noise and harm from the outside environment. Its cable is equipped with all the necessary wires for the excitation of the PZT crystals (178).

Steering and Focusing:

Huygens Principle

A probe is constructed from numerous PZT crystals that serve as independent sound sources. Each generates a pulse and sound waves. Each PZT-generated wave is referred to as a Huygens wavelet, and together they produce a single ultrasonic wave (Figure A.8). A delay in

the emission of PZT crystals at the probe's borders compared to centre crystals occurs due to the electronic resistors. This results in a curve in the wavefront, which effectively concentrates more ultrasound energy in the image's centre. This is referred to as electrical focusing and accounts for the brightest image in the centre of the screen. It is possible to apply the delay to only one side of the transducer; this effectively guides the beam in one direction at an angle, referred to as electronic beam steering (Figure A.8).

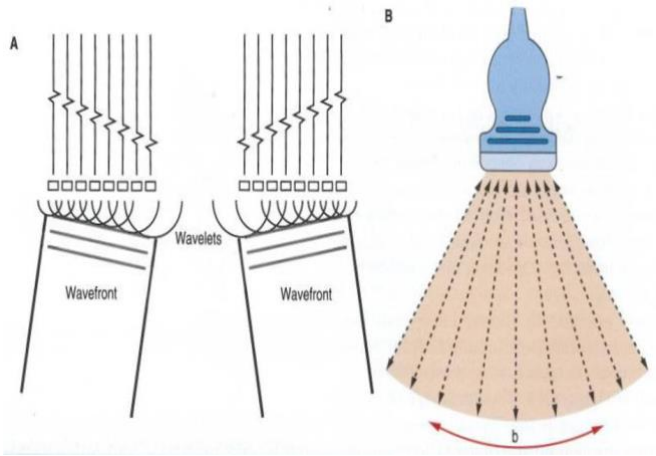

Figure A. 8 Beam steering is caused by individual PZT crystal time delays (184).

Ultrasound Beam Profile

The beam profile of an ultrasound image can be divided into three distinct sections due to the sound being focused. The close zone provides reasonable resolution because of the low number of reflections. The focal zone provides the maximum resolution because it contains the greatest concentration of ultrasonic energy concentrated in a compact region. With the divergence of the ultrasonic beam and energy loss, the far-field is often regarded as a low resolution. Generally, the focus remains on the focal zone and in the image's centre (Figure A. 9).

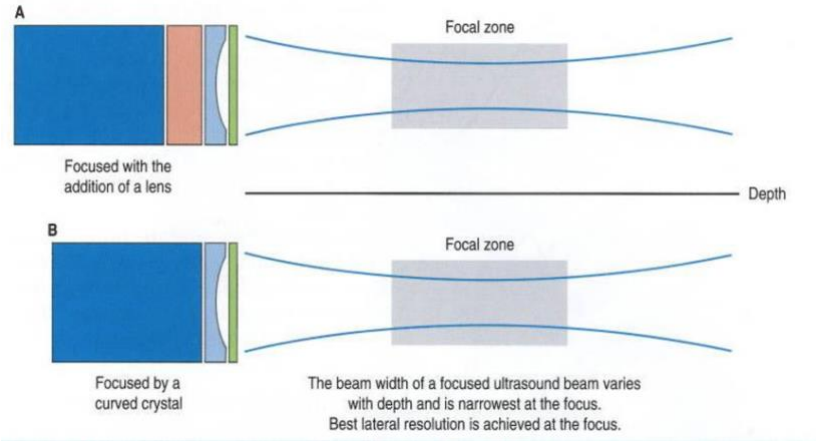

Figure A. 9 Focusing on the ultrasound beam(184).

Doppler:

The Doppler Effect

The Doppler effect is a change in frequency seen due to the relative motion of blood flow through an ultrasound probe which used to determine the blood flow. The Doppler shift is known as a sound pulse that transmits through the anatomical structure and interacts with red blood cells. The frequency of the sound pulse alters according to the blood's velocity (178). Blood direction is labelled to a red or blue colour on the scale and represents a positive or negative spectral waveform on the baseline aligning with the direction of the blood flow. The Doppler shift is calculated as follows:

$$fd = fr - ft$$

When analysing and comprehending the Doppler equation, the angle of insonation is critical as the equation employs the angle's cosine (178). The cosine of 90° is zero, and no flow is observed when the angle of insonation is vertical to the direction of the flow. The maximum Doppler shift is recorded when the angle of insonation is zero. In this case, angle adjustment

would be unnecessary. Transcranial Doppler is an example of this. Parallel flow is achievable in a minimal number of arteries (178).

There is an accompanying cosine error when employing Doppler and considering the cosine angle. The greater the angle, the greater the cosine error and the lower the detectable frequency of the Doppler shift. When utilising cosine, an acceptable error in estimated speed exists between 30° and 60° , which indicates that any angle between 30° and 60° may be employed. On the other hand, it is widely acknowledged that a 60 angle should be used to compare ultrasound scans performed over time. Fundamentally, if the angle of insonation can be computed appropriately, it makes no difference whether the angle is employed. Unfortunately, the angle of insonation cannot be calculated accurately using ultrasonography and thus contains an inaccuracy (178).

Doppler Effect

Generally, two distinct forms of Doppler application are used in vascular Ultrasound. The colour Doppler technique is used to demonstrate the blood flow, vessel patency, and flow turbulence. On the other hand, the Spectral Doppler measures blood velocity, turbulence upstream and downstream, and patency (178).

Spectral Doppler

Due to the pulsatile nature of blood flow, there are various speeds across the pulse. This indicates the range of frequencies within the Doppler shift when spread during the pulse duration.

Fast Fourier Transformation (FFT) is used to decompose the spectrum of frequencies into their component. The ultrasound machines present these as a spectral trace of frequency against time. The graphical representation of blood velocity as blood flow over time can be determined if the angle of insonation is known (178).

Colour Doppler

Essentially, colour Doppler visualises motion, mainly blood movement via an artery. The disadvantage of utilising FFT is that it is a relatively slow way of retrieving data. Colour Doppler must have a high temporal resolution to display data rapidly. The colour box is divided into numerous squares, requiring its sound pulse to detect so that several pulses can be transmitted down a single scan line simultaneously. Since only a single pulse may be transmitted down a single scan line at a time, a rapid technique of extracting the Doppler information is required to send the next pulse down the same scan line. This can occur on many scan lines concurrently (178). Therefore, it is essential to minimise the size of the colour box to get the maximum feasible temporal resolution.

Patient's movement is another significant disadvantage of Doppler colour imaging. The transducer or patient movement might alter the colour flow, misleading the readings which impair the readability of photographs (178).

Aliasing

The velocity displayed on the scale is adjustable by changing the PRF. When the mean velocity of the flow exceeds the PRF, an artefact known as aliasing occurs because the PRF's sample rate exceeds the number of times the flow is measured. (49) The Nyquist limit is the value of

half the PRF at which aliasing occurs. In this case, the colour scale loops around itself, allowing for identifying a blue in the vessel's centre due to images simulating reverse flow. A haemodynamically significant lesion indicated when aliasing occurs in vessels with stenosis which manifest as an increased blood velocity and turbulence within stenotic area (49,178).

Colour Bleeding

As in the case of grayscale imaging, colour imaging makes use of gain. If the gain time is too high, the mean velocity is amplified excessively, and the scanner's autocorrelation approach may display the colour information outside the vessel (178).

Nonlinear Propagation, Harmonics, and Pulse Inversion:

Nonlinear Propagation

Physics has explained that when the sound pulse is emitted, it moves and receives an irregular echo through soft tissue; however, this assumption is incorrect (178). A longitudinal ultrasonic wave propagates in a nonlinear manner. This occurs as a result of the sounds' density when it travels via regions of rarefaction and compression. Compression zones moves faster through soft tissue than rarefaction zones. Consequently, a compression zone can move to the next rarefaction zone. At this moment, the sound frequency will grow by multiples or fundamental transmission frequency. This phenomenon is referred to as nonlinear propagation. When the ultrasonic wave is distorted, harmonic echoes of the fundamental frequency are formed, for example, echoes at 2MHz, 4MHz, and 8MHz. Separating harmonic

frequencies from the fundamental frequency can be accomplished in two ways: by harmonic tissue imaging or using the pulse inversion approach (178).

Harmonic Imaging

Harmonics are particularly well-suited for ultrasound scan. A few harmonics are created at low depths with a fundamental solid frequency. Harmonics are created swiftly in the focus zone but are attenuated as quickly at depth. As a result, harmonics contribute to reducing artefacts by increasing the signal-to-noise ratio, which occurs because machine failure are frequently insufficiently strong to produce substantial harmonics.

Harmonic frequencies are used in the traditional approaches to aid image resolution. It is also used in electronic filters to ensure the scanner processes only signals with a second harmonic frequency. However, this can be regarded as an ineffective method as noise remains in the signal. This has encouraged the development of a clearer harmonic imaging techniques (178).

Pulse Inversion

Pulse inversion (the phase shift technique) uses a specific pulse with a uniquely defined bandwidth. Each manufacturer uses a unique pulse to mainstream its usage. When two sound pulses are sent into a patient along the same scan line, one of the pulses will replace the other. However, if nonlinear propagation occurs, the pulse transmits unevenly with more distortion in the positive pressure compression zone and less distortion in the negative rarefaction region. When these pulses are combined, an apparent signal is formed via harmonics (Figure A.10).

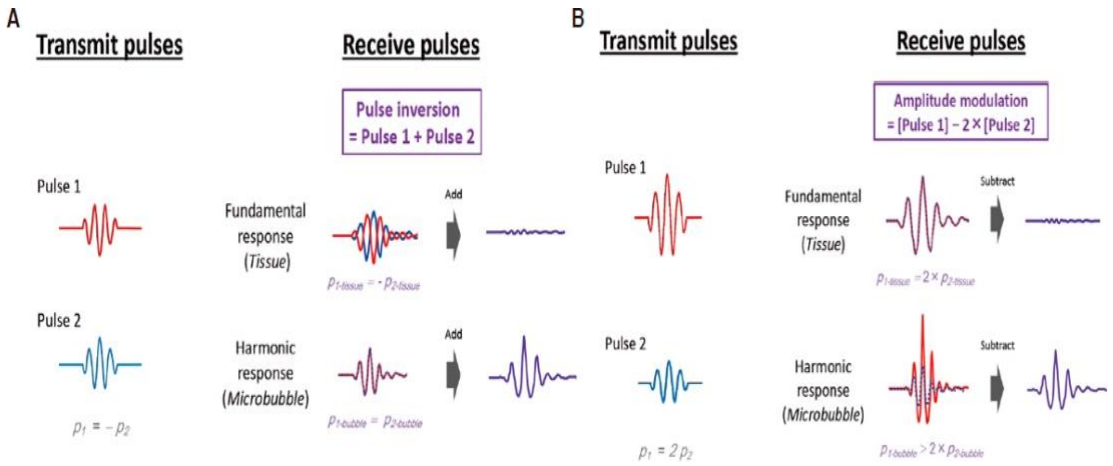

Figure A. 10 Pulse inversion process (185).

Safety:

The safety application of ultrasonography performance is essential to evaluate when the machine energy is manipulated as attempts made to increase the number of pulses per second. Quick pulses have a higher energy density over a shorter time, and because they are focussed, this energy is distributed across a smaller region. This often results in significant safety issues such as heat and mechanical damage.

Thermal Concerns

Ultrasound is m attenuated, and a burst of energy concentrated on a small area over time. Sound energy converts to heat when absorbed by soft tissue. Although thermal damage in adult is not a significant concern, it has been established that heating tissue influences cellular growth and may cause serious complications such as hyperthermia, which can result in abdominal wall abnormalities (178).

Mechanical Concerns

Radiation force, streaming, and cavitation are common mechanical issues when operating ultrasound machines. Radiation force occurs as the ultrasonic beam's energy distorts the soft tissue. Additionally, it can cause fluid objects to stream. This is when a stationary fluid begins to flow, causing formation of shear stress that can deform or damage the anatomical structure. While these concerns have been established in vitro, there have been no documented impacts in vivo, and hence the risks remain theoretical (178). Cavitation has been demonstrated in humans and is the foundation for the contrast imaging detailed below. Cavitation can develop when a radiation force generates a microbubble within a liquid medium or soft tissue with a high-water concentration. Cavitation can be stable or unstable. To grasp cavitation, it's necessary to realise that a sound wave oscillates between high and low pressure.

Stable Cavitation

When a sound wave travels over a micro-bubble, the bubble experiences oscillations in high and low pressure. As a result, the bubble's size will alter uniformly to the pressure change. This, in turn, can result in the streaming discussed previously—non-stable cavitation. When a sound wave oscillates over a bubble, it is possible that the bubble may not respond uniformly. In this case, the bubble's diameter rapidly expands and drops inconsistently over time. This can cause the bubble to rupture, resulting in shock waves and elevated temperatures in specific areas, which can cause tissue injury (178).

As Low As Reasonably Achievable (ALARA)

With the safety issues in mind, it makes sense to keep ultrasonic scans as brief as feasible and to use the lowest possible output power. The British Medical Ultrasound Society and the Society of Vascular Technology GB endorse the As Low As Reasonably Achievable (ALARA) philosophy to uphold this ethos.

Mechanical and Thermal Indices (MI and TI)

The American food and drug administration (FDA) requires that all commercially accessible devices capable of producing ultrasound have a mechanical and thermal index. According to tissue type, there are three sorts of indices; vascular ultrasonography is mainly concerned with MI and TI in soft tissue, though a few exceptions will not be mentioned here. When shown as 1, TI represents the theoretical effect of expanding the bodily tissue by one degree. A 1.5-degree increase in temperature is not regarded to pose any theoretical concern. MI indices quantify the theoretical possibility of creating cavitation. Cavitation is believed to be impossible below a MI of 0.7.

Appendix C: Published Abstract and Conference Presentation